Title
Second-order perturbative correction to state-specific, excited-state mean field theory

Author
Clune, Rachel

Publication Date
2023

Peer reviewed|Thesis/dissertation

Second-order perturbative correction to state-specific, excited-state mean field theory

by

Rachel A. Clune

A dissertation submitted in partial satisfaction of the

requirements for the degree of

Doctor of Philosophy

in

Chemistry

in the

Graduate Division

of the

University of California, Berkeley

Committee in charge:

Professor Eric Neuscamman, Chair
Professor Eran Rabani
Professor Burkhard Militzer

Spring 2023

Second-order perturbative correction
to state-specific, excited-state mean field theory

Abstract

Second-order perturbative correction
to state-specific, excited-state mean field theory

by

Rachel A. Clune

Doctor of Philosophy in Chemistry

University of California, Berkeley

Professor Eric Neuscamman, Chair

Obtaining predictions for the energies of electronic excited states, especially charge transfer states, is still a challenge in the field of electronic structure theory. Charge transfer states often play an important role in the function of solar cells and organic semiconductors, and having an accurate computational model for their energetics that is not computationally expensive is crucial for the development of new technologies that rely on the existence of these states. In this dissertation, two contributions towards this goal are discussed. First, the formulation of a state-specific perturbative method with a relatively low computational complexity of $O(N^5)$ is described. The approximations made to reduce the scaling from its original complexity of $O(N^7)$ had very little impact on the results of the method and it was shown that it provided accurate energetic predictions for valence and charge transfer excitations of small molecules. Next, this perturbative method was analyzed for its accuracy using a benchmarking set of 105 singlet valence excited states. Through this study it was found that, with regularization, the method can perform even better than many higher-scaling theories and can provide a warning for when a state being studied cannot be mainly described by single excitations. The demonstrated accuracy of the method combined with its relatively low computational cost makes it a promising theory that will be useful in its own right and which can act as a springboard for the development of even more sophisticated excited-state-specific correlation methods.

Rachel was here

Contents

List of Figures

List of Tables

Acknowledgments

There are so many people who helped me reach the end of this Ph.D. program, more than I can list here. However, I would be remiss if I did not explicitly thank these amazing people: My advisor, Eric Neuscamman for supporting my goals throughout the program, his research mentorship, and for finally reading the benchmarking paper.

Becky for doing their best to cheer me up whenever I felt overwhelmed, making the best oatmeal chocolate chip cookies I have ever had, and having the best dog anyone could ever be friends with.

Tarini for making sure I always made time for life outside of work.

Scott for making sure my ego never even had a chance of being inflated.

The best GSI a person could ask for, Sonja, for being so supportive and not letting me be too hard on myself. You're an amazing human, an amazing researcher, and you will be an amazing mom.

Trine for her infinite cheerfulness, willingness to try new things, and supporting me throughout the last year. You're going to do amazing things.

Connie for being a major part of the team that made sure my desk was the most recognizable in the Pitzer center.

Harrison for asking me questions that made me think deeper about my own project.

Leo for helping me sort through so many scientific topics and listening while I rambled about what I was working on.

The friends I made in undergrad, especially Vivian, Harshita, Sebastian, Charlotte, Rachel, Angela, Lauren, and Clara for helping me stay sane through the pandemic.

Our alumni, Sergio, Beatrice, Luning, Leon, and especially Jacki, for giving me the opportunity to learn from them.

The undergraduates in our group, Shuai, George, Billy, Shiloh, and Triet for letting me occasionally talk their ears off about what I was working on.

The math bootcamp team, especially Orion, Avishek, Dipti, and Elliot for giving me a chance to be part of a program that has been so meaningful to so many students and will hopefully carry on even after I graduate.

And last but not least, I would like to thank my family for their support throughout these last five years.

Chapter 1

Introduction

1.1 Motivation

Understanding the properties of electronic excited states is crucial for many aspects of science such as photochemistry and predicting chemical spectra.[1, 2] Theoretical models are necessary for understanding the underlying aspects of these chemical processes and can be used in conjunction with experimental data to give a more complete view of what is being studied. However, while a robust hierarchy of methods to study the ground states of systems exists – and will be discussed in more detail later on – excited states pose additional challenges. First, the change in electron density that comes from an electronic transition can cause the orbitals in the system to relax, a process that must be accounted for in order to obtain accurate results.[3] Second, determining the basic structure of an excited state can be difficult, as the molecular orbital picture of chemistry is just a model. As will be seen repeatedly in this thesis, electronic excitations, even ones dominated by singly excited character, are often best described as a linear combination of different configurations. For example, an excited state that is dominated by a HOMO/LUMO excitation can mix with the HOMO-1/LUMO+1 transition, meaning that a combination of both configurations is necessary to fully represent the state. Finding the linear combination of these configurations can be a daunting optimization problem. Having a hierarchy of excited state methods that fully account for orbital relaxations, can reliably find representations for specific vertical excitations while maintaining the computational complexity of their ground state counterparts, and can account for electron correlation effects would be an incredibly useful tool for the chemistry community.

In particular, modeling the properties of charge transfer states still poses a large challenge for the theoretical chemistry community.[4, 5] These states occur in materials being studied for their use in solar cells [6, 7] and in organic semiconductors, such as the well-studied DMABN molecule.[8] Methods that are more computationally complex (those that scale as $O(N^6)$ and higher) can be fairly accurate for these states, as will be discussed, but their high cost makes using them prohibitive for modeling realistic systems.[9] Lower scaling methods,

such as time-dependent density functional theory, while more tractable, tend to have issues with accuracy even with state-of-the-art exchange correlation functions.[5, 10] In this work, a method is presented that is capable of achieving accurate energies for valence and charge transfer excited states at O(N^5) scaling: excited-state-specific Møller-Plesset perturbation theory.[11, 12]

1.2 Underlying principles of electronic structure theory

To create these theoretical models that can describe molecular systems, we start with finding the solutions to

$$i\hbar\frac{\partial}{\partial t}\hat{H}\left|\Psi\right\rangle = \hat{H}\left|\Psi\right\rangle \tag{1.1}$$

known as the time-dependent Schrödinger equation. However, since the eigenstates of the Hamiltonian that control most molecular properties are stationary in time, we can instead focus on solving the time-independent Schrödinger equation

$$\hat{H}\left|\Psi\right\rangle = E\left|\Psi\right\rangle \tag{1.2}$$

where E is the energy of the system, $|\Psi\rangle$ is the corresponding eigenvector state, and $\hat{H}$ is given by

$$\hat{H} = \sum_{pq}\sum_{\sigma\in\{\alpha,\beta\}} h_{pq}\hat{p}^{\dagger}_{\sigma}\hat{q}_{\sigma} + \frac{1}{2}\sum_{pqrs}\sum_{\sigma,\tau\in\{\alpha,\beta\}} \langle pq|rs\rangle\, \hat{p}^{\dagger}_{\sigma}\hat{q}^{\dagger}_{\tau}\hat{s}_{\tau}\hat{r}_{\sigma} \tag{1.3}$$

in the syntax of second quantized algebra. Here p, q, r, s range over all one-electron basis functions used to approximately represent $|\Psi\rangle$, σ and τ denote spin up/down, operators of the form $\hat{p}^{\dagger}$ are creation operators that place electrons in the spatial orbital ϕ_p, and operators of the form $\hat{q}$ are destruction operators that remove electrons from spatial orbital ϕ_q. The first term is a one-body operator in that it only depends on the position of one electron can contains information about the electronic kinetic energy and electron-nuclear interaction:

$$h_{pq} \equiv \langle p|\,\hat{h}\,|q\rangle = \int \phi^{*}_{p}(\vec{r})\left(-\frac{1}{2}\nabla^2 - \sum_{M}^{N_{nuc}}\frac{Z_m}{\vec{r}-\vec{R}_M}\right)\phi_q(\vec{r})d\vec{r} \tag{1.4}$$

where N_{nuc} is the number of nuclei in the system, $\vec{r}$ is the position of a given electron, and R_M is the location of nuclei M. The second term in Equation 1.3 is a two-body describing electron-electron interactions where the integrals are given by

$$\langle pq|rs\rangle \equiv \langle pq|\,\hat{O}_2\,|rs\rangle = \int\int \phi^{*}_{p}(\vec{r}_1)\phi^{*}_{q}(\vec{r}_2)\frac{1}{|\vec{r}_1-\vec{r}_2|}\phi_r(\vec{r}_1)\phi_s(\vec{r}_2)d\vec{r}_1 d\vec{r}_2 \tag{1.5}$$

This is considered a two-body operator ($\hat{O}_2$) as these integrals depend on the positions of two electrons in the system. The nuclear-nuclear interactions are not considered because we

have adopted the Born-Oppenhiemer approximation. In this approximation it is assumed that the motion of the nuclei can be treated separately from that of the electrons because they are so much more massive, and thus move more slowly.[13]

The solutions to the time-independent electronic Schrödinger equation are the ground and electronic excited states of the system, within the basis set we are using to represent Ψ. These basis sets are typically a collection of Gaussian functions that are meant to recreate the atomic orbital shapes. Gaussians are chosen due to the existence of an analytical form for their integral expressions.[13] However, for many-body systems, the size of the basis becomes large very quickly, as functions are needed to describe the atomic orbitals on each individual atom in a system. For example, the cc-pVDZ basis set, which is typically not regarded as quite large enough to give chemically accurate results for many systems,[14, 15] needs 24 basis functions for a single water molecule. Extrapolating to systems such as a solute in a cluster of water molecules, it is easy to imagine modeling systems that would need thousands of basis functions. As the many-body basis grows exponentially with the number of electrons and orbitals, directly diagonalizing the Hamiltonian to obtain eigenfunctions and eigenvalues becomes computationally intractable for systems of this size, so in order to obtain results one must begin implementing approximations.

1.3 Ground state hierarchy of wave function methods

1.4 Hartree Fock

For calculating the properties of electronic ground states there exists a hierarchy of methods that allows one to systematically improve the expected accuracy of the prediction, usually at the cost of increased computational complexity. At the bottom of this hierarchy is Hartree Fock (HF), a mean field theory that is based around the assumption that the ground state of a system can be written as a single Slater determinant (SD):

$$|RHF\rangle \equiv |\psi\rangle = \frac{1}{\sqrt{N!}} \begin{vmatrix} \phi_1(\vec{r}_1) & \phi_2(\vec{r}_1) & \cdots & \phi_N(\vec{r}_1) \\ \phi_1(\vec{r}_2) & \phi_2(\vec{r}_2) & \cdots & \phi_N(\vec{r}_2) \\ \vdots & \vdots & \ddots & \vdots \\ \phi_1(\vec{r}_N) & \phi_2(\vec{r}_N) & \cdots & \phi_N(\vec{r}_N) \end{vmatrix} \tag{1.6}$$

where N is the number of electrons in the system, $\vec{r}_i$ are the locations of these electrons, and $\phi_i(\vec{r})$ are the molecular orbitals. The molecular orbitals are typically expressed as linear combinations of atomic orbitals, expressed as $\chi_\mu(\vec{r})$, which are in turn expressed using a (typically Gaussian) basis set, resulting in

$$\phi_i(\vec{r}) = \sum_\mu c_{\mu i} \chi_\mu(\vec{r}) \tag{1.7}$$

The variational principle, which states that any expectation value of the Hamiltonian gained from an approximate wave function must be greater than or equal to the lowest Hamiltonian

eigenvalue, is used to determine the set of coefficients ($c_{\mu i}$) via a minimization procedure. Typically one does this by solving the self-consistent Roothaan-Hall equations [13, 16, 17] given by

$$\boldsymbol{FC} = \boldsymbol{SC}\epsilon \tag{1.8}$$

where $\boldsymbol{F}$ is known as the Fock matrix, $\boldsymbol{C}$ is the rotation matrix for converting the basis functions into molecular orbitals, and $\{\epsilon\}$ are the Hartree Fock orbital energies. Using these equations is referred to as 'self-consistent' because the representation of the Fock matrix depends on the molecular orbital shapes, which is information that is contained within C. An iterative procedure must be used to slightly change the representation of the molecular orbitals, determine the impact this has had on the Fock matrix, use the Fock matrix to determine a new representation for the molecular orbitals, etc., until F and C change only negligibly.[13] There are ways to increase the convergence of this iterative procedure, such as using direct inversion of the iterative subspace (DIIS).[18] Direct minimization methods, such as gradient descent, may also be used if the self-consistent procedure fails.[19]

While this method of obtaining a representation of the ground state typically recovers around 99% of the total electronic energy for many systems, the remaining 1% of the energy, known as the correlation energy because it comes from effects beyond the statistically-independent mean-field picture, is crucial for depicting many chemical properties.[20] For an example of how large this 1% can be, comparing the reaction energy of the combustion of methane calculated from Hartree Fock to the reaction energy from a high level method such as CCSD(T) (this method is discussed in Section 1.4.3) shows that Hartree Fock errors by 14 kcal/mol.[21] It is therefore crucial to recover the correlation energy, but, instead of starting from scratch, we can use the Hartree Fock solutions as starting points for correlation treatments.

1.4.1 Møller-Plesset perturbation theory

The first step beyond HF in the overall hierarchy of wave function methods is usually considered to be second-order Møller-Plesset (MP) perturbation theory.[13] This is a form of Rayleigh-Schrodinger perturbation theory in which the zeroth order Hamiltonian is taken to be the Fock operator (F), as defined in Section 1.4. The perturbation is taken as the difference between the Fock operator and the full Hamiltonian (H) defined in Section 1.2. In order for the perturbation to be small, and thus the underlying assumption of any perturbative method to be valid, the description of the ground state gained from Hartree Fock theory must be fairly good. Typically this limits the usage of MP2 quite a bit as Hartree Fock can only be trusted for systems that can be represented with a single Slater determinant. For example, Hartree Fock in its restricted, spin-pure form fails qualitatively in the dissociation of symmetric molecules like H_2.[13, 22]

The perturbative equations are obtained by taking power series expansions in orders of the perturbing operator of the exact energy and wave function. A full description of the derivation can be found in *Modern Quantum Chemistry* by Szabo and Ostlund.[13] Largely

following the notation used there, we will express the set of energy corrections as $E^{(n)}$ and the set of wave function corrections as $\Psi^{(n)}$, where n is the order of the correction. The equations used to determine these corrections are

$$E^{(0)} |\Psi^{(0)}\rangle = F |\Psi^{(0)}\rangle \tag{1.9}$$

$$(H - F - E^{(1)}) |\Psi^{(0)}\rangle = -(F - E^{(0)}) |\Psi^{(1)}\rangle \tag{1.10}$$

$$E^{(2)} |\Psi^{(0)}\rangle = -(H - F - E^{(1)}) |\Psi^{(1)}\rangle - (F - E^{(0)}) |\Psi^{(2)}\rangle \tag{1.11}$$

and so on, to infinite n. Equation 1.9 is just the Hartree Fock eigenvalue problem, where $|\Psi^{(0)}\rangle$ is the Hartree Fock wave function and $E^{(0)} + E^{(1)}$ is the Hartree Fock energy. This comes from the fact that $E^{(0)}$ only includes the sum of the orbital energies. The Hartree Fock energy also includes contributions from the one-electron pieces of the Coulomb and exchange interactions, which happens to be retrieved by the first-order correction.[13] Since the first order correction to the energy does not actually give any new information about the system, one must go to the second order to obtain an estimate for the correlation energy.

In the ground state theory, an analytical form for the second order energy can be found due to the diagonal form of the Fock matrix:

$$E^{(2)} = \sum_{ijab} \frac{|\langle ij|ab\rangle - \langle ib|ji\rangle|^2}{\varepsilon_i + \varepsilon_j - \varepsilon_a - \varepsilon_b} \tag{1.12}$$

where a and b are indices of canonical virtual (unoccupied) molecular orbitals, i and j are indices of canonical occupied molecular orbitals, and ε_k are the set of orbital eigenvalues from Hartree Fock. It is important to note that while the summation in Equation 1.12 only runs over four indices, second-order Møller-Plesset perturbation theory (MP2) is actually $O(N^5)$, not $O(N^4)$ as this equation would make it seem, due to the transformation from atomic to molecular orbitals that must take place to obtain the two-electron integrals (the $\langle pq|rs\rangle$ values) in Equation 1.12.[23]

One key feature of MP2 is that it is both size consistent and size extensive. If a method is size consistent it means that the method can properly predict that the energy of two infinitely separated systems treated together is the same as the sum of the energies of each system treated individually.[13] Size extensivity is the property that a correlation method's correlation energy grows linearly with the number of electrons in the system, in the limit of a large system.[24] Methods that are not size consistent and extensive will have increasing accuracy issues as the studied systems become larger because there will be more long-range interactions that will be incorrectly accounted for.

1.4.2 Configuration interaction (CI)

Starting from the Hartree Fock molecular orbitals, a complete basis for the many-body Fock space can be formed from all possible configurations of the electrons within the orbitals. Typically these configurations are identified by their difference from the aufbau filling of

orbitals and grouped by how many of the electron placements differ. These are denoted singles if one electron differs from the aufbau filling, doubles if two, and so on. As this forms a complete basis, the exact wave function for a system can then be written as

$$|\Psi\rangle = c_0 |\psi\rangle + \sum_{ia} c_i^a |\psi_i^a\rangle + \sum_{ijab} c_{ij}^{ab} |\psi_{ij}^{ab}\rangle + \sum_{ijkabc} c_{ijk}^{abc} |\psi_{ijk}^{abc}\rangle + \dots \tag{1.13}$$

where the same notation from the previous section for occupied an virtual orbitals is used and $|\phi_i^a\rangle$ represents a configuration where an electron has been moved from the i^{th} occupied orbital in the aufbau filling to the a^{th} virtual orbital. The c coefficients are the weight each of these configurations has in the representation of the wave function. For small systems, the full expansion can be used to gain an exact energy, or at least exact up to the basis set limit, resulting in a method called full CI (FCI). However, this method has exponential scaling, so using CI on larger systems requires truncating the wave function expansion. This results in methods such as CIS, CID, CISD, etc., where the wave function has been truncated to include only singly excited configurations, doubly excited configurations, both singly excited and doubly excited configurations, etc., respectively.[23] The accuracy and computational complexity of the methods typically increases as the number of configurations in the expansion increases. Truncated configuration interaction methods are not extensive nor size consistent, leading to a degradation in accuracy as the system size increases, even when the size increase is from a far-away inert molecule.[24]

1.4.3 Coupled cluster

Similar to configuration interaction, coupled cluster improves on Hartree Fock by including configurations created by promoting electrons into higher orbitals. However, unlike configuration interaction, it has an exponential wave function ansatz:

$$|\Psi\rangle = e^T |\psi\rangle \tag{1.14}$$

where T is the cluster operator that produces a linear combination of configurations when acted on the reference (Hartree Fock) wave function. The operator can be expanded as

$$T = T_1 + T_2 + T_3 + \cdots \tag{1.15}$$

where T_1 is the operator that creates single excitations from the reference,

$$T_1 = \sum_{ia} c_i^a a^\dagger i \tag{1.16}$$

T_2 is the operator that creates double excitations from the reference,

$$T_2 = \sum_{ijab} c_{ij}^{ab} a^\dagger b^\dagger j i \tag{1.17}$$

and so forth. See Section 1.2 for the second quantization notation used here. Just as was the case for CI methods, the wave function must be truncated for the method to be tractable. For example, coupled cluster singles and doubles (CCSD) truncates T at the doubly excited operator. Truncating the cluster operator at higher orders creates a more accurate approximation to the exact energy, but also increases the computational complexity of the method.[25] Configurations can also be included perturbatively, such as in the CCSD(T), where the T in parentheses means that the triples configurations are approximated using a perturbative method based on the singles and doubles parameters from the converged CCSD wave function.[26] This can result in highly accurate methods, as can be seen from the analysis of CCSD(T) results where one study on the interactions of small molecule clusters found that the average error of the method was only 1.5% of the interaction energy.[27] The major difference between CI and CC methods is that CC methods are size consistent and extensive even after truncation, while truncated CI methods are not.[28, 25]

1.4.4 Complete active space methods

Complete active space methods allows one to choose which orbitals will be used to create the electronic configurations, in the same ways as discussed in Section 1.4.2, instead of using truncation to make the method computationally tractable like in the CI and CC methods.[29, 30] Within the 'active space' of chosen orbitals, the full number of configurations is created and treated like FCI. The energy is then minimized by varying the weights of these configurations and the molecular orbital shapes, usually in a self-consistent procedure, leading to the complete active space self consistent field theory (CASSCF) method. The remaining occupied and virtual orbitals that were not chosen to be in the active space are assumed not to play an important role in the calculation as they are either doubly occupied or empty in all configurations.[29] While this method is exponentially scaling in the number of active orbitals and requires quite a bit of knowledge to use correctly, it is accurate in strongly correlated situations such as bond dissociation where other methods often break down, as was discussed in Section 1.4.[25]

1.4.4.1 CASPT2

While the mutli-reference nature of the CASSCF wave function allows for the study of electronic correlation that cannot be captured by a single reference method, known as strong correlation, the lack of inclusion of other electronic configurations outside the active space in its wave function ansatz leads to a lack of dynamic electron correlation.[31, 32] A typical way to correct for this is to add a second-order perturbative correction to CASSCF, known as CASPT2.[32] In this method the zeroth order Hamiltonian is given by

$$\hat{H}_0 = PFP + QFQ \tag{1.18}$$

where F is the Fock operator built from the CASSCF density matrix, P is the projection operator to the CASSCF reference, and $Q = 1 - P$. This form ensures that the CASSCF

wave function is an eigenfunction of $\hat{H}_0$. Due to the nonzero off-diagonal elements in this zeroth order Hamiltonian, an analytical form for the second order energy correction cannot be found, unlike what was discussed in Section 1.4.1. Instead, $|\Psi^{(1)}\rangle$ is found by numerically solving the linear equation in Equation 1.10, with the perturbation still being $\hat{H} - \hat{H}_0$. The resulting set of first order amplitudes can be used to evaluate the second-order energy correction in Equation 1.11.[23]

1.4.5 Regularization

Perturbation theories, including MP2 and CASPT2, have a common "intruder state" issue which is perhaps easiest to see in the second order energy expression shown in Equation 1.12.[33] If the denominator in this expression becomes too close to zero, which often happens when the quality of the zeroth-order model provides a poor description of the system, the terms in the sum become artificially large leading to large errors in the perturbative energy correction. Regularization schemes can be implemented to mitigate this issue, the simplest being to add a constant, called the level shift parameter, to the denominator to bring these tiny energy differences away from zero. In theories like CASPT2, where there is no straightforward denominator, an equivalent regularization scheme can be implemented by shifting the diagonal of the zeroth order Hamiltonian.[34]

While the intruder state effect is clearly detrimental for the energy prediction, it also has a silver lining. If there are many portions of the sum that are large it offers a clear warning that the perturbation likely cannot be considered small and thus the method should not be used. An example of this will be seen in Chapter 3 where these warnings were shown to correspond with the onset of doubly excited character in the electronic excited states of many molecules.

1.4.5.1 Other regularization schemes

There are many other ways to mitigate the issue of intruder states beyond the addition of a level shift as described in the previous section. This level shifting procedure does not discriminate between large and small denominators very well[35] leading to attempts to use an imaginary level shift technique in methods such as CASPT2.[36] The Head-Gordon group has proposed exponential regularization schemes labeled by κ and σ that more selectively changes the weight of the terms in the MP2 energy expression,[37, 38] has also been implemented for CASPT2.[35] An example of a method that instead avoids intruder states via changing the structure of the zeroth-order Hamiltonian is driven similarity renormalization group, in which the Hamiltonian is continuously transformed to energetically separate nearly degenerate states.[39]

1.5 Overview of other existing excited state methods

To place the methods discussed in the body of this thesis in perspective an overview of other methods capable of calculating excited state energies will be given. While there are too many methods to even list here, the next few sections will given a description of some of the more prominent methods in this field.

1.5.1 Time-dependent density functional theory

The most widely used method to compute properties of excited states is time-dependent density functional theory (TD-DFT).[40] The main attraction of this method is its relatively low scaling of between O(N^3) and O(N^5), depending on the choice of functional.[41, 42] It does very well at predicting the energies of valence excitations and has the ability to predict the whole spectrum of singly excited states at once, instead of having to build it state by state.[4] However, TD-DFT faces many challenges. First, it takes quite a bit of expertise to use correctly, as results are sensitive to the choice of exchange-correlation functional so prior knowledge and expertise about the functional and molecules in question is necessary.[5] Second, while our own ESMP2 method also performs poorly for states with significant doubly excited character (see Chapter 3), in ESMP2 the first-order wave function amplitudes provide a warning that this breakdown is occurring. TD-DFT, under the standard approach of the adiabatic approximation, typically has no such warning system, and cannot even predict the existence of doubly excited configurations.[5] The final issue I want to discuss here is TD-DFT's difficulties in predicting the energies of charge transfer states. While range-separated hybrid functionals fix some of the local exchange issues that are otherwise inherent to TD-DFT, large changes in the distribution of electron density can still cause problems.[5] Mid-range charge transfer excitations also still pose a problem, as it is an area that even the range-separated hybrid functionals are not formally well-suited for, as the distance over which their exchange switches to full HF exchange may coincide with the charge transfer distance.[4] ESMP2's relatively black-box set up and suitability for charge transfer states at all ranges, see Chapters 2 and 3, makes it a promising alternative in this area where TD-DFT struggles.

1.5.2 Configuration Interaction

As discussed in Section 1.4.2 for the ground state, linear combinations of Slater determinants with different occupation patterns can also be used to study excited states. The inclusion of excited electronic configurations allows one to approximate (though it would be exact in the FCI limit) the representation of an electronic excited state as a linear combination of these configurations. To model excited states in CI theory, one can simply converge additional low-lying roots to the CI eigenvalue problem via a multi-root Davidson approach or some similar method.[43] However, as was mentioned previously, orbital relaxation can be incredibly important for modeling excited states, which CI does not include, though it

can be added.[44] The theory that comes from the lowest-level truncation of this method, CIS, also neglects almost all electronic correlation,[45] so while it can give a depiction of the excited states of a system, it cannot be expected to be accurate, especially for charge transfer states.[46] One of the reasons it is still used for the starting point of excited state methods is that it is size intensive, meaning that the excitation energies for two systems treated individually are correctly reproduced in a calculation that treats the two systems together, as long as those systems do not interact.[47] This level of truncation also results in a method is also relatively low scaling with a computational complexity of $O(N^4)$.[13] Taking a slightly further step in the truncation to obtain CISD, which increases the scaling to $O(N^6)$, also remove the size intensive property, making CIS the optimal starting point for higher-level excited state methods.[47]

1.5.3 Coupled cluster

1.5.3.1 Equation of motion coupled cluster

Equation of motion coupled cluster methods (EOM-CC) start with the ground state coupled cluster theory and level of truncation, as discussed in Section 1.4.3. The equation of motion approach is a type of linear response theory that can predict the energies and wave functions of excited states and via the linear excitation operator $\hat{\mathcal{R}}$:

$$\hat{\mathcal{R}} = 1 + \sum_{ia} r_i^a a^\dagger i + \frac{1}{4} \sum_{ijab} r_{ij}^{ab} a^\dagger b^\dagger j i + \cdots \tag{1.19}$$

see Section 1.3 for more information on the notation used here. Acting this operator on the ground state coupled cluster wave function effectively allows excitations out of the EOM-CC ground state:

$$|\Psi_{EOM}\rangle = \hat{\mathcal{R}} e^T |RHF\rangle \tag{1.20}$$

where T is the cluster operator defined in Section 1.4.3. While EOM-CC methods can be truncated to any level, similarly to their ground state counterparts EOM-CCSD and EOM-CCSD(T) are particularly widely used.[15, 48] However, EOM-CCSD and EOM-CCSD(T) are $O(N^6)$ and $O(N^7)$ scaling methods, respectively, making them too computationally expensive for large systems.[25] EOM-CC methods also only have a limited ability to include orbital relaxations,[49] which can be incredibly important for some excitations, especially charge transfer and core excitations.[50]

1.5.3.2 Approximate coupled cluster methods

Second-order approximate singles and doubles coupled cluster theory (CC2) and its extension to triples (CC3) can also be used to study the excited states of molecules. One obtains these methods by starting with the ground state coupled cluster theory truncated to the same level. For example, for CC2, one can start by looking at the CCSD energy expression:

$$E = \langle \psi | \hat{H} \exp \left[\hat{T}_1 + \hat{T}_2 \right] | \psi \rangle \tag{1.21}$$

The amplitudes for $\hat{T}_1$ and $\hat{T}_2$ can be gained from the equations

$$\langle k_1| \hat{H} + \left[\hat{H}, \hat{T}_2\right] |\psi\rangle = 0 \tag{1.22}$$

$$\langle k_2| \hat{H} + \left[\hat{H}, \hat{T}_2\right] + \frac{1}{2}\left[\left[\hat{H}, \hat{T}_2\right], \hat{T}_2\right] |\psi\rangle = 0 \tag{1.23}$$

where k_1 and k_2 represent the single and double excitation manifolds, respectively. If instead the doubles are approximated

$$\langle k_2| \left[\hat{F}, \hat{T}_2\right] + \hat{H} |\psi\rangle \tag{1.24}$$

where $\hat{F}$ is a Fock matrix, but the singles are still treated fully, the formulation for CC2 is obtained, which due to the lack of the last term in Equation 1.23, is O(N^5) scaling.[51] The formulation of CC3 is similar, only the singles and doubles are treated fully, while the triples are further approximated compared to CCSDT.[52] The linear response excited state incarnations of these methods are lower-scaling than their EOM counterparts,[51] however they still only treat orbital relaxations approximately, CC2 still does not reach chemical accuracy for many excited states, and CC3, while fairly accurate, scales as O(N^7), making it intractable for larger systems.[15]

1.6 Excited state-specific hierarchy of wave function methods

One of the overarching goals of the research being done in the Neuscamman group is to create a hierarchy of excited-state-specific correlation methods analogous to the ground state methods described in Section 1.3. While members of the group are actively working on excited state versions of coupled cluster theory[53] and complete active space methods[54, 55, 56], the work in this thesis is focused on the second rung of the hierarchy, namely an excited-state-specific version of second-order Møller-Plesset perturbation theory (ESMP2). Thus, only ESMP2 and it's reference method, excited state mean field theory (ESMF), will be discussed in detail.

1.6.1 Excited state mean field theory

ESMF is the lowest rung on this excited state hierarchy of methods and parallels Hartree Fock in many ways.[57, 58] First, while the ESMF wave function is a bit more complicated than Hartree Fock,

$$|ESMF\rangle = |\Phi\rangle = e^{\hat{X}} \left(c_0 |\psi\rangle + \sum_{ia} c_i^a |_i^a\rangle + \sum_{\bar{i}\bar{a}} c_{\bar{i}}^{\bar{a}} |_{\bar{i}}^{\bar{a}}\rangle \right) \tag{1.25}$$

where the absence/presence of bars on top of the orbital indices is used to denote spin up/down, this wave function, like Hartree Fock, defines a mean field theory that leads to

an effective one-electron equation.[58] In a sense, it is also minimally correlated similar to Hartree Fock: in Hartree Fock that minimum amount of correlation within the spatial distribution of electrons comes from enforcing the Pauli exclusion principle, in ESMF the only additional correlations are open-shell-singlet recoupling correlation and the correlation from the superposition of the different singly excited configurations. As these are both crucial for describing the qualitative structure of singly excited states they are necessarily included in the ESMF wave function ansatz, but further correlations are not in order to keep the theory as close to a mean-field approximation as possible. Second, the ESMF solutions are energy stationary points corresponding to specific electronic excited states, just as the Hartree Fock solution is the energy stationary point corresponding to the ground state. As mentioned in Section 1.4, Hartree Fock converges to the ground state by making use of the variational principle and a self-consistent procedure. ESMF states can be converged to via a similar self consistent method [58] or via the use of a generalized variational principle [59] that allows one to target a specific excited sate using approximate excitation energies, Mulliken populations, and several other state-specific properties. The exponential term multiplying the CIS wave function allows for orbital relaxation via the X operator,

$$\hat{X} = \sum_{p<q} X_{pq} \left(p^\dagger q - q^\dagger p \right) \tag{1.26}$$

which allows for a more accurate representation of an excited state as the movement of electron density in a system will naturally induce a relaxation of molecular orbital shapes. Whether by a self-consistent iteration or the generalized variational principle, the ESMF solution is found by making the ESMF energy stationary with respect to the CI coefficients c and the orbital rotation parameters X_{pq}.

Using this wave function ansatz provides a state-specific energy and wave function that provides a good *qualitative* characterization of the targeted excited state, provided the state has singly excited character. Like with Hartree Fock, correction schemes will need to be used on top of these results to gain quantitatively accurate information.

1.6.2 Second-order excited state Møller-Plesset perturbation theory (ESMP2)

An example for such a correction is ESMP2, which – just as ESMF was designed to have strong parallels to HF – was purposefully designed to be very similar in formulation to MP2 theory.[57] The derivation of ESMP2 starts with finding a zeroth operator, $\hat{H}_0$ for which the ESMF state is an eigenfunction. The perturbation is then defined as the difference between the full Hamiltonian, $\hat{H}$, and $\hat{H}_0$. $\hat{H}_0$ has a slightly more complex form than the ground state Fock operator, but still gives the property that the zeroth order energy obtained from this operator, $E^{(0)}$, needs to be added to the first order energy correction, $E^{(1)}$, to obtain the ESMF energy, just like is the case for the Hartree Fock. The zeroth order operator for

the perturbation theory, denoted H_0, can be written as

$$\hat{H}_0 = \hat{R}\left(\hat{F} - \hat{H}\right)\hat{R} + \hat{P}\hat{H}\hat{P} + \hat{Q}\hat{F}\hat{Q} \tag{1.27}$$

where $\hat{F}$ is the Fock operator built from the ESMF one-body density matrix, $\hat{R} = |\Phi\rangle\langle\Phi|$, $\hat{P}$ is the projector to the space spanned by the aufbau and singly excited configurations in the ESMF orbital basis, and $\hat{Q} = 1 - \hat{P}$.[57] This choice of zeroth-order operator also preserves the property that

$$\hat{H}_0|\Phi\rangle = E_0|\Phi\rangle = \langle\Phi|\hat{F}|\Phi\rangle|\Phi\rangle \tag{1.28}$$

in the same way as CASPT2, as discussed in Section 1.4.4.1. Also like CASPT2, it is important to point out that while the HF Fock matrix formed from the Hartree Fock one-body density matrix is diagonal, the ESMF Fock matrix is not, meaning that an analytical form for the second order energy correction, like that shown in Equation 1.12, is not possible for the excited state case. This means that the first order wave function must be found using Equation 1.10 in order to substitute it into Equation 1.11, as is the same for CASPT2. However, unlike CASPT2,[23] the choice of zeroth order Hamiltonian in ESMP2 leads to rigorously size intensive excitation energies.[57, 11]

The first order correction to the wave function in ESMP2 can be written as a linear combination of configurations of the arrangement of electrons in the ESMF orbitals, similar to the expansion shown in Equation 1.13:

$$|\Psi^{(1)}\rangle = \sum_{ijab} t_{ij}^{ab}|\psi_{ij}^{ab}\rangle + \sum_{ijkabc} t_{ijk}^{abc}|\psi_{ijk}^{abc}\rangle + \ldots \tag{1.29}$$

Note that the coefficients have been labeled with t's to purposefully distinguish them from the expansion coefficients in the ESMF wave function, which are optimized during the ESMF procedure. The aufbau state and singly excited configurations formed from the ESMF molecular orbitals are not part of this expansion since those contributions are included in the zeroth order (ESMF) wave function. However, like with coupled cluster and configuration interaction methods, this wave function must be truncated in order to create a computationally tractable method. Fortunately, a natural truncation to include only the doubles and triples configurations occurs due to the nature of the operators in the zeroth order and full Hamiltonians. The zeroth order Hamiltonian is a one-electron operator while the full Hamiltonian is at most a two-electron operator, so solving the first order amplitude equations in Equation 1.10 will only give nonzero amplitudes for the doubles and triples. However, a straightforward implementation of the method results in an $O(N^7)$ scaling method[57] due to the manipulations that would need to be done on the triples pieces of the first-order correction to the wave function. Chapter 2 describes how the theory can be slightly modified to reduce the computational complexity of the method to match that of the ground state MP2 without significantly affecting the results. Chapter 3 then establishes the accuracy of this approach through a study of its performance in predicting the energies of electronic excitations in a collection of organic compounds.

1.7 Outline

This thesis is the culmination of work on the first wave-function-based rung in this hierarchy beyond mean field theory: fully excited-state-specific second-order perturbation theory.

Chapter 2 details how the original ESMP2 method can be reformulated to reduce the computational complexity of the method to O(N^5) to match that of MP2. This work has been published in the article "An N^5-scaling excited-state-specific perturbation theory" *J. Chem. Theory Comput.* 16, 6132 (2020).

Chapter 3 shows the accuracy of this approach in comparison to other *ab intio* methods on a large set of electronic excitations in various types of organic molecules. This work has been accepted for publication in *J. Chem. Phys.* under the title "Studying excited-state-specific perturbation theory on the Thiel set." Finally, Chapter 4 summarizes the impacts of and work done on this state-specific perturbative method.

Chapter 2

An N^5-scaling excited-state-specific perturbation theory

2.1 Abstract

We show that by working in a basis similar to that of the natural transition orbitals and using a modified zeroth order Hamiltonian, the cost of a recently-introduced perturbative correction to excited state mean field theory can be reduced from seventh to fifth order in the system size. The $(\text{occupied})^2(\text{virtual})^3$ asymptotic scaling matches that of ground state second order Møller-Plesset theory, but with a significantly higher prefactor because the bottleneck is iterative: it appears in the Krylov-subspace-based solution of the linear equation that yields the first order wave function. Here we discuss the details of the modified zeroth order Hamiltonian we use to reduce the cost as well as the automatic code generation process we used to derive and verify the cost scaling of the different terms. Overall, we find that our modifications have little impact on the method's accuracy, which remains competitive with singles and doubles equation-of-motion coupled cluster.

2.2 Introduction

Although mean field methods like Hartree-Fock (HF) theory often succeed in making qualitatively correct predictions about how electrons distribute themselves within a molecule, making quantitative energetic predictions at the precision necessary to aid in designing and interpreting experiments usually requires grappling with the finer-grained wave function details that arise from electron correlation. In many contexts, especially when considering ground states in closed-shell molecules, density functional theory (DFT) fills this role at a relatively low computational expense. However, even in these DFT-friendly systems, there are areas – such as the treatment of weak intermolecular interactions [60] – where more expensive wave-function-based methods remain essential to, for example, help choose which empirical functional to trust. In electronically excited states, open-shell character is the

norm, and in practice DFT faces serious challenges and is less predictive than in ground states. These challenges include both the inability of time-dependent DFT (TD-DFT) to relax the shapes of orbitals not directly involved in the excitation [61, 62, 63] and the tendency of self-consistent DFT, as used for example in the restricted open-shell Kohn Sham (ROKS) [64, 65] method, to over-delocalize [66, 67] unpaired electrons or holes. Although the latter issue can be mitigated by using hybrid and range-separated functionals, [68] it nonetheless persists. [69] If wave-function-based methods are to help make up for DFT's difficulties in this area, it is highly desirable that they overcome these challenges while retaining electron correlation corrections that are as computationally affordable as possible. In this study, we take a step in this direction by reformulating a second-order perturbative correction to excited state mean field (ESMF) theory [57, 59, 69] so that its asymptotic cost scaling can reach parity with its ground state counterpart.

In the world of closed-shell ground states, the simplest and usually the most affordable approach to electron correlation aside from DFT is second-order Møller-Plesset perturbation theory (MP2). [70] In a canonical implementation, the asymptotic scaling of this method is $N_o^2 N_v^3$, where N_o and N_v denote the number of occupied and virtual orbitals in the HF reference, respectively. [71] Note that, for simplicity, we will throughout this paper consider N_v to be interchangeable with N, the total number of molecular orbitals, when discussing asymptotic scaling. Although significantly higher than the cost scaling of many widely used density functionals, the cost of MP2 is significantly lower than the sixth-order cost of coupled cluster theory with singles and doubles (CCSD), positioning it as the least expensive wave-function-based ground state correlation method in wide use. The excited-state-specific ESMP2 theory [57] that we focus on in this study was designed to closely mirror MP2 theory, correcting ESMF in the same way that MP2 corrects HF, achieving rigorous size intensivity, and working in an uncontracted first order interacting space. Unfortunately, the fact that the ESMF reference already contains single excitations means that this interacting space now includes both the doubles and triples excitations. Acting the zeroth order Hamiltonian in this space thus involves contracting a two-index Fock operator with a six-index amplitude tensor, leading to seventh order scaling with the system size and a theory that is decidedly less practical than the ground state theory that it seeks to mimic.

To overcome this difficulty, we exploit the fact that a wave function that is a linear combination of singles excitations, such as configuration interaction singles (CIS), can be written as a sum of just N_o configuration state functions (CSFs) under a particular occupied-occupied and virtual-virtual rotation of the orbital basis. Working in this basis — which for CIS itself is the natural transition orbital basis [72] but for ESMF will be slightly different due to its excited-state-specific orbital relaxations — the coulomb operator no longer connects the singly excited reference function to the whole triples space. Separating the triples in to those that connect with the reference and those that do not, one expects the unconnected triples (which are by far the larger group) to be less important, and so a more aggressive approximation of the zeroth order Hamiltonian in that space is somewhat justified. In particular, we will approximate the Fock operator in the unconnected space by its diagonal (note that, unlike for a HF reference, the Fock operator derived from the ESMF one-body density matrix

is not diagonal) at which point the unconnected triples no longer contribute to the theory at all, as they have no direct connection to the reference through the coulomb operator and no connection to the first order wave function through the zeroth order Hamiltonian. As we will discuss, this step immediately drops the scaling to sixth order. To drop the scaling further, we note that, in the vast majority of low-lying excitations in weakly correlated molecules, only a small number out of the N_o singly excited CSFs in the ESMF reference are expected to have large coefficients. By extending the diagonal approximation of the zeroth order Hamiltonian into the space of all triples that only connect to small parts of the reference, a reduction to $N_o^2 N_v^3$ cost scaling is achieved. Again, as these triples are less important, this approximation is not expected to make much difference, and indeed this expectation is confirmed by a comparison to results from the seventh-order parent method. Thus, by working in a particular orbital basis and slightly modifying the zeroth order Hamiltonian, the cost scaling of ESMP2 can be brought in line with that of MP2, even if the prefactor remains higher due to the off-diagonal zeroth order Hamiltonian and thus a need to iteratively solve a linear equation.

Although ESMP2, in either its original or its more efficient form, is similar to a number of other excited state perturbation theories, it also possesses important differences. When compared to CIS(D), which uses the HF orbitals and derives its triples amplitudes from the ground state MP2 doubles, [73] ESMP2 is instead wholly excited-state-specific: the orbitals are relaxed variationally for the excited state at the ESMF level, and the triples are derived via the excited state's first order wave function equation. In comparison to the recently-introduced driven similarity renormalization group VCIS-DSRG-PT2 approach, [74] ESMP2 again enjoys orbitals that are relaxed for the excited state, and it does not require the choice of an active space, making it easier to apply in a black-box manner. Finally, in contrast with complete active space second order perturbation theory (CASPT2), [75, 76] N-electron valence perturbation theory (NEVPT2), [77] and VCIS-DSRG-PT2, ESMP2 sticks to an uncontracted and thus orthonormal first order interacting space, which circumvents the need to address the potential for linear dependencies. That said, ESMP2 has much in common with CASPT2, and as we will see in the results, often hews rather closely to CASPT2 when it comes to predicting excitation energies. Again, ESMP2 achieves this without using an active space, which offers significant simplicity at the cost of being inappropriate for strongly correlated systems.

This paper is organized as follows. We begin by discussing the ESMF reference and how it can be simplified by working in a particular orbital basis, after which we discuss the first order wave function and the newly-modified zeroth order Hamiltonian. We then briefly discuss the automated approach we employ for term derivation and code generation, which allows us to make a detailed investigation of each term's scaling, the outcomes of which we present in the first subsection of the results. We then delve into the method's accuracy, first in a set of small molecules that are mostly single-CSF in character and then in a collection of ring excitations, in which multi-CSF character is more prevalent. We end our results section with an explicit test of size intensivity before concluding with a summary and a brief discussion of possible future directions.

2.3 Theory

To simplify our implementation, we have chosen to work with a slightly simplified version of the ESMF ansatz

$$|\Psi_0\rangle = e^{\hat{X}} \sum_{ia} C_{ia} \left(\hat{a}^+_{a\uparrow} \hat{a}_{i\uparrow} \pm \hat{a}^+_{a\downarrow} \hat{a}_{i\downarrow} \right) |\Phi\rangle \tag{2.1}$$

in which we have set the coefficient on the un-excited closed-shell reference determinant $|\Phi\rangle$ to zero. This simplification avoids a significant number of terms in the perturbation theory, but it does mean that we are assuming that the closed shell determinant is unimportant in the excited state, which is not universally true. Here the $\pm$ sign is plus (minus) for singlet (triplet) states, $\boldsymbol{C}$ is the matrix of single-excitation configuration interaction (CI) coefficients, $\hat{X}$ is an anti-Hermitian one-electron operator responsible for excited-state-specific orbital relaxations, and we adopt the convention of referring to occupied and unoccupied (virtual) orbitals in $|\Phi\rangle$ by the indices i,j,k,l and a,b,c,d, respectively. After relaxing $\hat{X}$ and $\boldsymbol{C}$ to find the energy stationary point corresponding to the excited state in question (which may for example proceed by guessing the CIS wave function and applying a generalized variational principle [59]), we take a singular value decomposition of the rectangular matrix $\boldsymbol{C}$

$$\boldsymbol{C} = \boldsymbol{U} \boldsymbol{\Lambda} \boldsymbol{V}^+ \tag{2.2}$$

where, if we assume that there are more virtual than occupied orbitals, $\boldsymbol{\Lambda}$ is the $N_o \times N_o$ diagonal matrix of singular values. Now, note that the Hamiltonian can be transformed into an orbital basis that eliminates $\boldsymbol{U}$ and $\boldsymbol{V}$ and thus renders the reference wave function in a particularly simple form.

$$\hat{H}^{\mathrm{HF}} \rightarrow\ e^{-\hat{Z}} e^{-\hat{Y}} e^{-\hat{X}} \hat{H}^{\mathrm{HF}} e^{\hat{X}} e^{\hat{Y}} e^{\hat{Z}} \tag{2.3}$$

Here we have started in the HF orbital basis (as indicated by the Hamiltonian $\hat{H}^{\mathrm{HF}}$), rotated via $\hat{X}$ into the ESMF orbital basis, and then rotated via the one-electron anti-Hermitian operators $\hat{Y}$ and $\hat{Z}$, which perform occupied-occupied and virtual-virtual rotations, respectively. The $\hat{Y}$ rotation can be chosen so as to eliminate $\boldsymbol{U}$, and likewise the $\hat{Z}$ rotation can be used to eliminate $\boldsymbol{V}$, leaving us with a greatly simplified CI expansion

$$|\Psi_0\rangle\ \rightarrow\ \sum_{i} \Lambda_{ii} \left(\hat{\sigma}^+_{i\uparrow} \hat{\tau}_{i\uparrow} \pm \hat{\sigma}^+_{i\downarrow} \hat{\tau}_{i\downarrow} \right) |\Phi\rangle \tag{2.4}$$

involving a sum over the singular values of $\boldsymbol{C}$. The corresponding virtual-orbital creation operators $\hat{\sigma}^+$ and occupied-orbital destruction operators $\hat{\tau}$ now come in pairs, one for each occupied orbital. We refer to each of these pairs as a transition orbital pair (TOP), and note that, if the optimal ESMF orbitals were the same as the RHF orbitals, the TOPs would be equivalent to the natural transition orbital (NTO) pairs. [72] It is important to emphasize that Eqs. (2.1) and (2.4) refer to exactly the same zeroth order wave function, they simply express it in different orbital bases. We now turn to the definition of our first order wave function, where the TOP basis will allow for useful groupings of the triples excitations into separate categories that we will exploit in order to achieve a lower asymptotic cost scaling.

2.3.1 First Order Wave Function

To begin, let us specify the language we will use for describing excitations as well as the the different orbital labels that we employ when working in the TOP orbital basis. First, throughout this paper, we will refer to excitation levels relative to the closed shell. In this language, our reference is a superposition of single excitations, and our first-order interacting space consists of double and triple excitations. As for how we label orbitals, let us adopt an orbital ordering in which the spatial orbitals are numbered 1 through N. In addition to the occupied orbitals with destruction operators $\hat{\tau}_i$ (with i allowed to range from 1 through N_o) and the corresponding TOP virtual orbitals whose creation operators are $\hat{\sigma}_a^+$ (with a allowed to range from $N_o + 1$ through $2N_o$), there are additional virtual orbitals (AVOs), whose creation operators we will denote by $\hat{\nu}_a^+$ (with a allowed to range from $2N_o + 1$ through N). When necessary, we will denote virtual orbitals that may be either TOP virtuals or AVOs using the creation operators $\hat{w}_a^+$, where a can range from $N_o + 1$ through N. Finally, when we denote a TOP virtual orbital using an occupied index, as for example in the operator $\hat{\sigma}_{i\uparrow}^+$ in Eq. (2.4), this implies the TOP virtual orbital with index $a = i + N_o$ that is the partner of the ith occupied orbital in the TOP orbital basis representation of $|\Psi_0\rangle$.

With these orbital definitions in hand and working in the TOP orbital basis, we now point out that while the Hamiltonian, through its two-electron part, can connect the singly-excited wave function $|\Psi_0\rangle$ to the full space of doubly excited determinants, it only connects $|\Psi_0\rangle$ to a subset of the triply excited determinants. In particular, the matrix element

$$H_{ijk}^{abc} = \langle\Psi_0|\, \hat{\tau}_k^+ \hat{\tau}_j^+ \hat{\tau}_i^+ \hat{w}_a \hat{w}_b \hat{w}_c \hat{H}\, |\Psi_0\rangle \tag{2.5}$$

will only be nonzero if there is at least one TOP amongst the occupied and virtual orbitals i,j,k,a,b,c. Put another way, this matrix element is zero if $d \neq l + N_o$ for all $d \in \{a, b, c\}$ and $l \in \{i, j, k\}$, as a nonzero element is only possible if one of the three excitations was already present in $|\Psi_0\rangle$, and $|\Psi_0\rangle$ only contains TOP excitations. In contrast, this matrix element can be nonzero if $d = l + N_o$ for at least one d,l pair from $d \in \{a, b, c\}$ and $l \in \{i, j, k\}$. Thus,

in our first order wave function

$$\begin{aligned}
|\Psi_1\rangle = & \sum_{ijab} T_{ij}^{ab} \hat{w}_{a\uparrow}^{+} \hat{w}_{b\uparrow}^{+} \hat{\tau}_{j\uparrow} \hat{\tau}_{i\uparrow} |\Phi\rangle \\
& + \sum_{ijab} T_{ij}^{ab} \hat{w}_{a\downarrow}^{+} \hat{w}_{b\downarrow}^{+} \hat{\tau}_{j\downarrow} \hat{\tau}_{i\downarrow} |\Phi\rangle \\
& + \sum_{ijab} S_{ij}^{ab} \hat{w}_{a\uparrow}^{+} \hat{w}_{b\downarrow}^{+} \hat{\tau}_{j\downarrow} \hat{\tau}_{i\uparrow} |\Phi\rangle \\
& + \sum_{ijkabc} T_{ijk}^{abc} \hat{w}_{a\uparrow}^{+} \hat{w}_{b\uparrow}^{+} \hat{w}_{c\uparrow}^{+} \hat{\tau}_{k\uparrow} \hat{\tau}_{j\uparrow} \hat{\tau}_{i\uparrow} |\Phi\rangle \\
& + \sum_{ijkabc} T_{ijk}^{abc} \hat{w}_{a\downarrow}^{+} \hat{w}_{b\downarrow}^{+} \hat{w}_{c\downarrow}^{+} \hat{\tau}_{k\downarrow} \hat{\tau}_{j\downarrow} \hat{\tau}_{i\downarrow} |\Phi\rangle \\
& + \sum_{ijkabc} S_{ijk}^{abc} \hat{w}_{a\uparrow}^{+} \hat{w}_{b\downarrow}^{+} \hat{w}_{c\downarrow}^{+} \hat{\tau}_{k\downarrow} \hat{\tau}_{j\downarrow} \hat{\tau}_{i\uparrow} |\Phi\rangle \\
& + \sum_{ijkabc} S_{ijk}^{abc} \hat{w}_{a\downarrow}^{+} \hat{w}_{b\uparrow}^{+} \hat{w}_{c\uparrow}^{+} \hat{\tau}_{k\uparrow} \hat{\tau}_{j\uparrow} \hat{\tau}_{i\downarrow} |\Phi\rangle
\end{aligned} \tag{2.6}$$

we set to zero the values of all same-spin (T_{ijk}^{abc}) and mixed-spin (S_{ijk}^{abc}) triples coefficients whose indices do not contain at least one TOP. As we will choose our zeroth order Hamiltonian to be diagonal in the space of triples excitations that contain no TOPs (which we define as the N-triples space), setting these coefficients to zero is not an approximation, but merely the natural consequence of their Eq. (2.5) matrix elements being zero and $\hat{H}_0$ not connecting them to any other parts of $|\Psi_1\rangle$. Instead, the new approximation, and the key difference from our previous N^7-scaling excited-state-specific perturbation theory, [57] comes in the definition of $\hat{H}_0$, to which we now turn our attention.

2.3.2 Zeroth Order Hamiltonian

In our previous N^7-scaling version of the theory, we chose the zeroth order Hamiltonian to have the following form.

$$\hat{H}_0 = \hat{R}(\hat{F} - \hat{H})\hat{R} + \hat{P}\hat{H}\hat{P} + \hat{Q}\hat{F}\hat{Q} \tag{2.7}$$

Here, we will retain this form, but make some modifications in the triples space to improve efficiency. As before, we take $\hat{F}$ to be the Fock operator constructed from the one-body density matrix of $|\Psi_0\rangle$, $\hat{R} = |\Psi_0\rangle \langle\Psi_0|$ to be the projector on to the zeroth order wave function, $\hat{P}$ to be the projector on to the span of the closed shell determinant $|\Phi\rangle$ and all singly excited determinants, and $\hat{Q} = 1 - \hat{P}$. The difference between the present theory and our previous approach is that, in the present theory, we work in the TOP orbital basis and modify the $\hat{Q}\hat{F}\hat{Q}$ term so that it is diagonal in some parts of the triples space. To see how, let us first organize the triply excited determinants into three groups: the N-triples whose

six indices i,j,k,a,b,c do not contain any TOPs, the L-triples that contain at least one TOP whose singular value from Eq. (2.4) is large (above a threshold η), and the S-triples that contain at least one TOP but whose TOPs all have small singular values (below η). With the triples organized into these three groups, we make the modification

$$\begin{aligned}\hat{Q}\hat{F}\hat{Q} \;\rightarrow\; & \left(\hat{Q}_{\mathrm{D}} + \hat{Q}_{\mathrm{L}}\right) \hat{F} \left(\hat{Q}_{\mathrm{D}} + \hat{Q}_{\mathrm{L}}\right) \\ & + \;\left(\hat{Q}_{\mathrm{S}} + \hat{Q}_{\mathrm{N}}\right) \hat{F}^{(\mathrm{diag})} \left(\hat{Q}_{\mathrm{S}} + \hat{Q}_{\mathrm{N}}\right) \end{aligned} \tag{2.8}$$

in which $\hat{F}^{(\mathrm{diag})}$ is the Fock operator with its off-diagonal terms set to zero and $\hat{Q}_{\mathrm{D}}$, $\hat{Q}_{\mathrm{L}}$, $\hat{Q}_{\mathrm{S}}$, and $\hat{Q}_{\mathrm{N}}$ project on to the doubles, the L-triples, the S-triples, and the N-triples, respectively. As shown in Figure 2.1, we are making $\hat{H}_0$ diagonal for the presumably less important S-triples and N-triples, whereas our previous approach left it off-diagonal for all triples.

How much efficiency is gained by this approach depends on how one chooses to divide the TOP-containing triples between the large and small L-triples and S-triples spaces. In the $\eta = 0$ extreme, in which all the TOP-containing triples are placed in the L-triples space, the cost of forming the right-hand-side of and solving the usual Rayleigh-Shrödinger linear equation for $|\Psi_1\rangle$ grows as N^6. The reduction from the N^7 scaling of our previous approach comes from eliminating the N-triples, which as discussed in Section 2.3.1 have no Eq. (2.5) matrix elements and thus can only contribute to the theory by coupling through $\hat{H}_0$ to other parts of $|\Psi_1\rangle$, which is prevented by our modification in Eq. (2.8). In the other extreme, when only triples that contain the TOP with the largest singular value are placed in the L-triples space and all other TOP-containing triples are placed in the S-triples space, the cost of setting up and solving the linear equation for $|\Psi_1\rangle$ grows as only N^5. Note that, as we explain in Section 2.4.2, we have explicitly verified these scalings (the lower of which is actually $N_o^2 N_v^3$) by log-log regressions on the floating-point operation counts of each individual term entering in to the setup and iterative solution of the linear equation.

To put these extremes in to perspective, we note that for a size-intensive excitation, by which we mean one whose spatial extent does not grow indefinitely as the system is enlarged, the number of non-zero singular values in Eq. (2.4) will be constant with system size in the large system limit. This implies that for size-intensive excitations, setting η to a small but non-zero threshold will result in both a size-intensive excitation energy (a property we verify explicitly below) and N^5 scaling. Note that this efficiency gain is *not* due to assuming anything about the locality of electron correlation (which if exploited as in some ground state methods [78] could perhaps further lower the method's scaling) but instead comes from the natural tendency of molecular excitations to be localized. Of course, in practice, the length scale needed to see this benefit may be much larger than the simulation in a particular system, so let us make a more concrete statement about the scaling. If one limits $|\Psi_0\rangle$ to have only N_{TOP} nonzero singular values regardless of the system size, then the method has an N^5 scaling. The obvious practical case where this approach should be useful is for excitations that are dominated by a single configuration state function (CSF), and thus for which only one singular value is nonzero anyways.

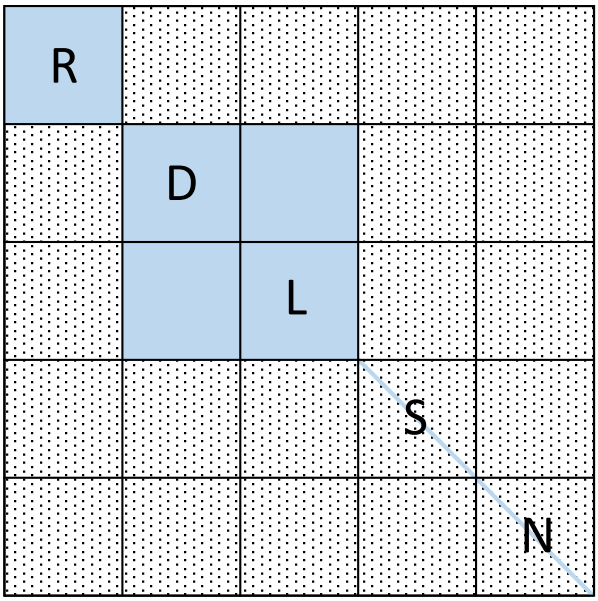

Figure 2.1: Block structure of the zeroth order Hamiltonian. The matrix is zero in the dotted regions and non-zero in the blue regions, including on the diagonal of blocks S and N. The blocks are labeled as R for $|\Psi_0\rangle$, D for double excitations, L for triple excitations containing at least one TOP with a large singular value, S for all other triple excitations containing at least one TOP, and N for the triple excitations that contain no TOPs. Note that no singly excited states are included in our first-order interacting space, on the theory that the effects of these states have already been included by the variational optimization of the reference.

2.3.3 Automated Implementation

For the construction and solution of the linear equation for $|\Psi_1\rangle$, we have written a simple for-loop generator. The approach is to start with a symbolic representation of the for-loops belonging to each orbital index, and then to use Wick's theorem to derive the different contraction schemes that connect indices and thus eliminate for-loops via the resulting Kronecker delta functions. This entire process is automated and includes the detailed logic needed to a) identify which triples reside in the L-triples space and thus must be included in the iterative solution of the linear equation (triples in the S and N spaces are not part of the iterative solver, as their part of the linear equation is diagonal and can be inverted directly) and b) avoid double counting redundant terms, such as T_{ijk}^{abc} and T_{jik}^{bac}. Of course, the result is a code build of "dumb" loops, which will not be cache-optimal, but does provide us with a correct reference implementation to start from. Further, it allows us to automatically implement careful operation counting, such that each contraction can have its cost scaling analyzed independently. Having thus identified the most expensive term (which turns out to be a contraction between the mixed-spin-L-triples and the Fock operator) we have verified that

by hand-coding this term in terms of dense linear algebra, the cost can be reduced by more than an order of magnitude. In future, we will work to convert all other contractions whose cost is not trivial into dense linear algebra. In the present study, however, our focus is not on a production-level code, but instead on completing a detailed analysis of the cost-scaling as well as the accuracy of the new N^5 approach.

For an example of how the code generation works, consider how the Fock operator might map double excitation coefficients to L-triples excitation coefficients in the case where all orbitals are spin up. The corresponding tensor contractions come from the different ways of contracting the indices in

$$\sum_{pq} \sum_{i'j'a'b'} F_{pq} T_{i'j'}^{a'b'} \left\langle \Phi \right| \hat{\tau}_k^+ \hat{\tau}_i^+ \hat{\tau}_j^+ \hat{w}_b \hat{w}_a \hat{\sigma}_c \hat{a}_p^+ \hat{a}_q \hat{w}_{a'}^+ \hat{w}_{b'}^+ \hat{\tau}_{j'} \hat{\tau}_{i'} \left| \Phi \right\rangle , \tag{2.9}$$

where the L-triple's indices are i,j,k,a,b,c and we assume, without loss of generality, that c and k form a TOP such that $c = k + N_o$ (at least one TOP must be present as this is an L-triple). The automatically generated code for one of the contractions resulting from Eq. (2.9) is seen in Figure 2.2, where we see explicitly in the second line of code the simplification and lower scaling that comes if we fix the number N_{TOP} of large TOPs. This particular term has $N_o^2 N_v^2$ scaling if the number of large-singular-value TOPs is fixed, or $N_o^3 N_v^2$ if it grows with system size (e.g. if all TOPs are considered large). Across all the different pieces needed to construct the linear equation's right-hand-side and to operate by $\hat{H}_0$, the automated generator found 185 contractions with non-zero contributions. When N_{TOP} is set to one, only 18 of the contractions involving triples showed fifth-order cost-scaling, and only 9 of those showed the most expensive $N_o^2 N_v^3$ scaling, suggesting that converting the worst terms to hand-coded dense linear algebra (i.e. BLAS) should be feasible in future work. See section 2.4.2 below for a more detailed cost scaling analysis.

2.4 Results

2.4.1 Computational Details

For ESMP2, we used the iterative conjugate-gradient algorithm to solve the linear equation for $|\Psi_1\rangle$. The EOM-CCSD and δ-CR-EOM-CC(2,3) [79, 80, 81, 82] calculations were performed with GAMESS,[83, 84] whereas CIS and TDDFT calculations were performed with QChem. [85] CASPT2 calculations for the ring excitations were performed with Molpro. [86, 87, 88] Note that, although some CASPT2 calculations relied on state-averaged CASSCF reference functions, the CASPT2 calculations themselves were single-state. In the pyrrole molecule, CASSCF was performed with a (10o,6e) active space, in which an equal-weight 4-state state-average was employed, with 2, 1, and 1 states from the A_1, A_2, and B_2 representations, respectively. Note that pyrrole's 2^1A_1 excitation was not stable in CASPT2 without a level shift, and so in this molecule a level shift of 0.2 E_h was used for all states. In the rest of the ring excitations, CASPT2 was stable without a level shift, and so no shift was

```
for ( int k = 0; k < nocc; k++ ) {
  if ( k >= ntop ) continue;
  const int c = (k+nocc);
  for ( int i = 0; i < nocc; i++ ) {
    if ( i == k ) continue;
    for ( int j = i+1; j < nocc; j++ ) {
      if ( j == k ) continue;
      for ( int a = nocc; a < norb; a++ ) {
        if ( a == c ) continue;
        if ( a == i + nocc && i <= k ) continue;
        if ( a == j + nocc && j <= k ) continue;
        for ( int b = a+1; b < norb; b++ ) {
          if ( b == c ) continue;
          if ( b == i + nocc && i <= k ) continue;
          if ( b == j + nocc && j <= k ) continue;
          const int ip = i;
          if ( ip >= nocc ) continue;
          const int jp = j;
          if ( jp <  ip+1 ) continue;
          if ( jp >= nocc ) continue;
          const int ap = a;
          if ( ap <  nocc ) continue;
          const int bp = b;
          if ( bp <  ap+1 ) continue;
          const int p = c;
          const int q = k;
          out(k,i,j,a,b) += fm(p,q) * in(ip,jp,ap,bp);
} } } } }
```

Figure 2.2: The generated code for the $\delta_{aa'}\delta_{bb'}\delta_{ii'}\delta_{jj'}\delta_{kq}\delta_{cp}$ contraction resulting from Eq. (2.9). Note the second line, where the scaling is explicitly reduced if the number N_{TOP} of TOPs that are considered large does not grow with system size.

used in other molecules. For pyridine, CASSCF employed an (8o,10e) active space and four separate state averaging calculations, one in each representation of its C_{2v} point group. No level shift was necessary for stability in pyridine, but each of these four calculations used an equal-weight 3-state state average, which was necessitated by the fact that at the CASSCF level the 1^1B_2 and 2^1B_2 states come first and third in the energy ordering of the $^1B_2$ states. For benzene, CASSCF employed a (6o,6e) active space for an equal-weight 6-state state-average with two states each in the A_g, B_{1u}, and B_{2u} representations (the computational point group was D_{2h}). Finally, for pyrimidine, CASSCF employed an (8o,10e) active space. As all the states investigated in pyrimidine are ground states within their own symmetries, state averaging was not used in this case.

2.4.2 Cost Scaling Analysis

Before looking at the energetic accuracy of reduced-scaling ESMP2, let us first inspect how the different components scale with the number of occupied and virtual orbitals. Using our automatic code generator, we have inserted operation counting into all of the terms, allowing for a contraction-by-contraction scaling analysis. For each contraction, we measured occupied scaling by fixing the number of virtual orbitals at 100 and varying the number of occupied orbitals between 30 and 50, after which we perform a log-log linear regression on

each contraction's operation count. Similarly, for scaling with virtual orbitals, we have fixed the number of occupied orbitals at 30 and varied the number of virtuals between 50 and 100, again feeding the information into log-log linear regressions. We present two sets of scaling data, representing the two cost extremes that one can get from the new approach. First, Table 2.1 shows the scaling data for ESMP2-TOP(1), in which only one TOP is considered large. Second, Table 2.2 shows the scaling data for ESMP2-TOP(all), in which all TOPs are considered large and the S-triples space is thus empty.

This detailed scaling analysis reveals that the worst-scaling terms all reside in the linear transformation part of solving the PT2 linear equation, which is to say evaluating the action of H_0 on a vector in the first-order interacting space as required in each iteration of the conjugate gradient algorithm we use to solve the linear equation. These terms are fifth and sixth order in the system size for ESMP2-TOP(1) and ESMP2-TOP(all), respectively, showing that it is indeed possible to improve over the seventh order scaling of the original formulation of ESMP2. Of course, prefactors matter, and the fact that ESMP2-TOP(1) carries 13 terms with $N_o^2 N_v^3$ scaling means that, for small systems, it will almost certainly be slower than EOM-CCSD despite its lower scaling, as EOM-CCSD has a smaller number of N^5 and N^6 terms. The scaling does guarantee, though, that ESMP2-TOP(1) will be faster in larger systems. This prefactor difference will also matter for the comparison between the $N7$- and $N5$-scaling codes, however a quick calculation on water with a cc-pVDZ basis set, resulting in $N = 24$ orbitals, revealed that the $N7$-scaling code took 9.84 seconds while the $N5$-scaling code only took 1.28. Extrapolating this with the scaling of the codes shows that the $N5$ scaling method becomes faster when the number of orbitals in the system is 8. We now turn our attention to the question of whether energetic accuracy is maintained when we aggressively limit the number of TOPs that are considered large.

2.4.3 Small Molecule Testing

Let us begin by testing the fifth order method on the same set of small molecules and two charge transfer (CT) examples that were studied recently with the original seventh order incarnation of ESMP2. To make the comparison direct, we use the same cc-pVDZ basis and the same molecular geometries as in the previous study. [59] Here, we restrict the L-triples space as much as possible by treating only the dominant TOP (or, in the case of N_2, the pair of equal-weight dominant TOPs) as large, relegating triples that do not contain the dominant TOP to the S-triples space with its diagonally-approximated zeroth order Hamiltonian. In Table 2.3, we see that for this set of small molecules, this $N_o^2 N_v^3$-scaling variant of ESMP2 is, like its seventh order predecessor, competitive in accuracy with EOM-CCSD. Thus, by working with excited-state-specific orbitals from the ESMF reference and an excited-state-specific correlation treatment from ESMP2, it is possible, at least in these test systems, to achieve EOM-CCSD accuracies with a method that scales as the fifth order of the system size. As with the original formulation of ESMP2, we find it especially encouraging that the method is equally accurate for CT and non-CT states, as practical uses of CT in biological

Table 2.1: Scaling data for ESMP2-TOP(1), in which only one TOP is treated as large and which is thus most appropriate when the reference is dominated by a single CSF. For the different parts of the PT2 linear equation's right-hand side (RHS) and linear transformation, we report how many of that part's contractions fall in to the different asymptotic scaling categories.

	N^3	$N_o^3 N_v$	$N_o^2 N_v^2$	$N_o^3 N_v^2$	$N_o^2 N_v^3$
T_{ij}^{ab} (RHS)	4	12	6	0	0
S_{ij}^{ab} (RHS)	2	6	3	0	0
T_{ijk}^{abc} (RHS)	16	0	4	0	0
S_{ijk}^{abc} (RHS)	3	0	5	0	0
$T_{ij}^{ab} \leftrightarrow T_{ij}^{ab}$	0	0	1	2	2
$S_{ij}^{ab} \leftrightarrow S_{ij}^{ab}$	0	0	1	2	2
$T_{ijk}^{abc} \leftrightarrow T_{ijk}^{abc}$	0	0	3	4	4
$S_{ijk}^{abc} \leftrightarrow S_{ijk}^{abc}$	0	0	2	5	5
$T_{ijk}^{abc} \leftrightarrow T_{ij}^{ab}$	0	0	18	0	0
$S_{ijk}^{abc} \leftrightarrow S_{ij}^{ab}$	0	0	8	0	0
$S_{ijk}^{abc} \leftrightarrow T_{ij}^{ab}$	0	0	2	0	0

and energy-related chemistry often involve large system sizes where lower-scaling methods are essential.

Interestingly, the results here are barely changed compared to the results from the previous seventh order method, which displayed mean absolute errors of 0.13 eV and 0.12 eV for the full set and the non-CT subset, respectively. [59] This finding suggests that the basic idea here is sound: using a diagonal approximation to H_0 in the space of less-important triples does not have a significant effect on the accuracy. Note that we have tested whether having any off-diagonal H_0 character in the triples manifold is necessary by testing what happens if no TOPs are treated as large. In that case, we find that accuracy suffers significantly, suggesting that, for the triples that connect directly via the coulomb operator to the large parts of the zeroth order reference, the fact that the Fock operator is not diagonal is significant. Thus, it appears that we get away with the reduction in scaling not because the off-diagonal parts of the Fock operator are unimportant, but because their effects are small for the triples that do not connect to the reference or that only connect to small components (TOPs with small weights) of the reference.

2.4.4 Ring Excitations

We now turn to a set of low-lying excitations in aromatic ring systems, where it is common to see excited states in which more than one TOP has a large weight. For these systems

Table 2.2: Scaling data for ESMP2-TOP(all), in which all TOPs are treated as large. For the different parts of the PT2 linear equation's right-hand side (RHS) and linear transformation, we report how many of that part's contractions fall in to the different asymptotic scaling categories. We omit the RHS doubles terms and the doubles-only parts ($T_{ij}^{ab} \leftrightarrow T_{ij}^{ab}$ and $S_{ij}^{ab} \leftrightarrow S_{ij}^{ab}$) of the linear transformation, as their scaling is the same as in Table 2.1. Note that in cases where the log-log scaling regression exponents for occupied or virtual orbitals were significantly fractional (i.e. differed from integers by more than 0.3) we took the conservative approach of transferring enough fractional exponent from occupied to virtual in order to move the virtual exponent up to the next integer, and then rounded what remained of the fractional occupied exponent up or down if it was above or below 0.3. For example, $N_o^{2.6}N_v^{2.5}$ is converted to $N_o^2N_v^3$, while $N_o^{2.99}N_v^{1.35}$ is converted to $N_o^3N_v^2$. Note that, although this conservative rounding may slightly rearrange the contractions among the N^4 and N^5 categories, we have explicitly verified (by inspecting the code) that each of the N^6 contractions has the asymptotic scaling reported here.

	N^4	N_o^5	$N_o^4N_v$	$N_o^3N_v^2$	$N_o^2N_v^3$	$N_o^4N_v^2$	$N_o^3N_v^3$
T_{ijk}^{abc} (RHS)	16	0	0	4	0	0	0
S_{ijk}^{abc} (RHS)	3	0	0	5	0	0	0
$T_{ijk}^{abc} \leftrightarrow T_{ijk}^{abc}$	0	25	8	13	10	7	4
$S_{ijk}^{abc} \leftrightarrow S_{ijk}^{abc}$	0	2	5	6	1	5	5
$T_{ijk}^{abc} \leftrightarrow T_{ij}^{ab}$	0	10	10	20	10	0	0
$S_{ijk}^{abc} \leftrightarrow S_{ij}^{ab}$	0	0	0	8	0	0	0
$S_{ijk}^{abc} \leftrightarrow T_{ij}^{ab}$	0	0	4	2	2	0	0

(whose geometries have been taken from the cc-pVDZ MP2 entries in the CCCBDB NIST database [21]) we have defined large TOPs as those whose singular values are above 0.1, resulting in two or fewer large TOPs in each excitation and thus a method that remains at the fifth-order end of the continuum between ESMP2-TOP(1) and ESMP2-TOP(all). Unlike the small molecules of the previous section, some of these ring excitations have at least a modest (although not dominant) degree of doubly excited character. As CASPT2 is often used to address double excitations, we have also included a comparison against its results in the table, although we stress that δ-CR-EOM-CC(2,3) is the better reference in these states thanks to its ability to handle double excitations and its higher-order treatment of electron correlation. This comparison makes clear that, at least on average, ESMP2 is more similar to CASPT2 than to δ-CR-EOM-CC(2,3), which is perhaps not surprising given the fact that ESMP2 and CASPT2 approach these states via second order perturbation theory from a qualitatively correct reference, making them methodologically similar. Of course, the fact that ESMP2 need not specify an active space is a significant practical advantage.

Across the twelve ring excitations shown in Table 2.4, we find that the differences between

Table 2.3: For the lowest singlet excitations in several small molecules, as well as for two simple CT excitations, we report the reference δ-CR-EOM-CC(2,3) excitation energy in eV, as well as other methods' errors relative to the reference. All calculations are in the cc-pVDZ basis. Only the dominant TOPs were considered large in ESMP2, meaning one TOP in all cases except N_2, where by symmetry there are two dominant TOPs with equal weights. Below each method, we report the canonical cost scaling with respect to system size. At bottom, we report mean and maximum absolute (i.e. unsigned) deviations from the reference both with and without the CT systems included, as well as the number of deviations larger than 0.3 eV.

	δ-CR-EOM-CC(2,3) $O(N^7)$	CIS $O(N^4)$	TDDFT/B3LYP $O(N^4)$	TDDFT/ωB97X $O(N^4)$	EOM-CCSD $O(N^6)$	ESMP2 $O(N^5)$
Acetaldehyde $1^1A"$	4.36	0.71	0.09	0.14	0.21	0.16
Ammonia 2^1A_1	7.57	0.95	-0.52	-0.07	0.05	0.01
Carbon Monoxide $1^1\Pi$	8.76	0.61	0.16	0.31	0.30	-0.09
Cyclopropene 2^1B2	7.97	0.57	-0.83	-0.33	-0.08	-0.07
Diazomethane 1^1A_2	3.01	0.38	0.05	0.09	0.45	-0.00
Dinitrogen $1\Pi_g$	10.36	-1.31	-0.03	0.00	0.44	0.09
Ethylene 1^1B_3	8.80	-0.25	0.11	0.10	0.19	-0.30
Formaldehyde 1^1A_2	4.08	0.63	0.07	0.10	0.19	0.15
Formamide $2^1A"$	5.86	0.88	0.04	0.11	0.21	0.15
Hydrogen Sulfide 2^1B_2	7.05	0.58	-0.27	0.20	0.11	-0.07
Ketene 1^1A_2	3.78	0.70	0.22	0.31	0.36	-0.01
Methanimine $1^1A"$	5.35	0.66	0.00	0.11	0.22	-0.00
Nitrosomethane $1^1A"$	1.85	0.27	0.13	0.12	0.25	0.17
Streptocyanine Cation 1^1B_2	7.53	1.55	1.08	1.07	0.28	-0.40
Thiofromaldyhyde 1^1A_2	2.18	0.58	0.13	0.17	0.24	-0.08
Water 1^1B_2	8.30	1.02	-0.57	-0.22	-0.01	0.06
Ammonia $\rightarrow$ Diflourine 2^1A_1	9.27	2.38	-6.91	-2.69	0.51	-0.26
Dinitrogen $\rightarrow$ Methylene 1^1B_2	15.49	1.66	-6.58	-1.79	0.06	0.15
Mean Abs. Dev. (with CT)		0.87	0.99	0.44	0.23	0.12
Max Abs. Dev. (with CT)		2.38	6.91	2.69	0.51	0.40
Mean Abs. Dev. (without CT)		0.73	0.27	0.22	0.22	0.11
Max Abs. Dev. (without CT)		1.55	1.08	1.07	0.45	0.40
Deviations above 0.3 eV		16	6	6	4	1

EOM-CCSD and ESMP2 are more significant than in the small-molecule excitations of the last section. While EOM-CCSD has a slightly higher mean absolute deviation from δ-CR-EOM-CC(2,3), its deviations are more regular than those of ESMP2. Indeed, in all twelve cases, EOM-CCSD predicts excitation energies to be between 0.2 and 0.55 eV higher than does δ-CR-EOM-CC(2,3), whereas the span of ESMP2's deviations is significantly larger at just over an eV. Table 2.5 shows that a similar story plays out for EOM-CCSD and ESMP2 in a triple-zeta basis, reassuring us that these tendencies are not specific to the double-zeta basis, on which we now focus our attention.

Notably, while Table 2.4's ESMP2 results are within 0.3 eV of δ-CR-EOM-CC(2,3) for eight out of the twelve states, in the other four states — pyrrole 2^1A_1, benzene 1^1B_{2u}, benzene 2^1B_{1u}, and pyrimidine 1^1B_1 — its prediction is low by 0.7 eV or more. Two of these are errors likely due to doubly excited character, one an error related to intruder states issues,

Table 2.4: Excitation energies (eV) for small ring systems in the cc-pVDZ basis. For the δ-CR-EOM-CC(2,3) reference, we report the excitation energy, while for other methods we report deviations from the reference. ESMP2 treated TOPs with singular values above 0.1 as large, which led to two or fewer large TOPs in all states included here. A diagonal H_0 was used in the space of triples that do not contain any large TOPs. At the bottom, we report mean and maximum absolute deviations from the reference, the number of these deviations that were larger than 0.3 eV, and the mean absolute deviation from CASPT2.

State	δ-CR-EOM-CC(2,3)	CIS	TDDFT/B3LYP	TDDFT/ωB97X	EOM-CCSD	CASPT2	ESMP2
Pyrrole 2^1A_1	6.15	1.60	0.45	0.84	0.51	-0.18*	-0.90
Pyrrole 1^1A_2	6.39	0.86	-0.48	0.70	0.36	0.10	0.09
Pyrrole 1^1B_2	6.56	0.37	0.01	0.10	0.47	0.38	-0.21
Pyridine 1^1B_1	4.84	1.33	-0.01	0.36	0.44	0.10	0.11
Pyridine 1^1B_2	4.76	1.44	0.75	0.83	0.52	0.07	-0.25
Pyridine 2^1B_2	6.51	2.05	0.86	1.05	0.45	0.29	0.11
Pyridine 1^1A_2	5.26	2.19	-0.16	0.33	0.44	-0.05	-0.05
Benzene 1^1B_{2u}	4.69	1.33	0.72	0.83	0.50	0.06	-0.71
Benzene 1^1B_{1u}	6.35	-0.08	-0.21	-0.06	0.42	-0.35	-0.26
Benzene 2^1B_{1u}	7.33	0.94	-0.14	-0.01	0.43	-0.69	-0.82
Pyrimidine 1^1B_1	4.50	1.40	-0.21	0.18	0.22	-0.32	-0.82
Pyrimidine 1^1B_2	5.23	1.28	0.52	0.61	0.28	-0.22	-0.28
Mean Abs. Dev. (MAD)		1.24	0.38	0.49	0.42	0.23	0.38
Max Abs. Dev.		2.19	0.86	1.05	0.52	0.69	0.90
Deviations above 0.3 eV		11	6	8	10	4	4
MAD vs CASPT2		1.30	0.44	0.59	0.49	0.00	0.28

*Level shift was necessary for convergence. See text.

and one is not necessarily much of an error at all. Start with the 2^1A_1 state of pyrrole, where CASPT2 displays intruder-state behavior and is not stable without the application of a level shift. Given that the zeroth order Hamiltonians are similar, and that the CASSCF reference used by CASPT2 should be a better starting point than ESMF, ESMP2's difficulty in this state is likely related to these intrude state difficulties. In the 2^1B_{1u} state of benzene, on the other hand, ESMP2 is energetically very similar to CASPT2, which is known to be highly accurate for the low-lying excitations of benzene, [91, 92, 89] and so this appears to be a case where ESMP2 is reasonably accurate, at least if CASPT2 is used as the reference. Indeed, the MAD of ESMP2 relative to CASPT2 across all twelve states is significantly lower than its MAD relative to δ-CR-EOM-CC(2,3), which is perhaps not so surprising given that both ESMP2 and CASPT2 are second-order perturbation theories based on orbital-optimized reference functions (although for CASPT2 the orbital optimization is state-averaged, rather than state-specific). However, the agreement is certainly not perfect, and the large deviations between ESMP2 and δ-CR-EOM-CC(2,3) in the benzene 1^1B_{2u} and pyrimidine 1^1B_1 states cannot be explained by either similarity to CASPT2 or by intruder state issues in CASPT2, which were not present. The errors in these two states are likely due instead to doubly excited character that the singly-excited ESMF reference function cannot capture. Indeed, the doubly excited fractions of the CASSCF wave functions for benzene 1^1B_{2u} and pyrimidine 1^1B_1 were 15% and 8%, respectfully. It is interesting to note that, at least in these two cases, this modest fraction of doubly excited character caused less trouble for EOM-CCSD. This

Table 2.5: Excitation energies (eV) for small ring systems in the cc-pVTZ basis. For the δ-CR-EOM-CC(2,3) reference, we report the excitation energy, while for other methods we report deviations from the reference. ESMP2 treated TOPs with singular values above 0.1 as large, which led to two or fewer large TOPs in all states included here. A diagonal H_0 was used in the space of triples that do not contain any large TOPs. At the bottom, we report mean and maximum absolute deviations from the reference and the number of these deviations that were larger than 0.3 eV.

State	δ-CR-EOM-CC(2,3)	EOM-CCSD	ESMP2
Pyrrole 2^1A_1	5.95	0.59	-0.89
Pyrrole 1^1A_2	5.93	0.41	0.13
Pyrrole 1^1B_2	6.25	0.15	-0.18
Pyridine 1^1B_1	4.69	0.52	0.15
Pyridine 1^1B_2	6.22	0.51	0.12
Pyridine 2^1B_2	4.61	0.60	-0.21
Pyridine 1^1A_2	5.14	0.51	-0.03
Benzene 1^1B_{2u}	4.55	0.58	-0.66
Benzene 1^1B_{1u}	7.01	0.51	-0.76
Benzene 2^1B_{1u}	6.06	0.48	-0.23
Pyrimidine 1^1B_1	4.14	0.54	-0.60
Pyrimidine 1^1B_2	4.82	0.62	-0.23
Mean Abs. Dev. (MAD)		0.51	0.35
Max Abs. Dev.		0.62	0.89
Deviations above 0.3 eV		11	4

raises the interesting question of whether, for cases with modest amounts of doubly excited character, EOM-CCSD is more robust than ESMP2, which seems like a question worth studying more systematically in future work.

2.4.5 Rydberg Excitations

To check whether ESMP2 achieves a similar quality in Rydberg excitations, we have tested it on relevant excitations in neon, formaldehyde, and benzene. Although the comparison is less straightforward than those of the previous sections due to a lack of a single high-level benchmark, comparisons to literature values are shown in Table 2.6. We find that the overall accuracy for ESMP2 is similar to that seen in the ring systems above and that it makes a substantial correction to the uncorrelated ESMF reference, which in most cases underestimates these excitations (although interestingly not in neon).

Table 2.6: Results for a few Rydberg states in neon, formaldehyde, and benzene. Molecular geometries were taken from the NIST CCCBDB database.[21] All values are reported in eV.

State	Basis	ESMF	N5-ESMP2	Error
Neon ($2s \rightarrow 3p$)	cc-pVTZ	65.6781	64.6521	0.35[a]
Formaldehyde 2^1A_1	d-aug-cc-pVTZ	7.0967	8.3287	0.23[b]
Formaldehyde 3^1A_1	d-aug-cc-pVTZ	8.1856	9.3947	0.13[b]
Benzene $1E_{2g}$	aug-ANO1[c]	6.7758	7.4583	-0.38[c]
Benzene $2A_{1g}$	aug-ANO1[c]	6.7619	7.4557	-0.39[c]
Benzene $1A_{2g}$	aug-ANO1[c]	6.8013	7.4856	-0.38[c]

[a] Compared to EOM-CCSD in the same basis.[57]
[b] Compared to the theoretical best estimate for these states.[89]
[c] Compared to CCSD calculations in the same basis set.[90]

Table 2.7: Size intensivity test, in which we report the first singlet excitation energy in eV for a water molecule surrounded by a variable number of distant He atoms. Methods' asymptotic cost scalings are given in parentheses.

He atoms	ESMF (N^4)	ESMP2 (N^5)	ESMP2 (N^7)	EOM-CCSD (N^6)	CISD (N^6)
0	7.7286	8.4508	8.4353	8.1946	10.1593
1	7.7286	8.4508	8.4353	8.1946	10.5369
2	7.7286	8.4508	8.4353	8.1946	10.9118
3	7.7286	8.4508	8.4353	8.1946	11.2841
4	7.7286	8.4508	8.4353	8.1946	11.6537
5	7.7286	8.4508	8.4353	8.1946	12.0207
6	7.7286	8.4508	8.4353	8.1946	12.3852

2.4.6 Size Intensive Excitation Energies

Finally, although ESMP2 is rigorously size intensive — by which we mean that the excitation energy is unchanged by adding a second, infinitely-far-away system that does not participate in the excitation — it is worth testing that this property has been realized in our implementation. To this end, we treated a water molecule with various numbers of far-away helium atoms in a 6-31G basis. We performed seven calculations, one with just the water molecule and then six more, each with one additional He atom placed 10 Å away from the water at the different points of an octahedron. As seen in Table 2.7, the ESMP2 prediction for the excitation energy was unchanged by the addition of the He atoms, both for the

original N^7-scaling approach and the N^5-scaling approach introduced here in which only the dominant TOP is considered large. While ESMP2's size intensivity is a formal advantage over CASPT2, which is only approximately size consistent, [93] CASPT2's size intensivity error turns out to be less than 10^{-6} eV in this example. In contrast, the excitation energy of configuration interaction with singles and doubles (CISD), which is not even approximately size consistent or intensive, changes significantly upon adding the He atoms, despite the fact that they have essentially no interaction with the water molecule. This alarming behavior is a reminder of why size-intensivity is such a high priority in excited state methods, as artificial energy shifts of the size displayed here by CISD could spoil predictions of solvation properties such as solvatochromic shifts.

2.5 Conclusion

We have shown that, by working in an orbital basis similar to that of the natural transition orbitals and by making a small modification to the zeroth order Hamiltonian, the cost scaling of the ESMP2 correction to the ESMF energy can be lowered from the seventh to the fifth power of the system size. In particular, the scaling matches the $N_o^2 N_v^3$ scaling of ground state MP2 theory, although the prefactor remains significantly higher due to the off-diagonal nature of ESMP2's zeroth order Hamiltonian, which necessitates an iterative solution to the central linear equation. Initial testing of this lower-scaling incarnation of ESMP2 theory shows that its accuracy remains competitive with EOM-CCSD in many scenarios, but that it may break down more rapidly when doubly excited character is present. Given that this approach to ESMP2 gives it a lower cost-scaling than EOM-CCSD, these findings strongly motivate more systematic and widespread testing in future. The potential for a low-scaling method that is robust in charge transfer contexts is especially strong, as DFT still struggles in this area and modeling these systems reliably often requires the explicit inclusion of solvent species and can thus easily entail hundreds of atoms.

Going forward, the immediate priority is to work towards a production-level implementation of the most expensive terms within the theory. Happily, our automatic code-generation and cost-analysis has revealed that the number of terms with fifth order scaling is relatively small, and so a hand-tuned implementation employing dense linear algebra should be quite feasible. Once the practical efficiency of the implementation is addressed, it will be important to test the method in a significantly larger and more systematic set of excitations in order to more firmly establish in which contexts ESMP2 can be used as a lower-cost alternative to EOM-CCSD and in which contexts it cannot. Looking a bit farther ahead, it would be interesting to further exploit locality. The new approach here derives its scaling from the fact that molecular excitations' spatial extents typically do not grow indefinitely with system size, but it does not exploit localities of electron correlation in the way many ground state methods now do. Finally, the realization of an excited state analogue of MP2 theory at the same cost scaling further motivates the study of applying a cluster operator to the ESMF reference wave function, which would be an important step towards the type

of systematically improvable hierarchy of correlation methods that Hartree Fock theory has long enjoyed.

2.6 Acknowledgements

This work was supported by the National Science Foundation's CAREER program under Award Number 1848012. The Berkeley Research Computing Savio cluster performed the calculations.

J.A.R.S. acknowledges that this material is based upon work supported by the National Science Foundation Graduate Research Fellowship Program under Grant No. DGE 1752814. Any opinions, findings, and conclusions or recommendations expressed in this material are those of the author(s) and do not necessarily reflect the views of the National Science Foundation.

Chapter 3

Studying excited-state-specific perturbation theory on the Thiel set

3.1 Abstract

We explore the performance of a recently-introduced N^5-scaling excited-state-specific second order perturbation theory (ESMP2) on the singlet excitations of the Thiel benchmarking set. We find that, without regularization, ESMP2 is quite sensitive to π system size, performing well in molecules with small π systems but poorly in those with larger π systems. With regularization, ESMP2 is far less sensitive to π system size and shows a higher overall accuracy on the Thiel set than CC2, EOM-CCSD, CC3, and a wide variety of time-dependent density functional approaches. Unsurprisingly, even regularized ESMP2 is less accurate than multi-reference perturbation theory on this test set, which can in part be explained by the set's inclusion of some doubly excited states but none of the strong charge transfer states that often pose challenges for state-averaging. Beyond energetics, we find that the ESMP2 doubles norm offers a relatively low-cost way to test for doubly excited character without the need to define an active space.

3.2 Introduction

Quantum chemistry approaches to modeling singly excited states have been highly successful, but it remains true that the methods that are most reliably accurate are also highly computationally intensive. As in ground state theory, coupled cluster (CC) methods that go beyond doubles but stop short of a full treatment of triples are often used as reliable benchmarks.[94, 96, 97, 98, 99, 100, 101, 102, 103, 95] However, with a cost that scales as N^7 with the system size N, these methods are quite limited in the size of molecule that they can treat. Density functional theory (DFT), and in particular time-dependent DFT (TD-DFT), is much more affordable, with costs ranging from N^3 to N^5 depending on the functional, with N^4 being typical for many hybrid functionals. By choosing a functional that

is known to work well for the chemistry in question, TD-DFT can offer impressive accuracy, especially for its computational price, but it would be an overstatement to claim that it is as reliable as CC methods that include some triples effects. Lower cost CC options for excited states, especially in the linear response (LR) and equation of motion (EOM) formalisms, are also widely used, but without triples effects, these methods are more varied in their reliability. Examples include EOM-CC with singles and doubles (EOM-CCSD), [104] which has an N^6 cost but tends to overestimate excitation energies, and CC2, [51, 105] which has an N^5 cost and typically displays lower average errors than EOM-CCSD. These methods are both widely used and have been quite successful, but nonetheless there is room for improvement, as they can produce surprisingly large errors in some cases that are not obviously ill-suited to their assumptions, as in the $2^1\mathrm{A}'$ state of formamide. Adding partial triples contributions – as in CC3, [52, 106, 105] EOM-CCSD(T), [107, 108] δ-CR-EOM(2,3)D, [79] and many related methods – can certainly improve matters, but brings us back to N^7 scaling. In this study, we will use a large test set to investigate to what degree it may be helpful to move away from the linear response paradigm and instead build traditional correlation methods upon a mean field reference, starting, for now, with second order perturbation theory.

Like ground state second order Møller-Plesset perturbation theory (MP2), [13] the recently introduced excited-state-specific Møller-Plesset theory (ESMP2) [57, 59, 11] seeks to provide a second order Rayleigh-Schrödinger correction atop a mean field starting point. In the ground state, MP2 perturbs around Hartree-Fock theory, while in ESMP2 the starting point is provided by excited state mean field (ESMF) theory, [57, 59] which refines the configuration interaction singles (CIS) picture [109] through excited-state-specific orbital relaxations to create a method that shares much in common with ground state mean field theory. [58] The early studies of ESMP2 have shown promising accuracy, which has become more relevant thanks to a refinement of the theory [11] that brings its cost scaling down to N^5. This is asymptotically comparable to MP2, although it should be noted that ESMP2's cost is an iterative N^5 due to its zeroth order Hamiltonian not being diagonal. With a relatively low scaling and early promise in initial tests, we now seek to deepen our understanding of the strengths and weaknesses of ESMP2 by exploring its performance on a widely used excited state benchmark.

The Thiel set [15] offers theoretical best estimates (TBEs) for over one hundred singlet excited states (and also many triplet states) spread over 28 molecules, which include nucleobases, carbonyls, aromatic rings, heterocyclic rings, small polyenes, and other small unsaturated hydrocarbons. In the original work, both complete active space second-order perturbation theory (CASPT2) [75, 76] as well as the LR or EOM coupled cluster methods CC2, EOM-CCSD, and CC3 were compared across these molecules. Since then, a large number of other research groups have used the Thiel set to make further comparisons between methods. [40, 117, 118, 119, 120, 121, 122, 123, 124, 110, 111, 112, 113, 114, 115, 116, 48] Both the quality of the initial test set and its broad subsequent use make the Thiel set especially attractive for helping to put ESMP2 in context and for understanding its strengths and weaknesses. We note that, for consistency with this significant body of previous work, we have employed the original test set's TBEs in our analysis below, although we acknowledge

that in some cases, such as the nucleobases, [125, 126] more recent studies may offer even more reliable best estimates.

Thiel and coworkers organized their test set into four groups of molecules. In one group they placed aldehydes, ketones, and amides, in which, with the exception of benzoquinone, ESMP2 shows a highly competitive performance even without regularization. Another group contains unsaturated aliphatic hydrocarbons, some of whose excited states have large amounts of doubly excited character and so do not satisfy the assumptions of ESMP2's singly-excited zeroth order reference state. Although ESMP2 cannot treat doubly excited character accurately, it does prove to be a relatively cost-effective way to offer warning that such character is present. Thiel's third group consists of aromatic rings and heterocycles, in which ESMP2's sensitivity to π system size and the practical efficacy of regularization become especially apparent. In our discussion below, we reorganize these two groups into three – conjugated polyenes, heterocycles, and other rings – as the polyenes are particularly illuminating for ESMP2. The fourth and final Thiel group contains the nucleobases cytosine, thymine, uracil, and adenine. As in other cases, ESMP2 struggles with their π system sizes but improves substantially with regularization.

3.3 Theory

3.3.1 Zeroth Order Reference

The zeroth order reference state for ESMP2 is the ESMF wave function, which in its simplest form is an orbital-relaxed linear combination of single excitations that can be written as follows.

$$|\Phi_0\rangle = e^{\hat{X}} \left(\sum_{ia} c_{ia} \, |_i^a\rangle + \sum_{\bar{i}\bar{a}} c_{\bar{i}\bar{a}} \, |_{\bar{i}}^{\bar{a}}\rangle \right) \tag{3.1}$$

In this work, the indices i, j, k represent occupied alpha orbitals, a, b, c represent virtual alpha orbitals, and $\bar{i}$ and $\bar{a}$ likewise represent beta orbitals. Note that it is possible to formulate ESMF so as to also include the closed-shell Aufbau configuration, [57] but we have not yet implemented the corresponding ESMP2 terms in our N^5-scaling ESMP2 code, and so the ESMF reference used in this work is as shown in Eq. 3.1. Here $\hat{X}$ is an anti-Hermitian one-body operator that, when exponentiated, produces a unitary orbital rotation that moves the linear combination of single excitations from the HF to the ESMF orbital basis. To find each ESMF state, we employ either the recently-introduced generalized variational principle (GVP) [59] or, where possible, the more efficient ESMF self-consistent field (SCF) approach. [58] The latter is not as robust as the GVP, and so we fall back to using the GVP in cases where the SCF approach proves unstable.

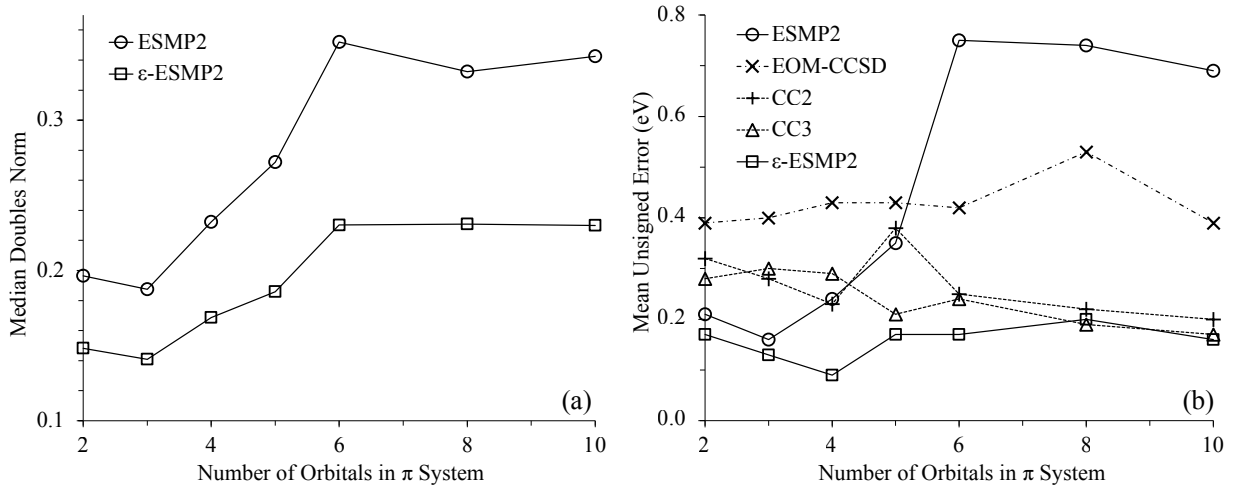

Figure 3.1: (a) Median $|T_2|$ doubles norms and (b) MUEs for excitation energies by π system size. States identified by ESMP2 to have strongly doubly excited character and states not found by ESMF (red and grey rows in Table 3.1) are excluded.

3.3.2 ESMP2

ESMP2 builds a second-order Rayleigh-Schrödinger perturbation theory atop ESMF in a way that parallels MP2's construction atop HF theory. As ESMF already contains singly excited components, the initial formulation [57] of ESMP2 included all doubly- and triply-excited determinants in its first order interacting space. This choice comes from the basic logic that if MP2 can stop at doubles when expanding around its Aufbau reference, ESMP2 should stop at triples. This approach led to promising accuracy in initial tests, but due to the large number of triples, it came with an N^7 cost scaling. More recently, an N^5 reformulation of ESMP2 has been introduced [11] that includes only the most important subset of triples by first converting the ESMF wave function into a "transition orbital pair" basis that shares much in common with the concept of a natural transition orbital basis. [127] For the present study, we employ the N^5 theory, and refer the reader to its original publication [11] for most of its details, but let us very briefly explain the added level shift as it has not been discussed previously.

The zeroth order Hamiltonian for ESMP2 is

$$\hat{H}_0 = \hat{R}(\hat{F} - \hat{H})\hat{R} + \hat{P}\hat{H}\hat{P} + \hat{Q}(\hat{F} + \epsilon)\hat{Q}, \tag{3.2}$$

where $\hat{R}$ projects onto the ESMF state, $\hat{P}$ projects onto the subspace containing the Aufbau and all singly-excited configurations, and $\hat{Q} = 1 - \hat{P}$. $\hat{H}$ is the full Hamiltonian, whereas $\hat{F}$ is the Fock operator formed from the ESMF one-body density matrix. Note that, in part, this choice of $\hat{H}_0$ is employed so as to ensure size intensivity. [11] In previous ESMP2

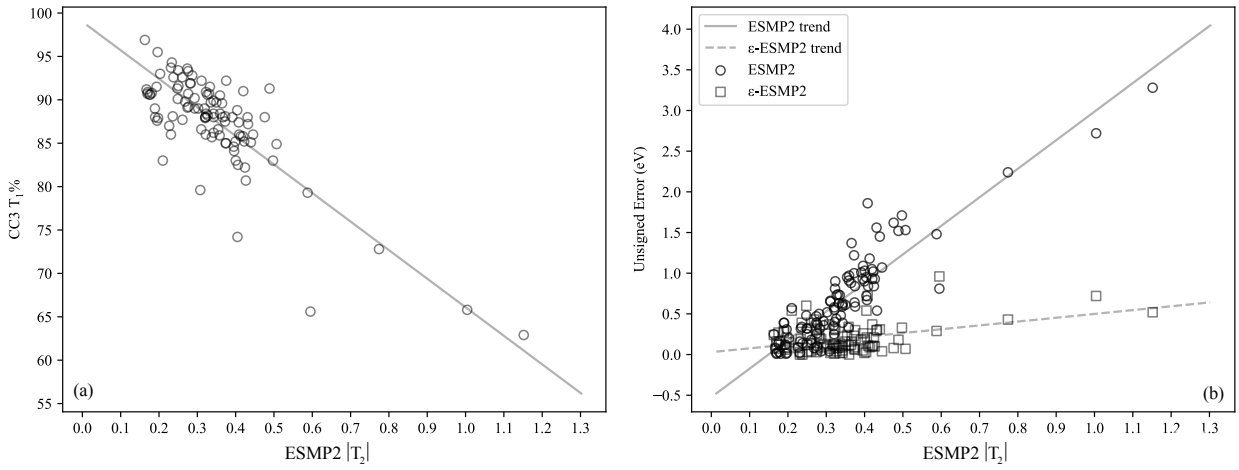

Figure 3.2: (a) CC3 T_1 percentages and (b) ESMP2 and ϵ-ESMP2 unsigned excitation energy errors plotted against the ESMP2 doubles norm $|T_2|$ for all states. The lines are linear fits to the points.

work, the level shift ϵ has not been used, and all results reported as "ESMP2" below use $\epsilon = 0$. By instead setting a positive value for ϵ, we can widen the zeroth order energy spacing that separates the singles from the doubles and triples, which as discussed above may help mitigate perturbative failures in larger π systems. Due to the structure of $\hat{H}_0$, the only modification that ϵ makes to ESMP2's working equations is to shift the zeroth order Hamiltonian matrix's diagonal in the amplitude equations, and so adopting a nonzero ϵ involves a trivial algorithmic change. As the ESMP2 excitation energy is

$$\Delta E = E_{\text{ESMP2}} - E_{\text{MP2}}, \tag{3.3}$$

we also add ϵ to the denominators in the standard MP2 energy expression so as to maintain a balanced treatment between the ground and excited state. Of course, the value chosen for ϵ will matter, and after some preliminary testing revealed that shifts below 0.2 E_h made very little difference, we ran the full test set with the substantially larger shift value of 0.5 E_h to find out what would happen with a much more aggressive shift. Interestingly, this resulted in substantially better excitation energies, and so we have not attempted to optimize ϵ any further in this study. We show examples of individual states' shift sensitivities in the Supplementary Material. All results presented below that are labeled "ϵ-ESMP2" employed $\epsilon = 0.5$ E_h.

3.3.3 Amplitude Diagnostics

Although they are not a perfect guide, [128] amplitude diagnostics such as the T_1 diagnostic [129] have long been used to help predict whether ground states are indeed weakly correlated

enough for single-reference methods to be reliable. Might similar diagnostics offer useful information for ESMP2? Unlike linear response excited state methods like EOM-CCSD in which doubly excited configurations must account for both orbital relaxation and correlation effects, ESMP2 is built on a reference in which mean-field orbital relaxations are already accounted for by the MO basis. Thus, its doubles amplitudes are more closely related to ground state singles amplitudes: both are singly excited relative to their reference state and both are only expected to be present in large amounts if the reference wave function is a poor approximation for the state. Certainly we would not expect ESMP2 to be accurate for a state in which any doubly excited configurations have large weights, as this would be a violation of the assumption that we are perturbing around the singly-excited ESMF reference. Thus, both from their similarity to the ground state singles at the heart of the T_1 diagnostic and from the perturbative argument that they should not be large, we expect that the ESMP2 doubles should be able to offer useful information about the reliability of ESMP2, and possibly other theories too, for a given excited state.

What functions of the doubles would make for good diagnostics? In many studies involving linear-response coupled cluster theory, the percentage of the wave function that is described by single excitations is used as a gauge[105]. While we could adopt a similar method for ESMP2, except using the percentage of the first order wave function coming from the doubles instead, we choose not to as the resulting diagnostic is not size consistent. Instead we make use of the fact that in ESMP2 any excitation that is localized to some molecule or molecular region (as most excitations in chemistry are) will see the triples percentage of its wave function grow indefinitely with system size as additional far-away molecules are added, as the size intensivity of the theory guarantees that those far-away molecules will simplify to MP2 descriptions, thus adding additional triples (MP2 doubles on top of the ESMF single excitation) components for every far-away molecule that is added.[11] Therefore, the ESMP2 doubles percent will drop to zero in the large system limit, in the same way that the RHF determinant's percentage of the MP2 wave function goes to zero in the large system limit. This effect implies that the meaning of the $\%T_1$ and $\%T_2$ measures will vary with system size in ESMP2, even when one is simply adding far-away molecules that do not interact with the original system. This is clearly undesirable.

In contrast, the norm of the doubles amplitudes (when working in intermediate normalization) is unaffected by the addition of far-away molecules, as the size intensivity of ESMP2 guarantees that, so long as the excitation is still on the original molecule, the new molecules add only triples in the form of the far-away molecules' MP2 doubles acting atop the ESMF singles. Further, like many other diagnostics, $|T_2|$ is invariant to occupied-occupied and virtual-virtual rotations. Thus, $|T_2|$ offers ESMP2 a size-consistent, orbital-invariant measure of the quality of ESMF's assumption of a purely singly-excited state. It should therefore allow us to flag cases, like states with large doubly excited components, for which ESMF and ESMP2 are not appropriate.

3.4 Computational Details

Following the general considerations described by Thiel and coworkers, [15] we have employed the same ground state MP2/6-31G* geometries and TZVP basis set [130] in all calculations. Our ESMP2 code does not currently make use of point group symmetry, so calculations were run in C1 and manual checks were performed to ensure that states' symmetry labels are correct. In part to ensure the same states were being used when comparing to existing results and in part for convenience, we employed the largest singles components from EOM-CCSD calculations as the guess singles in ESMF. We employed PySCF [131] for most EOM-CCSD calculations, while QChem [85] and Molpro [132] were used for the 2^1E_{2g} benzene state and the 2^1A_u and 1^1B_{2g} states of tetrazine. We also verified state characters by direct comparisons of the converged ESMF and EOM-CCSD wave functions, including visual inspection of the most relevant orbitals for each state using Molden v2.0. [133] We further verified state character and, in particular, the nature of doubly excited states, using Thiel and coworkers' active spaces [15] and Molpro's implementation of state-averaged CASSCF. Detailed information on these various comparisons can be found in the Supplementary Material. Note that in some of our comparisons below, we have excluded states not found by ESMF or that are flagged by ESMP2 as having large amounts of doubly excited character, as these either cannot be compared or are not appropriate for treatment by any of the single-reference methods. We have verified that crunching the numbers with these states included makes little difference, as discussed in the next section and as seen in the additional tables in the Supplementary Material.

3.5 Results

3.5.1 Overview

Table 3.1 shows our results on the 103 singlet states that have CC results and TBEs in the Thiel benchmark, [15] with the ESMP2 and CC methods' accuracies summarized in Figure 3.1 and Table 3.2. Orbital-optimized ESMF stationary points were successfully located for 100 of these 103 states, which, while not perfect, represents the clearest evidence to date that ESMF energy stationary points can be expected to exist for the vast majority of low-lying singlet excited states in single-reference molecules. Six of the states showed especially large ESMP2 doubles norms with $|T_2| > 0.5$, and five of these six likewise had CC3 T1 percentages below 80, indicating that ESMP2's $|T_2|$ can indeed help predict states with challenging amounts of doubly excited character. As seen in Figure 3.2, ESMP2's $|T_2|$ also shows the expected correlations with both ESMP2 excitation energy errors and the CC3 T1 percentage across a wider range of $|T_2|$ values. With regards to excluding states from some comparisons, we note that the exclusion of the three missing ESMF states from the statistics, for example in Table 3.2, changes the overall mean unsigned error (MUE) by 0.01 eV or less for CC2, EOM-CCSD, and CC3. Excluding the states with $|T_2| > 0.5$ improves

the overall MUEs of CC2, EOM-CCSD, CC3, and ϵ-ESMP2 by just 0.04, 0.03, 0.0, and 0.02 eV, respectively, and so does not affect the ordering of their overall accuracy. As there were only three states out of about 100 that ESMF did not find, we do not expect their absence from the ESMP2 statistics to alter any of the broad conclusions drawn from this study. The Supplementary Material has additional tables in which fewer states are excluded.

As seen in Figure 3.1, unregularized ESMP2's accuracy for excitation energies in singly-excited states depends strongly on the size of a molecule's π system, while ϵ-ESMP2 is insensitive to π system size and highly accurate. The degradation of ESMP2's accuracy with increasing π system size closely follows the rise of its $|T_2|$ doubles norm, indicating that the poor accuracy in molecules with larger π systems is indeed related to a perturbative failure born of small zeroth order energy spacings between the reference and the lowest-lying doubles. With its level shift suppressing the spurious growth of large doubles contributions, ϵ-ESMP2 is significantly more reliable, displaying an accuracy that is as good or better than the other single-reference methods at all π system sizes. Among the methods compared, only the multi-reference CASPT2 approach using Thiel's active spaces offers better overall accuracy on this test set than ϵ-ESMP2. With an N^5 scaling and no need to choose an active space, these results suggest that ϵ-ESMP2 has much to offer in modeling singly excited states, while ESMP2 can act as a relatively affordable detector of doubly excited character.

3.5.2 Amplitude Diagnostics

As seen in Figure 3.2, the ESMP2 $|T_2|$ values tend to increase as the CC3 $\%T_1$ values decrease, in line with expectation. With one exception, the most worrying CC3 $\%T_1$ values (those significantly below 80%) all correspond to ESMP2 $|T_2|$ values above 0.5. The exception is the 1^1B_{3u} state of benzoquinone, which has a CC3 $\%T_1$ of 75.2% but an ESMP2 doubles norm of just 0.4. Interestingly, both CC2 and CC3 are reasonably accurate for this state despite the low $\%T_1$ value, although EOM-CCSD and ϵ-ESMP2 are not. This exception makes it tempting to recommend that states with $|T_2| > 0.4$ be considered "hard" for ϵ-ESMP2, but Figure 3.2 also makes clear that there are many states with doubles norms this large that ϵ-ESMP2 is quite accurate for, and a couple with lower doubles norms where ϵ-ESMP2 struggles. So we see 0.5 as a better rough threshold for when to firmly set ϵ-ESMP2 and other single-reference methods aside and reach for multi-reference approaches. For ESMP2, large energy errors clearly start much earlier, and it would be difficult to recommend relying on it for any state where $|T_2| > 0.3$.

Table 3.1: Singlet excitation energies in eV. TBEs and results for CASPT2, CC2, EOM-CCSD, and CC3 are from the original Thiel benchmark, [15] except for CC3 results on cytosine, thymine, uracil, and adenine, which are from Kánnár and Szalay. [126] CASPT2 "a" refers to Roos's results, while CASPT2 "b" refers to Thiel's. States where no ESMF solution was found are highlighted in gray, those with known Rydberg character are in blue, and those in which ESMP2's $|T_2|$ was above 0.5 are in red.

Molecule	π size	State	TBE	CASPT2 a	CASPT2 b	CC2	CCSD	CC3 (%T_1)	ESMP2	ϵ-ESMP2	ESMP2 $\lvert T_2\rvert$
formaldehyde	2	1^1A_2	3.88	3.91	3.98	4.09	3.97	3.95 (91.2)	3.96	3.81	0.17
		1^1B_1	9.10	9.09	9.14	9.35	9.26	9.18 (90.9)	9.12	8.98	0.17
		2^1A_1	9.30	9.77	9.31	10.34	10.54	10.45 (91.3)	9.78	9.90	0.25
acetone	2	1^1A_2	4.40	4.18	4.42	4.52	4.43	4.40 (90.8)	4.39	4.28	0.18
		1^1B_1	9.10	9.10	9.27	9.29	9.26	9.17 (91.5)	9.22	9.16	0.19
		2^1A_1	9.40	9.16	9.31	9.74	9.87	9.65 (90.1)	9.08	9.28	0.25
benzoquinone	8	1^1A_u	2.80	2.50	2.80	2.92	3.19	2.85 (83.0)	1.77	2.61	0.40
		1^1B_{1g}	2.78	2.50	2.78	2.81	3.07	2.75 (84.1)	1.69	2.52	0.40
		1^1B_{3g}	4.25	4.19	4.25	4.69	4.93	4.59 (87.9)	3.67	4.12	0.32
		1^1B_{1u}	5.29	5.15	5.29	5.59	5.89	5.62 (88.4)	4.70	5.31	0.34
		1^1B_{3u}	5.60	5.15	5.60	5.69	6.55	5.82 (75.2)	4.88	6.14	0.40
		2^1B_{3g}	6.98	6.34	6.98	7.36	7.62	7.27 (88.8)	6.03	7.01	0.40
formamide	3	$1^1A''$	5.63	5.61	5.63	5.76	5.66	5.65 (90.7)	5.62	5.47	0.17
		$2^1A'$	7.44	7.41	7.44	8.15	8.52	8.27 (87.9)	7.42	7.52	0.20
acetamide	3	$1^1A''$	5.80	5.54	5.80	5.77	5.71	5.69 (90.6)	5.66	5.53	0.18
		$2^1A'$	7.27	7.21	7.27	7.66	7.85	7.67 (89.1)	6.88	7.30	0.27
propanamide	3	$1^1A''$	5.72	5.48	5.72	5.78	5.74	5.72 (90.6)	5.69	5.56	0.18
		$2^1A'$	7.20	7.28	7.20	7.56	7.80	7.62 (89.2)	6.83	7.26	0.28
ethene	2	1^1B_{1u}	7.80	7.98	8.62	8.40	8.51	8.37 (96.9)	8.05	8.04	0.16
butadiene	4	1^1B_u	6.18	6.23	6.47	6.49	6.72	6.58 (93.7)	6.02	6.18	0.23
		2^1A_g	6.55	6.27	6.83	7.63	7.42	6.77 (72.8)	4.31	6.98	0.77
hexatriene	6	1^1B_u	5.10	5.01	5.31	5.41	5.72	5.58 (92.6)	4.92	5.14	0.26
		2^1A_g	5.09	5.20	5.42	6.67	6.61	5.72 (65.8)	2.37	5.81	1.00

octatetraene	8	2^1A_g	4.47	4.38	4.64	5.87	5.99	4.97 (62.9)	1.19	4.99	1.15
		1^1B_u	4.66	4.42	4.70	4.72	5.07	4.94 (91.9)	4.16	4.43	0.28
cyclopropene	2	1^1B_1	6.76	6.36	6.76	6.96	6.96	6.90 (93.0)	6.56	6.61	0.20
		1^1B_2	7.06	7.45	7.06	7.17	7.24	7.10 (95.5)	6.75	6.85	0.20
cyclopentadiene	4	1^1B_2	5.55	5.27	5.51	5.69	5.87	5.73 (94.3)	5.23	5.36	0.23
		2^1A_1	6.31	6.31	6.31	7.05	7.05	6.61 (79.3)	4.83	6.60	0.60
norbornadiene	2	1^1A_2	5.34	5.28	5.34	5.57	5.80	5.64 (93.4)	5.09	5.31	0.25
		1^1B_2	6.11	6.20	6.11	6.37	6.69	6.49 (91.1)	5.79	6.31	0.28
benzene	6	1^1B_{2u}	5.08	4.84	5.05	5.27	5.19	5.07 (85.8)	4.03	4.98	0.42
		1^1B_{1u}	6.54	6.30	6.45	6.68	6.74	6.68 (93.6)	6.07	6.24	0.27
		1^1E_{1u}	7.13	7.03	7.07	7.44	7.65	7.45 (92.2)	6.48	7.11	0.31
		2^1E_{2g}	8.41	7.90	8.21	9.03	9.21	8.43 (65.6)	7.60	9.37	0.60
naphthalene	10	1^1B_{3u}	4.24	4.03	4.24	4.45	4.41	4.27 (85.2)	3.22	4.13	0.42
		1^1B_{2u}	4.77	4.56	4.77	4.96	5.21	5.03 (90.6)	4.33	4.73	0.33
		2^1A_g	5.90	5.39	5.90	6.22	6.23	5.98 (82.2)	5.06	6.11	0.42
		1^1B_{1g}	6.00	5.53	6.00	6.21	6.53	6.07 (79.6)	5.96	6.37	0.31
		2^1B_{3u}	6.07	5.54	6.07	6.25	6.55	6.33 (90.7)	5.33	5.99	0.33
		2^1B_{1g}	6.48	5.87	6.48	6.82	6.97	6.79 (91.3)	4.96	6.30	0.49
		2^1B_{2u}	6.33	5.93	6.33	6.57	6.77	6.57 (90.5)	5.42	6.22	0.36
		3^1A_g	6.71	6.04	6.71	7.34	7.77	6.90 (70.0)	N/A	N/A	N/A
furan	5	1^1B_2	6.32	6.04	6.43	6.43	6.80	6.60 (92.6)	6.18	6.32	0.24
		2^1A_1	6.57	6.16	6.52	6.87	6.89	6.62 (84.9)	5.04	6.50	0.51
		3^1A_1	8.13	7.66	8.22	8.83	8.83	8.53 (90.7)	7.87	8.38	0.28
pyrrole	5	2^1A_1	6.37	5.92	6.31	6.61	6.61	6.40 (86.0)	5.30	6.41	0.45
		1^1B_2	6.57	6.00	6.33	6.83	6.87	6.71 (91.6)	6.25	6.45	0.25
		3^1A_1	7.91	7.46	8.17	8.44	8.44	8.17 (90.2)	7.50	8.04	0.29
imidazole	5	$1^1A''$	6.81	6.52	6.81	6.86	7.01	6.82 (87.6)	6.80	6.72	0.19
		$2^1A'$	6.19	6.72	6.19	6.73	6.80	6.58 (87.2)	5.65	6.49	0.43
		$3^1A'$	6.93	7.15	6.93	7.28	7.27	7.10 (89.8)	7.01	7.36	0.27
pyridine	6	1^1B_2	4.85	4.84	5.02	5.32	5.27	5.15 (85.9)	4.52	5.19	0.36
		1^1B_1	4.59	4.91	5.14	5.12	5.25	5.05 (88.1)	4.93	4.98	0.24
		2^1A_2	5.11	5.17	5.47	5.39	5.73	5.50 (87.7)	5.25	5.50	0.26

		2^1A_1	6.26	6.42	6.39	6.88	6.94	6.85 (92.8)	6.22	6.45	0.29
		3^1A_1	7.18	7.23	7.46	7.72	7.94	7.70 (91.5)	6.55	7.29	0.33
		2^1B_2	7.27	7.48	7.29	7.61	7.81	7.59 (89.7)	6.54	7.25	0.34
pyrazine	6	1^1B_{3u}	3.95	3.63	4.12	4.26	4.42	4.24 (89.9)	3.34	4.00	0.34
		1^1A_u	4.81	4.52	4.70	4.95	5.29	5.05 (88.4)	3.84	4.81	0.36
		1^1B_{2u}	4.64	4.75	4.85	5.13	5.14	5.02 (86.2)	4.25	4.86	0.34
		1^1B_{2g}	5.56	5.17	5.68	5.92	6.02	5.74 (85.0)	4.92	5.65	0.37
		1^1B_{1g}	6.60	6.13	6.41	6.70	7.13	6.75 (85.8)	5.42	6.69	0.41
		1^1B_{1u}	6.58	6.70	6.89	7.10	7.18	7.07 (93.3)	6.48	6.66	0.28
		2^1B_{1u}	7.72	7.57	7.79	8.13	8.34	8.06 (90.9)	6.91	7.62	0.32
		2^1B_{2u}	7.60	7.70	7.65	8.07	8.29	8.05 (89.7)	6.99	7.76	0.35
pyrimidine	6	1^1B_1	4.55	3.81	4.44	4.49	4.70	4.50 (88.4)	3.65	4.24	0.32
		1^1A_2	4.91	4.12	4.81	4.84	5.12	4.93 (88.2)	4.18	4.83	0.33
		1^1B_2	5.44	4.93	5.24	5.51	5.49	5.36 (85.7)	4.96	5.55	0.34
		2^1A_1	6.95	6.72	6.64	7.12	7.17	7.06 (92.2)	6.36	7.25	0.38
pyridazine	6	1^1B_1	3.78	3.48	3.78	3.90	4.11	3.92 (89.0)	3.26	3.67	0.30
		1^1A_2	4.32	3.66	4.32	4.40	4.76	4.49 (86.6)	3.66	4.25	0.31
		2^1A_1	5.18	4.86	5.18	5.37	5.35	5.22 (85.2)	4.28	5.16	0.40
		2^1A_2	5.77	5.09	5.77	5.81	6.00	5.74 (86.6)	4.82	5.53	0.35
triazine	6	$1^1A_1''$	4.60	3.90	4.60	4.70	4.96	4.78 (88.0)	3.23	4.44	0.37
		$1^1A_2''$	4.66	4.08	4.68	4.80	4.98	4.76 (88.0)	3.65	4.48	0.39
		$1^1E''$	4.71	4.36	4.71	4.77	5.01	4.81 (88.1)	3.49	4.48	0.37
		$1^1A_2'$	5.79	5.33	5.79	5.82	5.84	5.71 (85.1)	4.34	5.48	0.44
tetrazine	6	1^1B_{3u}	2.24	1.96	2.24	2.47	2.71	2.53 (89.6)	1.36	2.12	0.36
		1^1A_u	3.48	3.06	3.48	3.67	4.07	3.79 (87.5)	2.48	3.55	0.37
		1^1B_{1g}	4.73	4.51	4.73	5.10	5.32	4.97 (82.5)	4.06	4.94	0.41
		1^1B_{2u}	4.91	4.89	4.91	5.20	5.27	5.12 (84.6)	3.98	4.86	0.40
		2^1A_u	5.47	5.28	5.47	5.50	5.70	5.46 (87.4)	3.61	4.75	0.41
		1^1B_{2g}	5.18	5.05	5.18	5.53	5.70	5.34 (80.7)	4.25	5.28	0.43
cytosine	8	$2^1A'$	4.66	4.39	4.68	4.80	4.98	4.72 (86)	N/A	N/A	N/A
		$1^1A''$	4.87	5.00	5.12	5.13	5.45	5.16 (86)	4.47	5.06	0.32
		$2^1A''$	5.26	6.53	5.54	5.01	5.99	5.52 (83)	5.83	5.80	0.21
		$3^1A'$	5.62	5.36	5.54	5.71	5.95	5.61 (85)	4.78	5.56	0.37
thymine	8	$1^1A''$	4.82	4.39	4.94	4.94	5.14	4.98 (87)	4.91	4.90	0.23

	$2^1A'$	5.20	4.88	5.06	5.39	5.60	5.34 (89)	4.84	5.29	0.29
	$3^1A'$	6.27	5.88	6.15	6.46	6.78	6.34 (83)	4.56	5.94	0.50
	$2^1A''$	6.16	5.91	6.38	6.33	6.57	6.45 (89)	6.55	6.44	0.19
	$4^1A'$	6.53	6.10	6.52	6.80	7.05	6.71 (88)	4.91	6.45	0.48
uracil	$1^1A''$	4.80	4.54	4.90	4.91	5.11	4.90 (86)	4.82	4.83	0.23
	$2^1A'$	5.35	5.00	5.23	5.52	5.70	5.44 (88)	4.80	5.36	0.32
	$3^1A'$	6.26	5.82	6.15	6.43	6.76	6.29 (83)	N/A	N/A	N/A
	$3^1A''$	6.56	6.37	6.97	6.26	6.50	6.77 (91)	5.63	6.93	0.42
	$2^1A''$	6.10	6.00	6.27	6.73	7.68	6.32 (88)	6.49	6.39	0.19
	$4^1A'$	6.70	6.46	6.75	6.96	7.19	6.87 (88)	5.14	6.40	0.43
adenine	$2^1A'$	5.25	5.13	5.20	5.28	5.37	5.18 (86)	4.41	5.36	0.41
	$3^1A'$	5.25	5.20	5.30	5.42	5.61	5.39 (89)	4.90	5.37	0.32
	$1^1A''$	5.12	6.15	5.21	5.27	5.58	5.34 (88)	4.87	5.44	0.32
	$2^1A''$	5.75	6.86	5.97	5.91	6.19	5.96 (88)	5.12	5.84	0.34

Table 3.2: Mean unsigned errors and standard deviations for singlet excitation energies in eV. States without ESMF solutions and states identified by ESMP2 to have large doubly excited components (gray and red rows in Table 3.1) are excluded.

	SA-CASPT2	MS-CASPT2	CC2	EOM-CCSD	CC3	ESMP2	ϵ-ESMP2
Ketones and amides	0.20 ± 0.18	0.02 ± 0.05	0.29 ± 0.26	0.45 ± 0.38	0.26 ± 0.31	0.39 ± 0.37	0.17 ± 0.16
Conjugated polyenes	0.14 ± 0.09	0.34 ± 0.34	0.32 ± 0.22	0.57 ± 0.13	0.43 ± 0.12	0.27 ± 0.16	0.13 ± 0.13
Conjugated rings	0.32 ± 0.17	0.01 ± 0.03	0.22 ± 0.07	0.36 ± 0.16	0.18 ± 0.12	0.60 ± 0.40	0.15 ± 0.10
Heterocycles	0.34 ± 0.21	0.10 ± 0.13	0.28 ± 0.19	0.43 ± 0.19	0.23 ± 0.16	0.68 ± 0.42	0.17 ± 0.14
Nucleobases	0.41 ± 0.37	0.15 ± 0.10	0.21 ± 0.13	0.47 ± 0.33	0.17 ± 0.08	0.68 ± 0.52	0.19 ± 0.15
All	0.31 ± 0.24	0.09 ± 0.13	0.26 ± 0.18	0.43 ± 0.26	0.23 ± 0.19	0.60 ± 0.43	0.17 ± 0.14

Table 3.3: Mean unsigned errors and standard deviations for singlet excitation energies in eV. States without ESMF solutions and states identified by ESMP2 to have large doubly excited components (gray and red rows in Table 3.1) are excluded.

	BP86	B3LYP	BHLYP	DFT/MRCI	ESMP2	ϵ-ESMP2
Ketones and amides	0.55 ± 0.35	0.29 ± 0.19	0.35 ± 0.44	0.34 ± 0.21	0.39 ± 0.37	0.17 ± 0.16
Conjugated polyenes	0.52 ± 0.32	0.40 ± 0.22	0.22 ± 0.11	0.22 ± 0.13	0.27 ± 0.16	0.13 ± 0.13
Conjugated rings	0.51 ± 0.34	0.36 ± 0.19	0.29 ± 0.22	0.16 ± 0.13	0.60 ± 0.40	0.15 ± 0.10
Heterocycles	0.44 ± 0.29	0.21 ± 0.18	0.49 ± 0.26	0.17 ± 0.12	0.68 ± 0.42	0.17 ± 0.14
Nucleobases	0.83 ± 0.30	0.50 ± 1.20	0.57 ± 0.29	0.15 ± 0.12	0.68 ± 0.52	0.19 ± 0.15
All	0.54 ± 0.34	0.31 ± 0.54	0.44 ± 0.31	0.20 ± 0.16	0.60 ± 0.43	0.17 ± 0.14

Table 3.4: Mean unsigned errors and standard deviations for singlet excitation energies in eV. States without ESMF solutions and states identified by ESMP2 to have large doubly excited components (gray and red rows in Table 3.1) are excluded.

π system size	SA-CASPT2	MS-CASPT2	CC2	EOM-CCSD	CC3	ESMP2	ϵ-ESMP2
2	0.19 ± 0.17	0.11 ± 0.24	0.32 ± 0.27	0.39 ± 0.36	0.28 ± 0.34	0.21 ± 0.14	0.17 ± 0.16
3	0.12 ± 0.11	0.00 ± 0.00	0.28 ± 0.26	0.40 ± 0.43	0.30 ± 0.32	0.16 ± 0.18	0.13 ± 0.09
4	0.17 ± 0.16	0.17 ± 0.18	0.23 ± 0.12	0.43 ± 0.16	0.29 ± 0.16	0.24 ± 0.12	0.09 ± 0.13
5	0.41 ± 0.13	0.10 ± 0.10	0.38 ± 0.20	0.43 ± 0.18	0.21 ± 0.15	0.35 ± 0.34	0.17 ± 0.14
6	0.31 ± 0.22	0.11 ± 0.13	0.25 ± 0.17	0.42 ± 0.20	0.24 ± 0.17	0.75 ± 0.39	0.17 ± 0.14
8	0.34 ± 0.26	0.11 ± 0.11	0.22 ± 0.14	0.53 ± 0.31	0.19 ± 0.10	0.74 ± 0.47	0.20 ± 0.16
10	0.48 ± 0.34	0.04 ± 0.07	0.20 ± 0.08	0.39 ± 0.13	0.17 ± 0.10	0.69 ± 0.41	0.16 ± 0.10
5 or less	0.24 ± 0.18	0.09 ± 0.17	0.32 ± 0.23	0.41 ± 0.31	0.26 ± 0.27	0.24 ± 0.23	0.16 ± 0.13
6 or more	0.34 ± 0.26	0.10 ± 0.10	0.24 ± 0.15	0.45 ± 0.23	0.21 ± 0.14	0.74 ± 0.41	0.18 ± 0.14

3.5.3 Comparison to TD-DFT

Shortly after the introduction of the Thiel benchmark set, a followup study evaluated the performance of TD-DFT and DFT/MRCI on the same molecules and states. [134] In Table 3.3, we compare the results of that study to ESMP2 and ϵ-ESMP2. Due to its sensitivity to π system size, ESMP2 without regularization is clearly less accurate than typical TD-DFT approaches, which, having a very different mathematical structure, do not suffer the

same issue of small denominators as the lowest doubly excited configurations come down in energy. Indeed, TD-DFT under the usual adiabatic approximation leads to a formalism in which doubles do not participate in excited states at all. [109] ϵ-ESMP2, on the other hand, proves to be more accurate on the Thiel set singlet states than any of the TD-DFT functionals originally tested by Thiel, and this favorable comparison holds even when considering more recent benchmarking [40] of a much wider range of functionals, where MUEs were seen to range from just above 0.2 eV up to more than 0.5 eV. Even when the states with large $|T_2|$ are included (see tables in SI), ϵ-ESMP2 shows a MUE of 0.19 eV, although it is far from obvious that such states should be used in comparing these methods as TD-DFT cannot treat their doubly excited parts at all. Table 3.3 also shows that ϵ-ESMP2's accuracy is largely consistent across different types of molecules, whereas the density functionals tested by Thiel have accuracies that vary more widely, with the nucleobases proving the most difficult.

Another difference between TD-DFT and ESMP2 is the latter's ability to offer diagnostic information about the presence of doubly excited character. Although TD-DFT at N^4 is less expensive than ESMP2, it offers no information on such character, whereas ESMP2 can do so at N^5 cost. This is substantially lower than the N^7 cost of CC3, and the original Thiel set study makes clear that lower-level CC methods like EOM-CCSD are much less effective at predicting doubly excited character. [15] Thus, when checking for doubly excited character when trying to assess the trustworthiness of TD-DFT for a particular excited state, ESMP2 may offer a relatively affordable approach.

3.5.4 Group 1: Aldehydes, Ketones, and Amides

These molecules have many uses as functional groups in biological and photocatalytic settings,[135, 136, 137, 138] making them interesting both from a formal and a practical perspective. Thiel's CASPT2 approach (CASPT2 b) is especially accurate in this set of molecules with a MUE of just 0.02 eV. ϵ-ESMP2 is the next most accurate, followed by Roos's CASPT2, CC3, and CC2, with EOM-CCSD and ESMP2 being the least accurate. Previous TD-DFT work shows that TD-DFT methods with hybrid functionals usually give results comparable to EOM-CCSD in these molecules.[139, 140, 134] ϵ-ESMP2 proves to be more accurate than B3LYP in these molecules, which in turn is interestingly significantly more accurate than DFT/MRCI, which has more difficulty with this set of molecules than with any other.

3.5.4.1 Formaldehyde and Acetone

For formaldehyde and acetone three states were studied: 1^1A_2 of $n \rightarrow \pi^*$ character, 1^1B_1 of $\sigma \rightarrow \pi^*$ character, and 2^1A_1 of $\pi \rightarrow \pi^*$ character. It should be noted that the 2^1A_1 states of these molecules are known to have considerable Rydberg character, which cannot be described properly in the TZVP basis set as it lacks diffuse functions. We have chosen not to exclude these states from our analysis, because many other states in the Thiel set also have some Rydberg character to varying degrees, making it difficult to draw a clear line

between what to include and what not to. Of course, all the methods we are comparing with each other use the same TZVP basis and so are faced with this same issue.

These two molecules are particularly interesting for ESMP2, as they are the only cases in this benchmark where ESMP2 did as well as ϵ-ESMP2. Both methods produced errors with a relatively small magnitude of 0.1 eV for the non-Rydberg states. Interestingly, the addition of the level shift actually increased errors for the 1^1B_1 state in formaldehyde and the 1^1A_2 state in acetone, although ϵ-ESMP2 remains quite accurate. Another interesting and potentially noteworthy observation we made was that ESMP2 showed larger doubles norms for the Rydberg states and a much larger maximum individual amplitude value, raising the question of whether it would have any value in flagging Rydberg character. We don't have enough data in this study to say anything conclusive on this front, but it may be interesting to study further.

3.5.4.2 *p*-Benzoquinone

For benzoquinone, three $n \rightarrow \pi^*$ states - 1^1A_u, 1^1B_{1g}, 1^1B_{3u} - and three $\pi \rightarrow \pi^*$ states - 1^1B_{3g}, 1^1B_{1u}, 2^1B_{3g} - were studied. Within this group of molecules, benzoquinone showed by far the largest amount of doubly excited character, as seen in both the CC3 $\%T_1$ and the ESMP2 $|T_2|$ values. Unsurprisingly, unregularized ESMP2 performed quite poorly in benzoquinone, with ϵ-ESMP2 performing much better and more comparably to CC2 and CC3. ϵ-ESMP2's largest error in this molecule was 0.54 eV for the 1^1B_{3u} state, which has the most significant doubly excited character. This reminds us that, although ϵ-ESMP2 can improve significantly over ESMP2 when such character is present, it is no substitute for multi-reference methods in cases where the doubly excited component is large enough.

3.5.4.3 Formamide, Acetamide, and Propanamide

For each of these molecules, the $1^1A''$ $n \rightarrow \pi^*$ state, and the $2^1A'$ $\pi \rightarrow \pi^*$ state were studied. In the $2^1A'$ state of propanamide and especially acetamide, the excitation within the converged ESMF wave function contained fewer components than in EOM-CCSD, placing a higher fraction of the overall weight on the dominant HOMO→LUMO+2 component. We see this as a good reminder that both orbital relaxation and the degree to which correlation effects are captured can affect the degree of predicted mixing between excitation components.

ESMP2 was quite accurate for the $1^1A''$ excitation energies, with ϵ-ESMP2 less so, while ϵ-ESMP2 was much more accurate than ESMP2 for the $2^1A'$ states .Although none of these states has a particularly high degree of doubly excited character, the ESMP2 doubles norms do correctly predict the relative accuracy for the unregularized theory between these two states.A final noteworthy point is the unusually high errors made by CC2, EOM-CCSD, and CC3 in the $2^1A'$ state of formamide. It is not obvious what is driving this error, especially considering ESMP2's accuracy and the small effect of introducing regularization.

3.5.5 Group 2: Conjugated Polyenes

The four unsaturated polyene molecules in this group – ethene, butadiene, hexatriene, and octatetraene – provided a great deal of insight into how ESMP2 performs in the presence of doubly excited character, as the 2^1A_g states of butadiene, hexatriene, and octatetraene all have large doubly excited components, [141] which can for example be seen in their CC3 $\%T_1$ values. The ESMP2 doubles norm correctly flags all three of these doubly excited 2^1A_g states as likely to be problematic for ESMP2 and other single-reference methods. Although far superior to the other methods in the doubly excited state, Thiel's CASPT2 results (CASPT2 b) are not especially competitive for the 1^1B_2 states. Even more surprising is the degree of difficulty that CC3 has with the 1^1B_2 states, as they are dominated by singly excited components. Excited-state-specific DFT in the form of restricted open-shell Kohn Sham (ROKS) has also shown difficulty in these states, [139] with accuracy appearing to decrease as the basis set is enlarged. In the TD-DFT benchmark presented by Wiberg et al., [140] it was shown that the ethene and butadiene singly excited states were modeled best by functionals with higher amounts of Hartree Fock exchange. Indeed, in Thiel's TD-DFT benchmark, [134] BHLYP significantly outperformed B3LYP and BP86 in the 1^1B_2 states, although we find that ϵ-ESMP2 does better still.

3.5.5.1 Ethene

The only state studied for ethene was the 1^1B_{1u} state as the other low lying excited states for the molecule are strongly Rydberg in character and cannot be accurately described using the TZVP basis set used here.[142, 143] The 1^1B_{1u} state also contains significant valence-Rydberg mixing, however, it is still mostly described as a valence excited state. The Thiel best estimate value of 7.80 eV is based on a mixture experimental data and high-level *ab initio* results, though it was noted in the paper that defined the best estimates that the vertical excitation of the 1^1B_{1u} state could not be assigned precisely based on experimental data.[15]

In this state, ESMP2 and ϵ-ESMP2 performed similarly with errors of 0.25 and 0.24 eV, respectively, which makes sense given how strongly dominated this state is by single excitations. The CC methods EOM-CCSD, CC2, and CC3 all perform relatively poorly for this state with errors around 0.6-0.7 eV, and Thiel's CASPT2 shows an unusually large error of 0.82 eV. Roos's CASPT2 error is much smaller at 0.18 eV, and Thiel et al. report an almost exact result with a greatly expanded (8,20) active space, [15] a useful reminder of how important the choice of active space can be.

3.5.5.2 Butadiene, Hexatriene, and Octatetraene

For these three molecules, two states were studied each: the single-excitation-dominated 1^1B_u state, and the substantially doubly excited 2^1A_g state. As expected, ESMP2 performs considerably better for the 1^1B_u states (errors of 0.5 eV or below) than for the 2^1A_g (errors between 2 and 3 eV). Its redeeming quality in the latter states is it's ability to signal its

own failure through unusually large doubles norms of 0.77, 1.0, and 1.15, clearly warning the user to get their hands on a multi-reference method instead. To put how extreme these norms are in context, remember that the weight of the zeroth order reference in intermediate normalization is 1, meaning that this perturbation theory's perturbation is coming out as big or bigger than the zeroth order piece! Such a grossly nonsensical result is a clear sign of failure, which if heeded can help guide a user in selecting a more appropriate method. As for the 1^1B_u state, because our summary tables exclude states flagged as strongly doubly excited by ESMP2, the entry in Table 3.2 offers at a glance the performance on this less challenging, singly-excited state. ϵ-ESMP2 is considerably more accurate for this state than the CC methods, rivaled only by CASPT2 approaches with well chosen active spaces.

3.5.6 Group 3: Conjugated rings

With their larger π systems, this group of molecules proved especially difficult for unregularized ESMP2, whose overall accuracy in this group was worse than the other wave function methods. ϵ-ESMP2, on the other hand, outperformed the CC methods, and was in turn outperformed by Thiel's CASPT2. Although Thiel's selecton of CASPT2 to be the TBE in cyclopropene, norbornadiene, and naphthalene no doubt gives it a statistical advantage, we certainly expect it to be more accurate than ϵ-ESMP2 in these molecules. As in the polyenes, ROKS has shown a tendency for its accuracy to decrease with increasing basis set size in a number of these conjugated rings, both with and without the use of range separation. [139] DFT/MRCI, on the other hand performs quite well in these molecules, as does CC3.

3.5.6.1 Cyclopentadiene

We look at two $\pi \rightarrow \pi^*$ excitations in cyclopentadiene – the 1^1B_2 and 2^1A_1 states. While both are valence excited states without significant Rydberg mixing,[144] the former state is dominated by a single excitation, while the latter is a superposition of components that includes doubly excited pieces. Thiel calculates a 5.55 eV excitation energy from EOM-CCSDT evaluated with an "exhaustive" basis set as the TBE for the 1^1B_2 state, which is a bit above the carefully estimated 5.43(5) eV experimental value. [145] For the 2^1A_1 state, Thiel uses CASPT2 for the TBE. ESMP2 successfully predicts its own failure in the 2^1A_1 state, while ϵ-ESMP2 is similar in accuracy to CC3. As expected, ESMP2 does better for the 1^1B_2 state, and in that case is further improved by ϵ-ESMP2, which errors low by about the same amount that CC3 errors high.

3.5.6.2 Norbornadiene

Norbornadiene can be seen as the third and most structurally complicated member of a series begun by cis-butadiene and cyclopentadiene. [146] For calculations on the excited states of norbornadiene, one must consider that while it is formally not conjugated, there is indirect conjugation of the double bonds, allowing for through-space and through-bond

interactions – thus, interactions between π and σ orbitals are more important. [146] Two $\pi \rightarrow \pi^*$ excitations are examined in this benchmark – an experimentally forbidden 1^1A_2 state and a 1^1B_2 excited state that can mix strongly with nearby Rydberg states. [146] CASSCF studies, [146] CC3, and ESMP2 all indicate that both states are dominated by single excitations. Thiel selects CASPT2/TZVP for both TBEs, 5.34 eV and 6.11 eV, which lie a little above the reported experimental values of 5.25 eV and 5.95 eV. [147] ESMP2 produces excitation energy errors of 0.25 eV and 0.32 eV for the 1^1A_2 and 1^1B_2 states, respectively, making it more accurate than EOM-CCSD and on par with CC2 and CC3. ϵ-ESMP2 is the most accurate non-active-space method for these states, but is not as accurate as CASPT2.

3.5.6.3 Benzene

For benzene, we looked at the 1^1B_{1u}, 1^1B_{2u}, 1^1E_{1u}, and 2^1E_{2g} $\pi \rightarrow \pi^*$ excitations. The first three of these excitations are dominated by equally-weighted superpositions of excitations out of the degenerate π system HOMOs, while the largest component of the 2^1E_{2g} state is a single excitation out of the lowest energy π orbital. Thiel adopts Sánchez de Merás et al.'s CC3/ANO1 results as best estimates for the states. [148]

Benzene is a good example of a molecule where the EOM-CCSD can overestimate the degree of singly excited character compared to CC3. This issue is particularly stark in the 2^1E_{2g} state, where EOM-CCSD and CC3 disagree in their % T1 measures by 19%. Similarly, the inclusion of triples drops CC3's excitation energy in this state by 0.6 eV compared to CC2. As pointed out by Sánchez de Merás et al, [148] not all of these states show a uniform convergence order between CCS, CC2, EOM-CCSD, and CC3, with EOM-CCSD's excitation energy in the 1^1B_{2u} state lying below that of CC2, which is atypical among Thiel set states. These authors go on to use benzene to support an argument that EOM-CCSD is not a reliable guide to doubly excited character. With such considerable changes when going from the inclusion of doubles to the inclusion of triples, we have some doubts about the accuracy of the CC3 results as a best estimate for the significantly doubly excited 2^1E_{2g} state, and might instead have adopted CASPT2 values.

As in many other cases, ESMP2's doubles norms tell a similar story about doubly excited character as the CC3 % T1, and in particular signal clearly that ESMP2 is not appropriate for use in the 2^1E_{2g} state. ESMP2's excitation energy accuracy is poor in all of benzene's states, as is common for systems with six or more orbitals in their π system, but, with the exception of the 2^1E_{2g} state, ϵ-ESMP2 makes a large improvement to the point that it is competitive with CC2 and CC3. In 2^1E_{2g}, where ESMP2 signals its own failure, it is difficult not to look to CASPT2 as the preferred method among those tested, all things considered.

3.5.6.4 Naphthalene

We looked at the 1^1B_{3u}, 1^1B_{2u}, 2^1A_g, 1^1B_{1g}, 2^1B_{3u}, 2^1B_{1g}, 2^1B_{2u}, and 3^1A_g states of naphthalene, all of which are $\pi \rightarrow \pi^*$ transitions. The TBEs for these states were taken directly

from the MS-CASPT2/TZVP results, as this molecule's size limits other options. Based on the T_1% values from CC3, it is likely that many of these states involve significant amounts of doubly excited character. The 3^1A_g state had a particularly low T_1% of 70%, and is the first state we come to for which the ESMF stationary point could not be found.

For the other states, ESMP2 displayed a range of accuracies. It showed a particularly small error of 0.04 eV for the 1^1B_{1g} state, which, despite a relatively low CC3 T_1%, was also treated accurately by CC3 and CC2. In fact, this is one of the rare states in which regularization made the excitation energy prediction worse, with ϵ-ESMP2 giving an error of 0.37 eV. ESMP2's errors in the other naphthalene states were much larger, with some states showing significantly larger doubles norms as well, although not as large as in the doubly excited polyene states. In these other states, regularization makes a large improvement, making ϵ-ESMP2 competitive with CC2 and CC3.

3.5.7 Group 4: Heterocycles

The molecules in this group are furan, pyrrole, imidazole, pyridine, pyrazine, pyrimidine, pyridazine, triazine, and tetrazine. A common theme in these molecules is that almost all of the states studied here have at least moderate contributions from double excitations, at least as measured by the CC3 T_1%. As one might therefore expect, ESMP2's predictions were fairly inaccurate in this group. Regularization via ϵ-ESMP2 dramatically reduces these errors, to the point that it is more accurate than CC2, EOM-CCSD, and CC3. As in many other cases, only CASPT2 with Thiel's active spaces did better. It should, however, be noted that the CASPT2 b error is somewhat artificially small in this group, as it was used as the TBE for imidazole, pyridazine, triazine, and tetrazine. [15] Among DFT approaches, DFT/MRCI and TD-DFT/B3LYP perform particularly well in the heterocycles, [134] while ROKS performs well for some cases but shows difficult basis set dependence in others. [139] Further analysis of TD-DFT in some of these molecules can be found in a study by Caricato, et al. [149]

3.5.7.1 Pyrrole and Furan

We consider the following $\pi \rightarrow \pi^*$ excitations in pyrrole and furan: the 1^1B_2, 2^1A_1, and 3^1A_1 states. We analyze these two molecules together as their spectra are similar. Pyrrole's 2^1A_1 state and furan's 1^1B_2 and 2^1A_1 states are valence excited states, while the remaining states are considered to have Rydberg character. [144] For both molecules, Thiel's TBEs are based on CC3 calculations with basis set corrections. [150, 151]

The ESMP2 predictions were mixed in terms of accuracy. Both molecules had two states, the 3^1A_1 and 1^1B_2 states, that produces errors lower than 0.5 eV and then a 2^1A_1 state with an error of 1.53 eV in furan and 1.07 eV in pyrrole. This is not surprising given the large ESMP2 doubles norms in these states and the relatively low CC3 T_1 percentages of 85% and 86% As in many other molecules, regularization makes a big difference, and ϵ-ESMP2

reduces the errors in the 2^1A_1 states to below 0.05 eV while also lowering errors in most other states as well.

3.5.7.2 Imidazole

Imidazole is a case where experimental comparison is particularly challenging, as the UV-Vis spectrum has only been taken in ethanol and aqueous solutions. [152, 153, 154, 155, 156, 157, 158, 159] Further, there is disagreement about whether imidazole and imidazolium (the protonated form) have overlapping broad bands or each form separate strong peaks. [152] In any case, Thiel selected their CASPT2 results as the TBE for three singlet vertical excitations: the 1^1A" $n \rightarrow \pi^*$ state at 6.81 eV, and two $\pi \rightarrow \pi^*$ excitations of A' symmetry at 6.19 eV and 6.93 eV. CASSCF and CASPT2 calculations have shown that these states are not Rydberg in nature. [152]

Interestingly, there is some disagreement between different CASSCF approaches and also ESMF about the nature of these three states. If we consider the 6-electron, 5-orbital π system in imidazole, we would not expect the lowest-energy and nodeless 1a" π orbital to participate strongly in low-lying excitations. Instead, the occupied 2a" and 3a" π orbitals, which both have an additional nodal plane, can form up to four singlet excitations into the unoccupied 4a" and 5a" π^* orbitals. Thiel's work on MS-CASPT2 and CC3 shows the $2^1A'$ state as being dominated by the 3a"$\rightarrow$4a" excitation, while the $3^1A'$ state involves a positive superposition of the 2a"$\rightarrow$4a" and 3a"$\rightarrow$5a" excitations.[125] However, Roos found the states of A' symmetry to both have significant contributions from each of the 3a"$\rightarrow$4a", 2a"$\rightarrow$4a", and 3a"$\rightarrow$5a" excitations. [152] In our ESMF results, the A' states are essentially the plus and minus combinations of the 3a"$\rightarrow$4a" and 3a"$\rightarrow$5a" transitions, with very little contribution from 2a"$\rightarrow$4a". Taken together, these results show that imidazole is a case where the exact mixing of the components within excited states is quite sensitive to the amount of correlation and orbital relaxation in play.

In terms of energetics, ESMP2's excitation energies have an overall accuracy similar to that of CC3. Regularization only improves the accuracy in one of the three states, making this an unusual molecule in that regard and raising the question of how accurately ESMF has captured the zeroth order representation, especially in light of the disagreement between it and multiple versions of CASSCF in the A' states. It seems possible that this is a case where the primary singly excited components are close enough in energy that how they mix is substantially affected by correlation effects from doubly excited determinants, which is an effect that is simply beyond the reach of ESMF.

3.5.7.3 Pyridine

We studied the 1 $^1B_1$ and 2 $^1A_2$ $n \rightarrow \pi^*$ excitations and four $\pi \rightarrow \pi^*$ states: 1^1B_2, 2^1A_1, 3^1A_1 and 2^1B_2. The best estimates for these states comes from Nakatsuji et al's SAC-CI calculations, [160] which are close to experimental gas-phase excitation values. Using ESMP2 to predict the excitation energies for these states led to a mixture of errors. 2^1A_1

and 2^1A_2 had the smallest errors of 0.04 and 0.14 eV, respectively. 1^1B_2 and 1^1B_1 had errors of 0.33 and 0.34 eV, and the largest errors were from the 3^1A_1 and 2^1B_2 states with 0.63 and 0.73 eV. None of these states show especially large doubles norms, at least not compared for example to those seen in the polyenes. Although ESMF and EOM-CCSD both agree that the excited states of A_1 symmetry are superpositions of two main components, ESMF predicts much more equal superpositions than EOM-CCSD. Compared to other methods, ESMP2 is overall slightly more accurate than the coupled cluster methods, although the accuracy of both varies significantly from state to state. The overall accuracy of ϵ-ESMP2 is better, but this comes from improvements in some states partially counteracted by detriments in others.

3.5.7.4 Pyrazine

For pyrazine, four $n \rightarrow \pi^*$ states – 1^1B_{3u}, 1^1A_u, 1^1B_{2g}, 1^1B_{1g} – and four $\pi \rightarrow \pi^*$ states – 1^1B_{2u}, 1^1B_{1u}, 2^1B_{1u}, 2^1B_{2u} – were studied. Thiel selected EOM-CCSD($\widetilde{T}$) calculations for the TBEs, [15] compared to which ESMP2 produced a wide variety of errors, ranging from 0.10 eV in the 1^1B_{1u} state to 1.18 eV in the 1^1B_{1g} state. ϵ-ESMP2 shows significant improvements, with errors of less than 0.25 eV in all states. The CC methods do better than ESMP2 but worse than ϵ-ESMP2. The same is true of CASPT2, although its accuracy is much closer to that of ϵ-ESMP2.

3.5.7.5 Pyrimidine

Four excited states were studied for pyrimidine, two $n \rightarrow \pi^*$ states – 1^1B_1 and 1^1A_2 – and two $\pi \rightarrow \pi^*$ states – 1^1B_2 and 2^1A_1. The Thiel best estimates for the excited states of pyrimidine were based on coupled cluster results with non-iterative triples and basis set corrections. Generally these values error a few tenths of an electron volt high compared to experimental values. Based on the work presented in benchmarking studies by Loos, et. al.[161] and Schreiber et. al.[15] most ab initio methods error high for these states compared to experiment, not only the ones based on coupled cluster. An unusual feature in pyrimidine as compared to the other azabenzenes studied here is that EOM-CCSD does comparably to Thiel's CASPT2 and only slightly worse than CC2 and CC3. In the other azabenzenes, EOM-CCSD had noticeably higher errors when compared to CC2 and CC3. Without a level shift, ESMP2 is most similar in accuracy to Roos's CASPT2, with both methods producing large errors. ϵ-ESMP2 shows smaller errors, ranging from 0.08 to 0.31 eV, which is closer to but not as accurate as Thiel's CASPT2 and the CC methods.

3.5.7.6 Pyridazine

Three $n \rightarrow \pi^*$ states were studied in pyridazine: 1^1B_1, 1^1A_2, and 2^1A_2. While all of these states had ESMP2 errors above 0.5 eV, those for the 2^1A_2 and 2^1A_1 states were particularly large at almost 1 eV. Pyridazine is thus another good example of ESMP2's difficulties in larger π systems, but it is also one of the most powerful examples of the practical efficacy

of regularization, with all of ϵ-ESMP2's errors coming in at less than 0.25 eV. Comparing these results to other wave function methods, ESMP2 was easily the least accurate, while ϵ-ESMP2 performed similarly to CC2, was more accurate than EOM-CCSD, and was only slightly less accurate than CC3. The TBEs for this molecule were directly taken from Thiel's CASPT2 values, so it is difficult to make a fair comparison to that method.

3.5.7.7 *s*-Triazine

In triazine we studied three $n \rightarrow \pi^*$ states – $1^1A_1''$, $1^1A_2''$, $1^1E''$ – and one $\pi \rightarrow \pi^*$ state, $1^1A_2'$. Even compared to its performance on other azabenzenes, ESMP2 did poorly here with typical errors around 1 eV, making it by far the least accurate among the wave function methods. The CC3 T_1 values are all below 90% and the ESMP2 doubles norms all above 0.35, suggesting that triazine is simply a particularly painful example of the difficulty unregularized ESMP2 has when an extended π system brings the lowest doubly excited configurations too close to the primary singly excited configurations. Again, ϵ-ESMP2 significantly mitigates this difficulty, reducing the worst error to 0.31 eV instead of 1.45 eV. ϵ-ESMP2 is still less accurate than CC2 and CC3, but is comparable to EOM-CCSD and noticeably better than Roos's CASPT2.

3.5.7.8 *s*-Tetrazine

In this molecule we look at four $n \rightarrow \pi^*$ excitations – 1^1B_{3u}, 1^1B_{1g}, 1^1B_{2g}, and 2^1A_u – and two $\pi \rightarrow \pi^*$ excitations – 1^1A_u and 1^1B_{2u}. Note that we have not studied the strongly doubly excited 1^1B_{3g} state, and indeed the original Thiel benchmark does not even contain CC numbers for this state. As in a number of other heterocycles, Thiel's TBEs for tetrazine were taken directly from the CASPT2(b) results without basis set extrapolation. Against this TBE, CC2 and CC3 show errors mostly below about 0.3 eV, whereas EOM-CCSD errors are higher. As in triazine, all of tetrazine's CC3 $\%T_1$ values for the states studied are between 80 and 90, again implying a difficult playing field for unregularized EMSP2, which duly makes errors on the order of 1eV and shows doubles norms above 0.35. ESMP2 was especially bad for the 2^1A_u state, with an error of 1.86 eV, its worst error among the heterocycles. Introducing regularization via ϵ-ESMP2 makes a huge difference, reducing errors to less than 0.22 eV in all states except for 2^1A_u. The 2^1A_u state's error only falls to 0.72 eV, making it one of the worst for ϵ-ESMP2, especially considering that the ESMP2 doubles norm, although not small at 0.41, is not as large as in the difficult benzene or polyene states and so it is not as clear in this case that ESMP2 would be able to predict ϵ-ESMP2's failure. Outside of the 2^1A_u state, the accuracy of ϵ-ESMP2 is similar to the other wave function based methods.

3.5.8 Group 5: Nucleobases

This group of molecules includes cytosine, thymine, uracil, and adenine. Due to the size of these molecules, there were no CC3/TZVP calculations reported in the original Thiel benchmark, [15] and we have instead taken the CC3 data from a more recent study. [126] Thiel selected CC2/aug-cc-pVTZ results for the TBEs in all nucleobase states. We note that many of the nucleobase states were difficult for ESMF to converge to, which was even true in some cases in which the state was dominated by a single singly excited component. In both of the cases where ESMF failed to converge to a stationary point (the $2^1A'$ state of cytosine and the $3^1A'$ state of uracil), we hypothesize that a loss of good orthogonality with lower states during the ESMF optimization was partially to blame. Still, it is not clear why this was such an issue in these cases, as at least a small loss of orthogonality is normal in ESMF due to its state-specific orbital relaxation, and the same difficulty was not present in most other states.

For the excited states in this group, ESMP2 had an MUE of 0.61 eV, making it the wave function method with the worst overall accuracy, as seen in Table 3.2. ϵ-ESMP2, on the other hand, had a much smaller MUE of 0.19 eV, putting it on par with CC2 and ahead of EOM-CCSD. ϵ-ESMP2 was also more accurate in the nucleobases than the TD-DFT methods shown in Table 3.3, while being a little less accurate than DFT/MRCI.

3.5.8.1 Cytosine

In cytosine, we studied two $\pi \rightarrow \pi^*$ states – $2^1A'$ and $3^1A'$ – and two $n \rightarrow \pi^*$ states – $1^1A''$ and $2^1A''$. In the states ESMF successfully converged, ESMP2 with no level shift did fairly poorly with errors between 0.5 and 1 eV, which is similarly inaccurate to EOM-CCSD and worse than the other wave function methods. ESMP2 shows a notably peculiar result for the $2^1A''$ state in that it overestimates the excitation energy. In most other cases, ESMP2 tends to error low. This $2^1A''$ state remains an outlier even after introducing regularization, with the error barely changing. In contrast, regularization brings the errors for the other two below 0.2 eV.

3.5.8.2 Uracil

Five states were successfully studied in uracil: the $n \rightarrow \pi^*$ states with symmetry labels $1^1A''$, $2^1A''$, and $3^1A''$ and the $\pi \rightarrow \pi^*$ states with symmetry labels $2^1A'$ and $4^1A'$. ESMF failed to converge the $3^1A'$ state in uracil. Similar to the cytosine state, this state is dominated by a single singly excited component, so the reasons for this failure are not obvious. In the other states, ESMP2 does very well for the $1^1A''$ state with an error of just 0.02 eV, somewhat poorly for the $2^1A'$ and $2^1A''$ states with errors around 0.5 eV, and very poorly for the $3^1A''$ and $4^1A'$ states. In the other states, ESMP2 does very well for the $1^1A''$ state with an error of just 0.02 eV, somewhat poorly for the $2^1A'$ and $2^1A''$ states with errors around 0.5 eV, and very poorly for the $3^1A''$ and $4^1A'$ states. Overall, ESMP2 performs comparably to EOM-CCSD, but worse than the other wave function methods. Regularization reduces error

for the $2^1A'$ state to just 0.01 eV, leaves the error in the $1^1A''$ state essentially unchanged, and brings the other states' errors to around 0.3 eV. This places the accuracy of ϵ-ESMP2 ahead of EOM-CCSD and CC2, but still behind that of Thiel's CASPT2.

3.5.8.3 Thymine

For thymine we studied two $n \rightarrow \pi^*$ states, $1^1A''$ and $2^1A''$, and three $\pi \rightarrow \pi^*$ states – $2^1A'$, $3^1A'$, and $4^1A'$. ESMP2 does very well for $1^1A''$, achieves errors of around 0.5 eV for $2^1A'$ and $2^1A''$, and has errors of over 1.5 eV for $3^1A'$ and $4^1A'$. For both of the latter states, large doubles norms of 0.497 and 0.476, respectively, warn of the trouble. ϵ-ESMP2 has much lower errors for all states and makes particularly large improvements in the $3^1A''$ and $4^1A'$ states, with an overall accuracy in this molecule better than EOM-CCSD or Roos's CASPT2 but worse than CC2 and Thiel's CASPT2.

3.5.8.4 Adenine

For adenine we studied two $\pi \rightarrow \pi^*$ states, $2^1A'$ and $3^1A'$, and two $n \rightarrow \pi^*$ states, $1^1A''$ and $2^1A''$. ESMP2 gives errors above 0.5 eV for $2^1A'$ and $2^1A''$ and errors of around 0.3 eV for the $3^1A'$ and $1^1A''$ states, with an overall accuracy comparable to EOM-CCSD but worse than the other wave function methods. ϵ-ESMP2's worst error was 0.32 eV for the $1^1A''$ state, with its other errors all around 0.1 eV, making it much more comparable to CC2, although not as accurate as Thiel's CASPT2.

3.6 Conclusion

We have applied ESMP2 and its regularized ϵ-ESMP2 cousin to the singlet excitations in the 28 molecules of the Thiel set, which has clarified multiple aspects of this excited-state-specific perturbation theory's behavior and performance. First, we found that the underlying ESMF possesses a well-defined excited-state-specific stationary point in 100 out of the 103 states tested, suggesting that such stationary points typically exist for singly excited singlet states in single-reference molecules. Second, we found that ESMP2 is highly sensitive to the size of a molecule's π system. For molecules with five or fewer orbitals in their π systems, unregularized ESMP2's mean unsigned error was 0.32 eV, while for molecules with six or more orbitals in their π system it was 0.71 eV. Third, this sensitivity closely tracks the size of the ESMP2 doubles norm, which helps us understand the issue as a straightforward failure of perturbation theory brought about by doubly excited configurations that are too close in energy to the primary singles in the zeroth order reference. Fourth, although this sensitivity is bad news for accuracy, it allows the unregularized ESMP2 doubles norm to act as a reasonably effective predictor of doubly excited character. Finally, this sensitivity can be mitigated by repartitioning the zeroth order approximation via a level shift, resulting in the regularized ϵ-ESMP2 method that outperforms TD-DFT, CC2, EOM-CCSD, and even CC3 in overall accuracy on the singlet states in the Thiel set. While CASPT2 showed the

highest overall accuracy, ϵ-ESMP2's unsigned error of just 0.17 eV on singly excited states was the lowest among methods that do not rely on an active space.

3.7 Acknowledgements

This work was supported by the National Science Foundation's CAREER program under Award Number 1848012. Calculations were performed using the Berkeley Research Computing Savio cluster, the Lawrence Berkeley National Lab Lawrencium cluster, and the National Energy Research Scientific Computing Center, a DOE Office of Science User Facility supported by the Office of Science of the U.S. Department of Energy under Contract No. DE-AC02-05CH11231. J.A.R.S. and H.T. acknowledge that this material is based upon work supported by the National Science Foundation Graduate Research Fellowship Program under Grant No. DGE 2146752. Any opinions, findings, and conclusions or recommendations expressed in this material are those of the author(s) and do not necessarily reflect the views of the National Science Foundation.

Chapter 4

Conclusions

ESMP2, anN^5-scaling excited-state-specific perturbation theory, was discussed in detail in the body of this work. By using an orbital basis similar to natural transition orbitals and by limiting the number of off-diagonal elements in the reference Hamiltonian, the scaling of the excited-state perturbative method was reduced by two orders of N without having a large impact on the accuracy of the results. The new scaling matches that of MP2, the ground state analogue. By testing the accuracy of this method on the Thiel benchmarking set, we found that the addition of a regularizer in the form of an empirical level shift dramatically increases the accuracy of ESMP2, especially for molecules with large π systems. The accuracy of the regularized method rivaled that of higher scaling methods such as CC3 and EOM-CCSD. Additionally, as the amplitudes of the first order correction to the wave function should be small if the perturbation theory is valid, creating a diagnostic based on these amplitudes can act as a predictor of doubly excited character in excited states. The collection of work presented in this thesis shows that ESMP2 is a promising method for the study of excited states and the relatively low scaling and high accuracy of this method will make it an exciting choice for the study of realistic systems, such as solutes in explicit solvents.

Appendix A

Supplementary material for studying excited-state-specific perturbation theory on the Thiel set

Table A.1: Mean unsigned errors and standard deviations for singlet excitation energies in eV. All states are included, except in the case of ESMP2 and ϵ-ESMP2, which by necessity exclude states that lack ESMF solutions (gray rows in Table I).

	SA-CASPT2	MS-CASPT2	CC2	EOM-CCSD	CC3	ESMP2	ϵ-ESMP2
Ketones and amides	0.20 ± 0.18	0.02 ± 0.05	0.29 ± 0.26	0.45 ± 0.38	0.26 ± 0.31	0.39 ± 0.37	0.17 ± 0.16
Conjugated polyenes	0.15 ± 0.09	0.31 ± 0.25	0.76 ± 0.59	0.88 ± 0.46	0.44 ± 0.15	1.33 ± 1.36	0.31 ± 0.26
Conjugated rings	0.33 ± 0.20	0.02 ± 0.05	0.29 ± 0.18	0.45 ± 0.25	0.18 ± 0.12	0.67 ± 0.43	0.21 ± 0.22
Heterocycles	0.34 ± 0.21	0.10 ± 0.13	0.28 ± 0.19	0.42 ± 0.19	0.23 ± 0.16	0.71 ± 0.43	0.17 ± 0.14
Nucleobases	0.40 ± 0.35	0.14 ± 0.10	0.20 ± 0.12	0.46 ± 0.31	0.15 ± 0.09	0.68 ± 0.52	0.19 ± 0.15
All	0.31 ± 0.24	0.10 ± 0.13	0.30 ± 0.26	0.47 ± 0.30	0.23 ± 0.19	0.68 ± 0.58	0.19 ± 0.17

Table A.2: Mean unsigned errors and standard deviations for singlet excitation energies in eV. States without ESMF solutions (gray rows in Table I) are excluded.

	SA-CASPT2	MS-CASPT2	CC2	EOM-CCSD	CC3	ESMP2	ϵ-ESMP2
Ketones and amides	0.20 ± 0.18	0.02 ± 0.05	0.29 ± 0.26	0.45 ± 0.38	0.26 ± 0.31	0.39 ± 0.37	0.17 ± 0.16
Conjugated polyenes	0.15 ± 0.09	0.31 ± 0.25	0.76 ± 0.59	0.88 ± 0.46	0.44 ± 0.15	1.33 ± 1.36	0.31 ± 0.26
Conjugated rings	0.31 ± 0.19	0.02 ± 0.05	0.27 ± 0.17	0.41 ± 0.20	0.18 ± 0.12	0.67 ± 0.43	0.21 ± 0.22
Heterocycles	0.34 ± 0.21	0.10 ± 0.13	0.28 ± 0.19	0.42 ± 0.19	0.23 ± 0.16	0.71 ± 0.43	0.17 ± 0.14
Nucleobases	0.41 ± 0.37	0.15 ± 0.10	0.21 ± 0.13	0.47 ± 0.33	0.17 ± 0.08	0.68 ± 0.52	0.19 ± 0.15
All	0.31 ± 0.24	0.10 ± 0.14	0.30 ± 0.27	0.47 ± 0.30	0.23 ± 0.19	0.68 ± 0.58	0.19 ± 0.17

Table A.3: Mean unsigned errors and standard deviations for singlet excitation energies in eV. All states are included, except in the case of ESMP2 and ϵ-ESMP2, which by necessity exclude states that lack ESMF solutions (gray rows in Table I).

	BP86	B3LYP	BHLYP	DFT/MRCI	ESMP2	ϵ-ESMP2
Ketones and amides	0.55 ± 0.35	0.29 ± 0.19	0.35 ± 0.44	0.34 ± 0.21	0.39 ± 0.37	0.17 ± 0.16
Conjugated polyenes	0.38 ± 0.30	0.40 ± 0.19	0.70 ± 0.62	0.27 ± 0.14	1.33 ± 1.36	0.31 ± 0.26
Conjugated rings	0.47 ± 0.33	0.35 ± 0.19	0.42 ± 0.36	0.23 ± 0.23	0.67 ± 0.43	0.21 ± 0.22
Heterocycles	0.43 ± 0.29	0.20 ± 0.18	0.50 ± 0.26	0.18 ± 0.12	0.71 ± 0.43	0.17 ± 0.14
Nucleobases	0.82 ± 0.30	0.47 ± 1.14	0.57 ± 0.27	0.16 ± 0.13	0.68 ± 0.52	0.19 ± 0.15
All	0.53 ± 0.34	0.31 ± 0.52	0.49 ± 0.35	0.22 ± 0.17	0.68 ± 0.58	0.19 ± 0.17

Table A.4: Mean unsigned errors and standard deviations for singlet excitation energies in eV. States without ESMF solutions (gray rows in Table I) are excluded.

	BP86	B3LYP	BHLYP	DFT/MRCI	ESMP2	ϵ-ESMP2
Ketones and amides	0.55 ± 0.35	0.29 ± 0.19	0.35 ± 0.44	0.34 ± 0.21	0.39 ± 0.37	0.17 ± 0.16
Conjugated polyenes	0.38 ± 0.30	0.40 ± 0.19	0.70 ± 0.62	0.27 ± 0.14	1.33 ± 1.36	0.31 ± 0.26
Conjugated rings	0.47 ± 0.34	0.36 ± 0.19	0.39 ± 0.34	0.20 ± 0.21	0.67 ± 0.43	0.21 ± 0.22
Heterocycles	0.43 ± 0.29	0.20 ± 0.18	0.50 ± 0.26	0.18 ± 0.12	0.71 ± 0.43	0.17 ± 0.14
Nucleobases	0.83 ± 0.30	0.50 ± 1.20	0.57 ± 0.29	0.15 ± 0.12	0.68 ± 0.52	0.19 ± 0.15
All	0.52 ± 0.34	0.31 ± 0.52	0.48 ± 0.35	0.21 ± 0.17	0.68 ± 0.58	0.19 ± 0.17

Table A.5: Mean unsigned errors and standard deviations for singlet excitation energies in eV. All states are included, except in the case of ESMP2 and ϵ-ESMP2, which by necessity exclude states that lack ESMF solutions (gray rows in Table I).

π system size	SA-CASPT2	MS-CASPT2	CC2	EOM-CCSD	CC3	ESMP2	ϵ-ESMP2
2	0.19 ± 0.17	0.11 ± 0.24	0.32 ± 0.27	0.39 ± 0.36	0.28 ± 0.34	0.21 ± 0.14	0.17 ± 0.16
3	0.12 ± 0.11	0.00 ± 0.00	0.28 ± 0.26	0.40 ± 0.43	0.30 ± 0.32	0.16 ± 0.18	0.13 ± 0.09
4	0.25 ± 0.15	0.15 ± 0.15	0.57 ± 0.42	0.62 ± 0.24	0.28 ± 0.10	1.05 ± 0.99	0.23 ± 0.18
5	0.41 ± 0.12	0.09 ± 0.10	0.37 ± 0.18	0.41 ± 0.17	0.19 ± 0.15	0.48 ± 0.50	0.16 ± 0.14
6	0.31 ± 0.22	0.12 ± 0.13	0.30 ± 0.28	0.46 ± 0.27	0.24 ± 0.18	0.80 ± 0.50	0.20 ± 0.21
8	0.33 ± 0.25	0.10 ± 0.11	0.27 ± 0.28	0.56 ± 0.36	0.19 ± 0.12	0.86 ± 0.72	0.22 ± 0.17
10	0.49 ± 0.33	0.03 ± 0.07	0.24 ± 0.15	0.44 ± 0.23	0.17 ± 0.09	0.69 ± 0.41	0.16 ± 0.10
5 or less	0.24 ± 0.18	0.09 ± 0.17	0.36 ± 0.27	0.43 ± 0.31	0.26 ± 0.26	0.40 ± 0.52	0.17 ± 0.14
6 or more	0.34 ± 0.25	0.10 ± 0.10	0.28 ± 0.26	0.49 ± 0.30	0.23 ± 0.17	0.80 ± 0.56	0.20 ± 0.18

Table A.6: Mean unsigned errors and standard deviations for singlet excitation energies in eV. States without ESMF solutions (gray rows in Table I) are excluded.

π system size	SA-CASPT2	MS-CASPT2	CC2	EOM-CCSD	CC3	ESMP2	ϵ-ESMP2
2	0.19 ± 0.17	0.11 ± 0.24	0.32 ± 0.27	0.39 ± 0.36	0.28 ± 0.34	0.21 ± 0.14	0.17 ± 0.16
3	0.12 ± 0.11	0.00 ± 0.00	0.28 ± 0.26	0.40 ± 0.43	0.30 ± 0.32	0.16 ± 0.18	0.13 ± 0.09
4	0.15 ± 0.15	0.15 ± 0.15	0.57 ± 0.42	0.62 ± 0.24	0.28 ± 0.10	1.05 ± 0.99	0.23 ± 0.18
5	0.41 ± 0.12	0.09 ± 0.10	0.37 ± 0.18	0.41 ± 0.17	0.19 ± 0.15	0.48 ± 0.50	0.16 ± 0.14
6	0.31 ± 0.22	0.12 ± 0.13	0.30 ± 0.28	0.46 ± 0.27	0.24 ± 0.18	0.80 ± 0.50	0.20 ± 0.21
8	0.32 ± 0.25	0.10 ± 0.11	0.27 ± 0.29	0.56 ± 0.29	0.20 ± 0.12	0.86 ± 0.72	0.22 ± 0.17
10	0.48 ± 0.34	0.04 ± 0.07	0.20 ± 0.08	0.39 ± 0.13	0.17 ± 0.10	0.69 ± 0.41	0.16 ± 0.10
5 or less	0.24 ± 0.18	0.09 ± 0.17	0.36 ± 0.27	0.43 ± 0.31	0.26 ± 0.26	0.40 ± 0.52	0.17 ± 0.14
6 or more	0.34 ± 0.25	0.10 ± 0.10	0.27 ± 0.26	0.48 ± 0.29	0.22 ± 0.15	0.80 ± 0.56	0.20 ± 0.18

A.1 Level shift examples

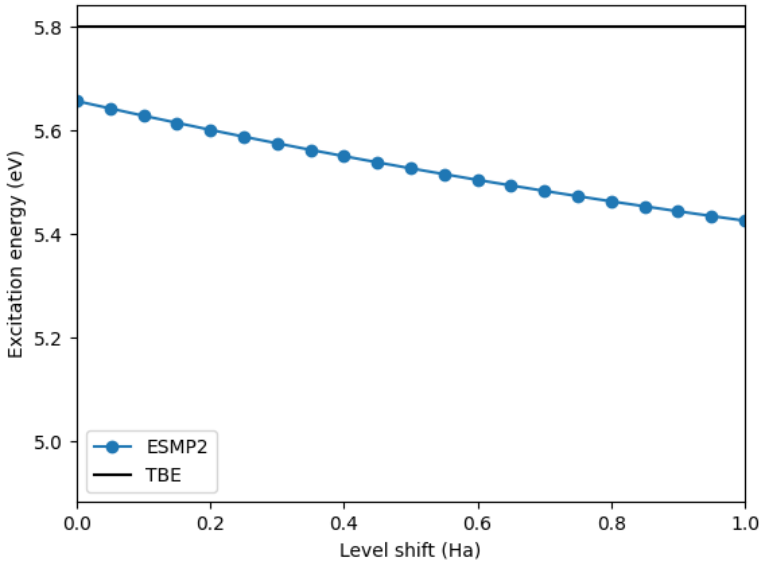

Figure A.1: Predicted excitation energies for the $1^1A''$ state of acetamide for different values of the level shift in ε-ESMP2. Note that the change in the excitation energy of this state between a level shift of 1.0 Ha and 0.0 Ha is about 0.1 eV, showing that the level shift had very little impact on the accuracy of the ESMP2 prediction.

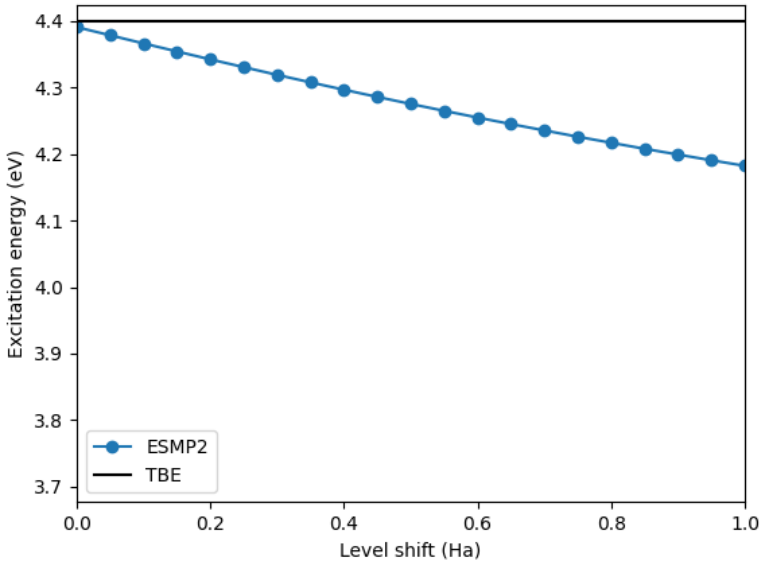

Figure A.2: Predicted excitation energies for the $2^1A'$ state of acetamide for different values of the level shift in ε-ESMP2. The change in the predicted excitation energy across the range of shifts is only about 0.2 eV, showing that the level shift has very little impact on the accuracy of the prediction.

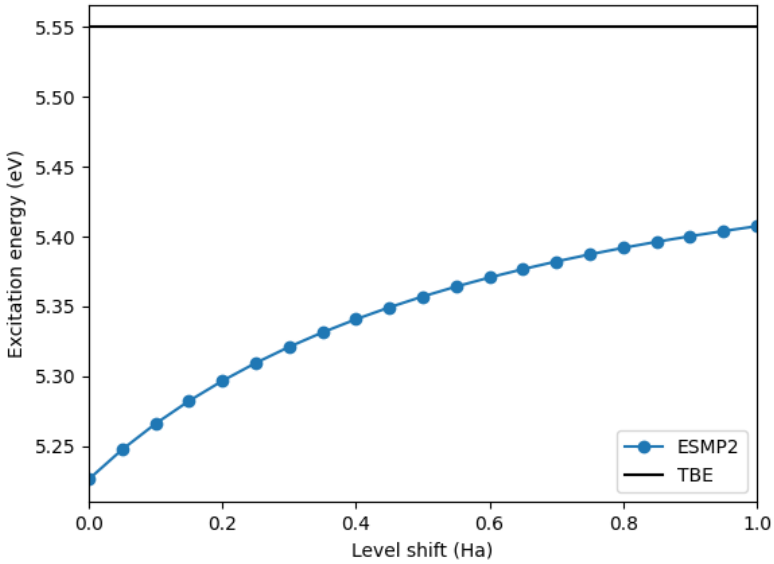

Figure A.3: Predicted excitation energies for the 1^1B_2 state of cyclopentadiene for different values of the level shift in ε-ESMP2. The change of predicted excitation energy for the shifts shown here is only 0.2 eV, showing that the predicted energy is not very sensitive to the choice of shift.

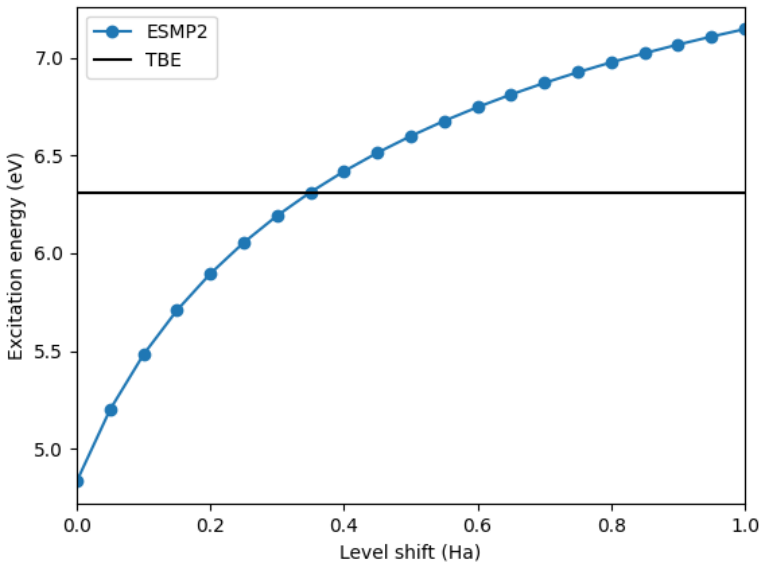

Figure A.4: Predicted excitation energies for the 2^1A_1 state of cyclopentadiene for different values of the level shift in ε-ESMP2. This state, likely because it has some doubly excited character, was very impacted by the addition of the level shift to the ESMP2 method.

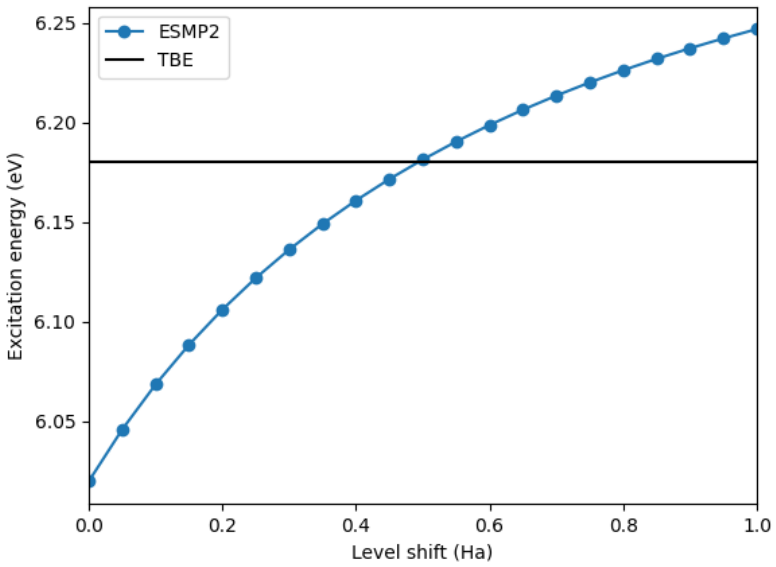

Figure A.5: Predicted excitation energies for the 1^1B_u state of butadiene for different values of the level shift in ε-ESMP2. The excitation energy only changes by 0.2eV across the range of tested level shifts, showing that this state is not very sensitive to the choice of shift.

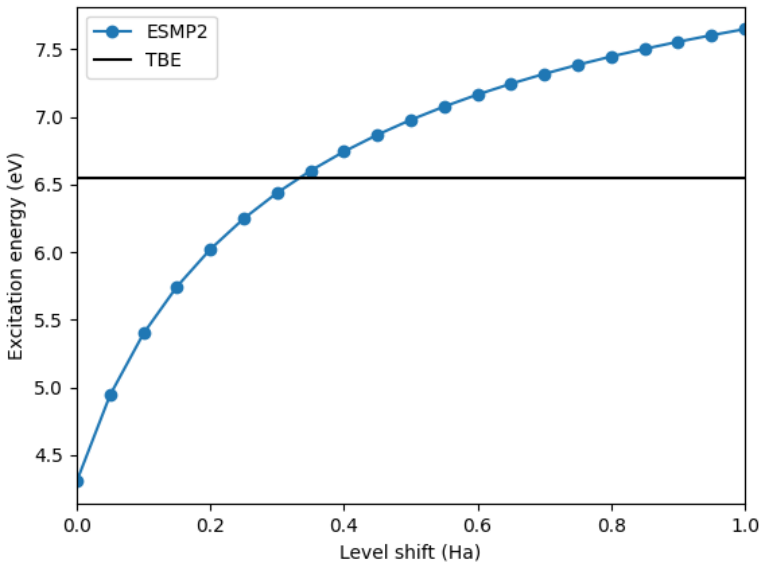

Figure A.6: Predicted excitation energies for the 2^1A_g state of butadiene for different values of the level shift in ε-ESMP2. Likely due to its partly doubly excited character, this state was highly sensitive to the level shift value.

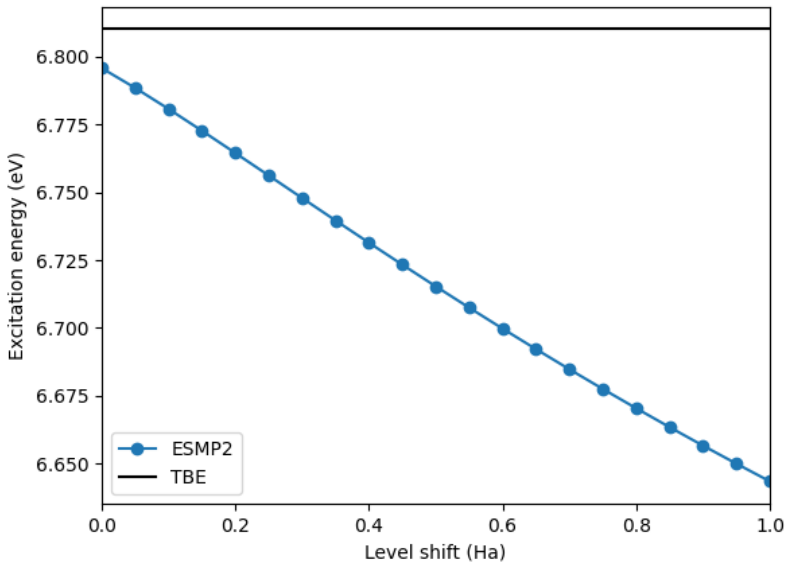

Figure A.7: Predicted excitation energies for the $1^1A''$ state of imidazole for different values of the level shift in ε-ESMP2. This state was only slightly impacted by the addition of the level shift, as the range of predicted excitation energies only varies by 0.15 eV.

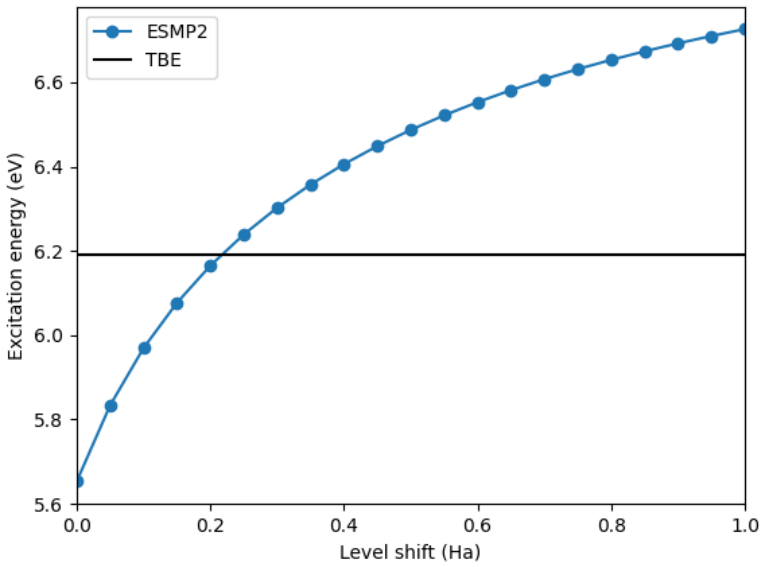

Figure A.8: Predicted excitation energies for the $2^1\mathrm{A}'$ state of imidazole for different values of the level shift in ε-ESMP2. This state is a good example of a state in a π system that is somewhat sensitive to regularization.

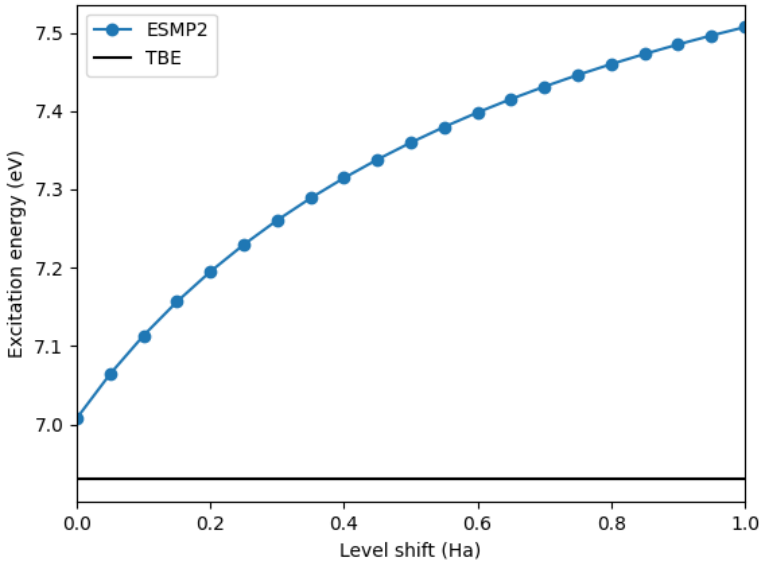

Figure A.9: Predicted excitation energies for the $3^1A'$ state of imidazole for different values of the level shift in ε-ESMP2. The addition of the level shift to ESMP2 had a large impact on the predicted excitation energy for this state, and it is a good example of a case where regularization does not improve accuracy.

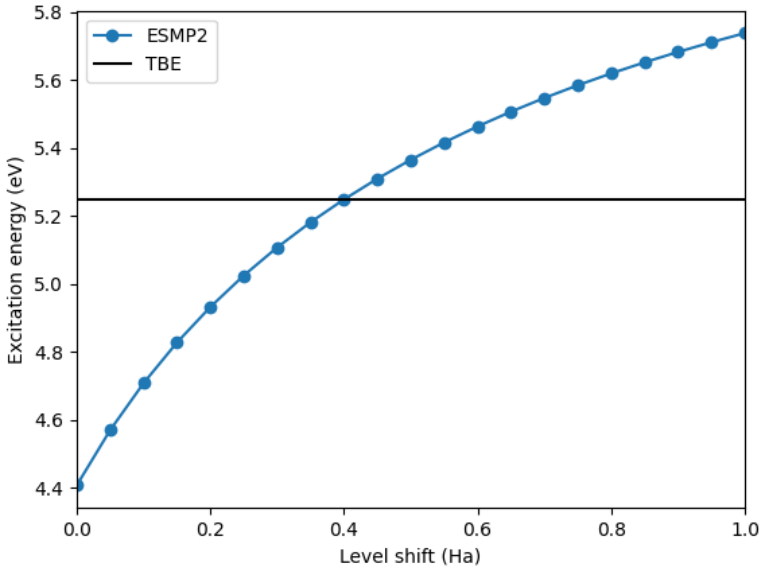

Figure A.10: Predicted excitation energies for the $2^1\mathrm{A}'$ state of adenine for different values of the level shift in ε-ESMP2. This is another example of a π system excitation that is sensitive to regularization.

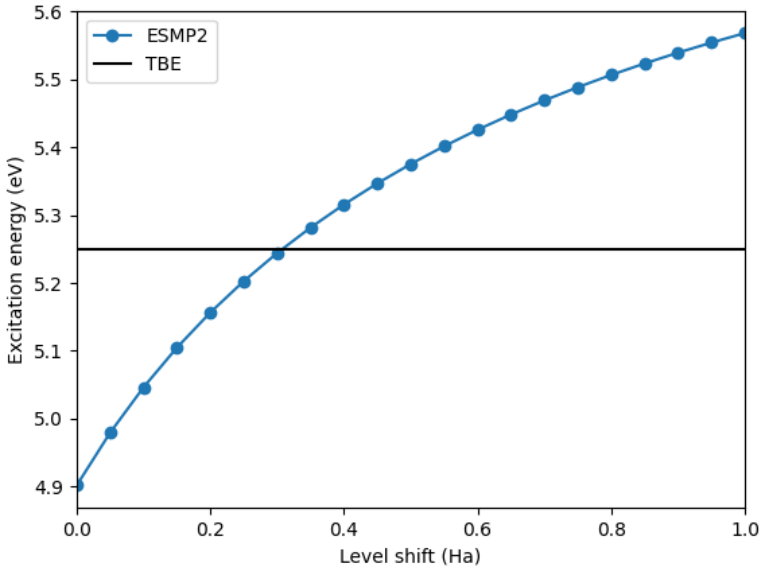

Figure A.11: Predicted excitation energies for the $3^1\mathrm{A}'$ state of adenine for different values of the level shift in ε-ESMP2. Similar to the $2^1\mathrm{A}'$ state above, adding regularization makes a significant difference here.

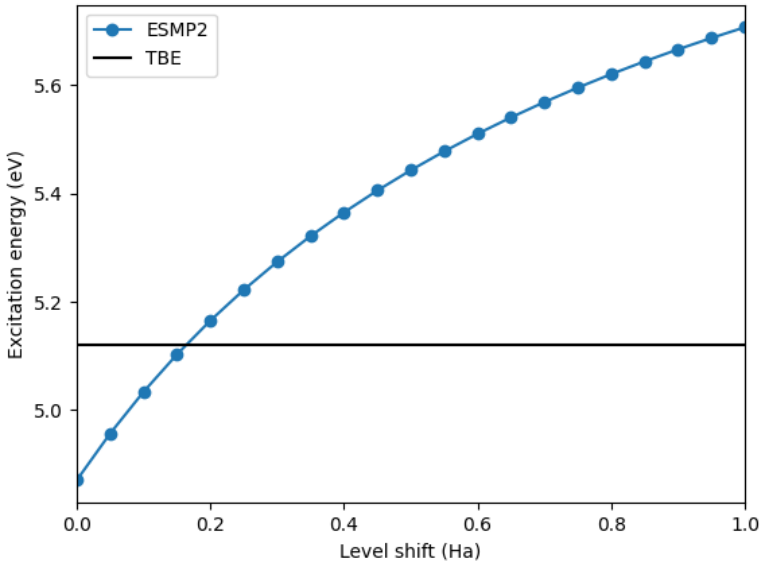

Figure A.12: Predicted excitation energies for the $1^1A''$ state of adenine for different values of the level shift in ε-ESMP2.

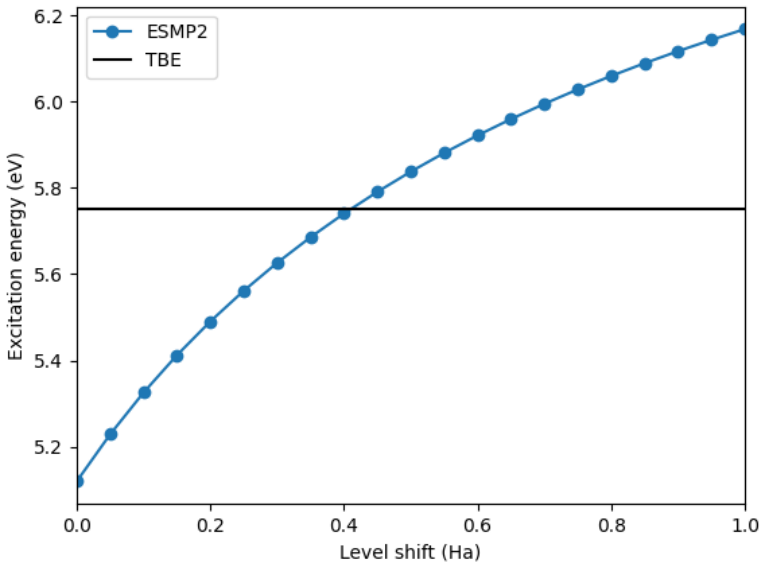

Figure A.13: Predicted excitation energies for the $2^1A''$ state of adenine for different values of the level shift in ε-ESMP2. Like the other adenine states studied here, the addition of a level shift makes a significant difference.

A.2 Formaldehyde

Table A.7: All methods singlet excitation energies in eV for molecule formaldehyde.

State	TBE	CASPT2[a]	CASPT2[b]	CC2	CCSD	CC3	ESMP2	lvl-ESMP2
1^1A_2	3.88	3.91	3.98	4.09	3.97	3.95	3.96	3.81
1^1B_1	9.10	9.09	9.14	9.35	9.26	9.18	9.12	8.98
2^1A_1	9.30	9.77	9.31	10.34	10.54	10.45	9.78	9.90

Table A.8: Absolute ESMF, ESMP2 and level shifted ESMP2 (level shift = 0.50 a.u.) results vs. the Thiel best estimates (TBEs) for formaldehyde.

State	TBE	ESMF	error	ESMP2	error	shift=0.50 a.u.	error
1^1A_2	3.88	2.93	0.95	3.96	0.08	3.81	0.07
1^1B_1	9.10	8.12	0.98	9.12	0.02	8.98	0.12
2^1A_1	9.30	9.22	0.08	9.78	0.48	9.90	0.60

Table A.9: Absolute ESMF, ESMP2 and level shifted ESMP2 (level shift = 0.50 a.u.) errors vs. the Thiel best estimates (TBEs) and the corresponding norm of the doubles amplitudes calculated from the norm of the first order ESMP wave function for formaldehyde.

State	lvl=0.0 error	norm	lvl=0.5 error	norm
1^1A_2	0.08	0.17	0.07	0.13
1^1B_1	0.02	0.17	0.12	0.14
2^1A_1	0.48	0.25	0.60	0.15

Table A.10: SA-CASSCF percentages for the amount of singles, doubles, and triples character for the excitations of formaldehyde.

State	%singles	%doubles	%triples
2^1A_1	92.50	2.04	0.26
1^1A_2	97.80	0.27	1.12
1^1B_1	100.00	0.00	0.00

Table A.11: Singles amplitudes with magnitudes above 0.2 from the ESMF and EOM-CCSD wave functions for the calculated states for formaldehyde.

State	ESMF	EOM
1^1A_2		
	H→L(0.62)	H→L(0.91)
	H−3→L(-0.20)	H→L+5(-0.23)
1^1B_1		
	H−2→L(0.63)	H−2→L(0.91)
		H−2→L+5(-0.24)
2^1A_1		
	H→L+2(0.60)	H→L+2(0.80)
		H−1→L(0.41)
		H→L(-0.28)

A.3 Acetone

Table A.12: All methods singlet excitation energies in eV for molecule acetone.

State	TBE	CASPT2[a]	CASPT2[b]	CC2	CCSD	CC3	ESMP2	lvl-ESMP2
1^1A_2	4.40	4.18	4.42	4.52	4.43	4.40	4.39	4.28
1^1B_1	9.10	9.10	9.27	9.29	9.26	9.17	9.22	9.16
2^1A_1	9.40	9.16	9.31	9.74	9.87	9.65	9.08	9.28

Table A.13: Absolute ESMF, ESMP2 and level shifted ESMP2 (level shift = 0.50 a.u.) results vs. the Thiel best estimates (TBEs) for acetone.

State	TBE	ESMF	error	ESMP2	error	shift=0.50 a.u.	error
1^1A_2	4.40	3.47	0.93	4.39	0.01	4.28	0.12
1^1B_1	9.10	8.48	0.62	9.22	0.12	9.16	0.06
2^1A_1	9.40	8.82	0.58	9.08	0.32	9.28	0.12

Table A.14: Absolute ESMF, ESMP2 and level shifted ESMP2 (level shift = 0.50 a.u.) errors vs. the Thiel best estimates (TBEs) and the corresponding norm of the doubles amplitudes calculated from the norm of the first order ESMP wave function for acetone.

State	lvl=0.0 error	norm	lvl=0.5 error	norm
1^1A_2	0.01	0.18	0.12	0.14
1^1B_1	0.12	0.19	0.06	0.15
2^1A_1	0.32	0.25	0.12	0.16

Table A.15: SA-CASSCF percentages for the amount of singles, doubles, and triples character for the excitations of acetone.

State	%singles	%doubles	%triples
1^1A_2	97.90	0.00	1.18
1^1B_1	100.00	0.00	0.00
2^1A_1	96.97	0.23	0.01

Table A.16: Singles amplitudes with magnitudes above 0.2 from the ESMF and EOM-CCSD wave functions for the calculated states for acetone.

State	ESMF	EOM
1^1A_2		
	H→L+1(0.58)	H→L+1(-0.88)
	H→L+4(-0.20)	H→L+4(-0.29)
	H−7→L+1(0.20)	
1^1B_1		
	H−3→L+1(-0.41)	H−3→L+1(-0.74)
	H−6→L+1(-0.41)	H−6→L+1(-0.48)
	H−8→L+1(0.23)	H−3→L+4(-0.23)
2^1A_1		
	H→L+2(0.60)	H→L+2(-0.68)
	H−1→L+1(0.17)	H−1→L+1(-0.58)

A.4 Benzoquinone

Table A.17: All methods singlet excitation energies in eV for molecule benzoquinone.

State	TBE	CASPT2[a]	CASPT2[b]	CC2	CCSD	CC3	ESMP2	lvl-ESMP2
1^1A_u	2.80	2.50	2.80	2.92	3.19	2.85	1.77	2.61
1^1B_{1g}	2.78	2.50	2.78	2.81	3.07	2.75	1.69	2.52
1^1B_{3g}	4.25	4.19	4.25	4.69	4.93	4.59	3.67	4.12
1^1B_{1u}	5.29	5.15	5.29	5.59	5.89	5.62	4.70	5.31
1^1B_{3u}	5.60	5.15	5.60	5.69	6.55	5.82	4.88	6.14
2^1B_{3g}	6.98	6.34	6.98	7.36	7.62	7.27	6.03	7.01

Table A.18: Absolute ESMF, ESMP2 and level shifted ESMP2 (level shift = 0.50 a.u.) results vs. the Thiel best estimates (TBEs) for benzoquinone.

State	TBE	ESMF	error	ESMP2	error	shift=0.50 a.u.	error
1^1A_u	2.80	3.52	0.72	1.77	1.03	2.61	0.19
1^1B_{1g}	2.78	3.50	0.72	1.69	1.09	2.52	0.26
1^1B_{3g}	4.25	4.56	0.31	3.67	0.58	4.12	0.13
1^1B_{1u}	5.29	6.03	0.74	4.70	0.59	5.31	0.02
1^1B_{3u}	5.60	8.14	2.54	4.88	0.72	6.14	0.54
2^1B_{3g}	6.98	8.27	1.29	6.03	0.95	7.01	0.03

Table A.19: Absolute ESMF, ESMP2 and level shifted ESMP2 (level shift = 0.50 a.u.) errors vs. the Thiel best estimates (TBEs) and the corresponding norm of the doubles amplitudes calculated from the norm of the first order ESMP wave function for benzoquinone.

State	lvl=0.0 error	norm	lvl=0.5 error	norm
1^1A_u	1.03	0.40	0.19	0.24
1^1B_{1g}	1.09	0.40	0.26	0.24
1^1B_{3g}	0.58	0.32	0.13	0.21
1^1B_{1u}	0.59	0.34	0.02	0.23
1^1B_{3u}	0.72	0.40	0.54	0.26
2^1B_{3g}	0.95	0.40	0.03	0.26

Table A.20: SA-CASSCF percentages for the amount of singles, doubles, and triples character for the excitations of benzoquinone.

State	%singles	%doubles	%triples
1^1A_u	66.62	22.22	2.86
1^1B_{1g}	66.83	21.61	2.52
1^1B_{3g}	71.31	20.76	1.16
1^1B_{1u}	76.71	15.96	1.60
1^1B_{3u}	27.93	53.72	5.59
2^1B_{3g}	68.82	18.78	2.90

Table A.21: Singles amplitudes with magnitudes above 0.2 from the ESMF and EOM-CCSD wave functions for the calculated states for benzoquinone.

State	ESMF	EOM
1^1A_u		
	H−3→L(-0.62)	H−2→L(0.89)
	H−2→L+3(-0.24)	H−3→L+3(0.26)
1^1B_{1g}		
	H−2→L(0.59)	H−3→L(-0.90)
	H−3→L+3(0.27)	H−2→L+3(-0.26)
1^1B_{3g}		
	H−1→L(0.69)	H−1→L(0.95)
1^1B_{1u}		
	H→L(0.66)	H→L(0.93)
1^1B_{3u}		
	H−2→L+1(-0.61)	H−2→L+1(-0.93)
	H−0→L(-0.30)	
2^1B_{3g}		
	H→L+1(-0.67)	H→L+1(-0.93)

A.5 Formamide

Table A.22: All methods singlet excitation energies in eV for molecule formamide.

State	TBE	CASPT2[a]	CASPT2[b]	CC2	CCSD	CC3	ESMP2	lvl-ESMP2
$1^1A''$	5.63	5.61	5.63	5.76	5.66	5.65	5.62	5.47
$2^1A'$	7.44	7.41	7.44	8.15	8.52	8.27	7.42	7.52

Table A.23: Absolute ESMF, ESMP2 and level shifted ESMP2 (level shift = 0.50 a.u.) results vs. the Thiel best estimates (TBEs) for formamide.

State	TBE	ESMF	error	ESMP2	error	shift=0.50 a.u.	error
$1^1A''$	5.63	4.56	1.07	5.62	0.01	5.47	0.16
$2^1A'$	7.44	7.03	0.41	7.42	0.02	7.52	0.08

Table A.24: Absolute ESMF, ESMP2 and level shifted ESMP2 (level shift = 0.50 a.u.) errors vs. the Thiel best estimates (TBEs) and the corresponding norm of the doubles amplitudes calculated from the norm of the first order ESMP wave function for formamide.

State	lvl=0.0 error	norm	lvl=0.5 error	norm
$1^1A''$	0.01	0.17	0.16	0.14
$2^1A'$	0.02	0.20	0.08	0.14

Table A.25: SA-CASSCF percentages for the amount of singles, doubles, and triples character for the excitations of formamide.

State	%singles	%doubles	%triples
$1^1A''$	99.34	0.00	0.00
$2^1A'$	91.20	0.00	0.00

Table A.26: Singles amplitudes with magnitudes above 0.2 from the ESMF and EOM-CCSD wave functions for the calculated states for formamide.

State	ESMF	EOM
$1^1A''$		
	H−1→L+2(-0.64)	H−1→L+2(-0.92)
		H−1→L+6(0.24)
$2^1A'$		
	H−1→L(-0.56)	H−1→L(0.74)
	H→L+2(-0.25)	H→L(0.53)

A.6 Acetamide

Table A.27: All methods singlet excitation energies in eV for molecule acetamide.

State	TBE	CASPT2[a]	CASPT2[b]	CC2	CCSD	CC3	ESMP2	lvl-ESMP2
$1^1A''$	5.80	5.54	5.80	5.77	5.71	5.69	5.66	5.53
$2^1A'$	7.27	7.21	7.27	7.66	7.85	7.67	6.88	7.30

Table A.28: Absolute ESMF, ESMP2 and level shifted ESMP2 (level shift = 0.50 a.u.) results vs. the Thiel best estimates (TBEs) for acetamide.

State	TBE	ESMF	error	ESMP2	error	shift=0.50 a.u.	error
$1^1A''$	5.80	4.67	1.13	5.66	0.14	5.53	0.27
$2^1A'$	7.27	7.85	0.58	6.88	0.39	7.30	0.03

Table A.29: Absolute ESMF, ESMP2 and level shifted ESMP2 (level shift = 0.50 a.u.) errors vs. the Thiel best estimates (TBEs) and the corresponding norm of the doubles amplitudes calculated from the norm of the first order ESMP wave function for acetamide.

State	lvl=0.0 error	norm	lvl=0.5 error	norm
$1^1A''$	0.14	0.18	0.27	0.14
$2^1A'$	0.39	0.27	0.03	0.20

Table A.30: SA-CASSCF percentages for the amount of singles, doubles, and triples character for the excitations of acetamide.

State	%singles	%doubles	%triples
$1^1A''$	93.51	4.23	0.00
$2^1A'$	85.23	8.08	0.10

Table A.31: Singles amplitudes with magnitudes above 0.2 from the ESMF and EOM-CCSD wave functions for the calculated states for acetamide.

State	ESMF	EOM
$1^1A''$		
	H−1→L+2(0.58)	H−1→L+2(0.85)
	H−1→L+5(0.27)	H−1→L+5(0.37)
$2^1A'$		
	H→L+2(-0.60)	H→L+2(-0.70)
		H−1→L(-0.50)
		H→L(-0.23)
		H−1→L+1(-0.21)
	H→L+5(0.25)	

A.7 Propanamide

Table A.32: All methods singlet excitation energies in eV for molecule propanamide.

State	TBE	CASPT2[a]	CASPT2[b]	CC2	CCSD	CC3	ESMP2	lvl-ESMP2
$1^1A''$	5.72	5.48	5.72	5.78	5.74	5.72	5.69	5.56
$2^1A'$	7.20	7.28	7.20	7.56	7.80	7.62	6.83	7.26

Table A.33: Absolute ESMF, ESMP2 and level shifted ESMP2 (level shift = 0.50 a.u.) results vs. the Thiel best estimates (TBEs) for propanamide.

State	TBE	ESMF	error	ESMP2	error	shift=0.50 a.u.	error
$1^1A''$	5.72	4.71	1.01	5.69	0.03	5.56	0.16
$2^1A'$	7.20	7.83	0.63	6.83	0.37	7.26	0.06

Table A.34: Absolute ESMF, ESMP2 and level shifted ESMP2 (level shift = 0.50 a.u.) errors vs. the Thiel best estimates (TBEs) and the corresponding norm of the doubles amplitudes calculated from the norm of the first order ESMP wave function for propanamide.

State	lvl=0.0 error	norm	lvl=0.5 error	norm
$1^1A''$	0.03	0.18	0.16	0.14
$2^1A'$	0.37	0.28	0.06	0.20

Table A.35: SA-CASSCF percentages for the amount of singles, doubles, and triples character for the excitations of propanamide.

State	%singles	%doubles	%triples
$1^1A''$	97.83	0.52	0.66
$2^1A'$	85.53	12.06	0.60

Table A.36: Singles amplitudes with magnitudes above 0.2 from the ESMF and EOM-CCSD wave functions for the calculated states for propanamide.

State	ESMF	EOM
$1^1A''$		
	H−1→L+2(-0.54)	H−1→L+2(-0.80)
	H−1→L+5(0.28)	H−1→L+5(-0.39)
		H−1→L+7(-0.23)
$2^1A'$		
	H→L+2(-0.58)	H→L+2(-0.63)
	H→L-5(0.26)	H−1→L(0.56)
		H−1→L+1(0.26)
		H→L(-0.22)

A.8 Ethene

Table A.37: All methods singlet excitation energies in eV for molecule ethene.

State	TBE	CASPT2[a]	CASPT2[b]	CC2	CCSD	CC3	ESMP2	lvl-ESMP2
1^1B_{1u}	7.80	7.98	8.62	8.40	8.51	8.37	8.05	8.04

Table A.38: Absolute ESMF, ESMP2 and level shifted ESMP2 (level shift = 0.50 a.u.) results vs. the Thiel best estimates (TBEs) for ethene.

State	TBE	ESMF	error	ESMP2	error	shift=0.50 a.u.	error
1^1B_{1u}	7.80	7.77	0.03	8.05	0.25	8.04	0.24

Table A.39: Absolute ESMF, ESMP2 and level shifted ESMP2 (level shift = 0.50 a.u.) errors vs. the Thiel best estimates (TBEs) and the corresponding norm of the doubles amplitudes calculated from the norm of the first order ESMP wave function for ethene.

State	lvl=0.0 error	norm	lvl=0.5 error	norm
1^1B_{1u}	0.25	0.16	0.24	0.13

Table A.40: SA-CASSCF percentages for the amount of singles, doubles, and triples character for the excitations of ethene.

State	%singles	%doubles	%triples
1^1B_{1u}	100.00	0.00	0.00

Table A.41: Singles amplitudes with magnitudes above 0.2 from the ESMF and EOM-CCSD wave functions for the calculated states for ethene.

State	ESMF	EOM
1^1B_{1u}		
	H→L(-0.69)	H→L(-0.96)

A.9 Butadiene

Table A.42: All methods singlet excitation energies in eV for molecule butadiene.

State	TBE	CASPT2[a]	CASPT2[b]	CC2	CCSD	CC3	ESMP2	lvl-ESMP2
1^1B_u	6.18	6.23	6.47	6.49	6.72	6.58	6.02	6.18
2^1A_g	6.55	6.27	6.83	7.63	7.42	6.77	4.31	6.98

Table A.43: Absolute ESMF, ESMP2 and level shifted ESMP2 (level shift = 0.50 a.u.) results vs. the Thiel best estimates (TBEs) for butadiene.

State	TBE	ESMF	error	ESMP2	error	shift=0.50 a.u.	error
1^1B_u	6.18	6.29	0.12	6.02	0.16	6.18	0.00
2^1A_g	6.55	8.85	2.30	4.31	2.24	6.98	0.43

Table A.44: Absolute ESMF, ESMP2 and level shifted ESMP2 (level shift = 0.50 a.u.) errors vs. the Thiel best estimates (TBEs) and the corresponding norm of the doubles amplitudes calculated from the norm of the first order ESMP wave function for butadiene.

State	lvl=0.0 error	norm	lvl=0.5 error	norm
1^1B_u	0.16	0.23	0.00	0.18
2^1A_g	2.24	0.77	0.43	0.31

Table A.45: SA-CASSCF percentages for the amount of singles, doubles, and triples character for the excitations of butadiene.

State	%singles	%doubles	%triples
1^1B_u	94.78	0.27	1.45
2^1A_g	54.77	41.30	1.52

Table A.46: Singles amplitudes with magnitudes above 0.2 from the ESMF and EOM-CCSD wave functions for the calculated states for butadiene.

State	ESMF	EOM
1^1B_u		
	H→L(-0.69)	H→L(-0.95)
2^1A_g		
	H−1→L(-0.48)	H→L+4(-0.63)
	H→L+4(0.45)	H−1→L(-0.54)

A.10 Hexatriene

Table A.47: All methods singlet excitation energies in eV for molecule hexatriene.

State	TBE	CASPT2[a]	CASPT2[b]	CC2	CCSD	CC3	ESMP2	lvl-ESMP2
1^1B_u	5.10	5.01	5.31	5.41	5.72	5.58	4.92	5.14
2^1A_g	5.09	5.20	5.42	6.67	6.61	5.72	2.37	5.81

Table A.48: Absolute ESMF, ESMP2 and level shifted ESMP2 (level shift = 0.50 a.u.) results vs. the Thiel best estimates (TBEs) for hexatriene.

State	TBE	ESMF	error	ESMP2	error	shift=0.50 a.u.	error
1^1B_u	5.10	5.34	0.25	4.92	0.18	5.14	0.04
2^1A_g	5.09	7.87	2.78	2.37	2.72	5.81	0.72

Table A.49: Absolute ESMF, ESMP2 and level shifted ESMP2 (level shift = 0.50 a.u.) errors vs. the Thiel best estimates (TBEs) and the corresponding norm of the doubles amplitudescalculated from the norm of the first order ESMP wave function for hexatriene.

State	lvl=0.0 error	norm	lvl=0.5 error	norm
1^1B_u	0.18	0.26	0.04	0.18
2^1A_g	2.72	1.00	0.72	0.32

Table A.50: SA-CASSCF percentages for the amount of singles, doubles, and triples character for the excitations of hexatriene.

State	%singles	%doubles	%triples
2^1A_g	43.16	51.05	1.31
1^1B_u	46.50	26.71	20.85

Table A.51: Singles amplitudes with magnitudes above 0.2 from the ESMF and EOM-CCSD wave functions for the calculated states for hexatriene.

State	ESMF	EOM
1^1B_u		
	H→L(0.68)	H→L(-0.95)
2^1A_g		
	H−1→L(0.43)	H−1→L(-0.59)
	H→L+2(-0.43)	H→L+2(-0.55)

A.11 Octatetraene

Table A.52: All methods singlet excitation energies in eV for molecule octatetraene.

State	TBE	CASPT2[a]	CASPT2[b]	CC2	CCSD	CC3	ESMP2	lvl-ESMP2
2^1A_g	4.47	4.38	4.64	5.87	5.99	4.97	1.19	4.99
1^1B_u	4.66	4.42	4.70	4.72	5.07	4.94	4.16	4.43

Table A.53: Absolute ESMF, ESMP2 and level shifted ESMP2 (level shift = 0.50 a.u.) results vs. the Thiel best estimates (TBEs) for octatetraene.

State	TBE	ESMF	error	ESMP2	error	shift=0.50 a.u.	error
2^1A_g	4.47	7.01	2.54	1.19	3.28	4.99	0.52
1^1B_u	4.66	4.71	0.05	4.16	0.50	4.43	0.23

Table A.54: Absolute ESMF, ESMP2 and level shifted ESMP2 (level shift = 0.50 a.u.) errors vs. the Thiel best estimates (TBEs) and the corresponding norm of the doubles amplitudes calculated from the norm of the first order ESMP wave function for octatetraene.

State	lvl=0.0 error	norm	lvl=0.5 error	norm
2^1A_g	3.28	1.15	0.52	0.33
1^1B_u	0.50	0.28	0.23	0.19

Table A.55: SA-CASSCF percentages for the amount of singles, doubles, and triples character for the excitations of octatetraene.

State	%singles	%doubles	%triples
2^1A_g	38.21	46.53	0.67
1^1B_u	36.52	46.90	0.00

Table A.56: Singles amplitudes with magnitudes above 0.2 from the ESMF and EOM-CCSD wave functions for the calculated states for octatetraene.

State	ESMF	EOM
2^1A_g		
	H→L+2(0.45)	H−1→L(-0.62)
	H−1→L(0.35)	H→L+2(-0.53)
1^1B_u		
	H→L(-0.68)	H→L(-0.95)

A.12 Cyclopropene

Table A.57: All methods singlet excitation energies in eV for molecule cyclopropene.

State	TBE	CASPT2[a]	CASPT2[b]	CC2	CCSD	CC3	ESMP2	lvl-ESMP2
1^1B_1	6.76	6.36	6.76	6.96	6.96	6.90	6.56	6.61
1^1B_2	7.06	7.45	7.06	7.17	7.24	7.10	6.75	6.85

Table A.58: Absolute ESMF, ESMP2 and level shifted ESMP2 (level shift = 0.50 a.u.) results vs. the Thiel best estimates (TBEs) for cyclopropene.

State	TBE	ESMF	error	ESMP2	error	shift=0.50 a.u.	error
1^1B_1	6.76	6.44	0.32	6.56	0.20	6.61	0.15
1^1B_2	7.06	6.76	0.30	6.75	0.31	6.85	0.21

Table A.59: Absolute ESMF, ESMP2 and level shifted ESMP2 (level shift = 0.50 a.u.) errors vs. the Thiel best estimates (TBEs) and the corresponding norm of the doubles amplitudes calculated from the norm of the first order ESMP wave function for cyclopropene.

State	lvl=0.0 error	norm	lvl=0.5 error	norm
1^1B_1	0.20	0.20	0.15	0.15
1^1B_2	0.31	0.20	0.21	0.15

Table A.60: SA-CASSCF percentages for the amount of singles, doubles, and triples character for the excitations of cyclopropene.

State	%singles	%doubles	%triples
1^1B_1	100.00	0.00	0.00
1^1B_2	100.00	0.00	0.00

Table A.61: Singles amplitudes with magnitudes above 0.2 from the ESMF and EOM-CCSD wave functions for the calculated states for cyclopropene.

State	ESMF	EOM
1^1B_1		
	H−1→L(0.68)	H−1→L(0.94)
		H−1→L+14(0.21)
1^1B_2		
	H→L(0.67)	H→L(0.93)

A.13 Cyclopentadiene

Table A.62: All methods singlet excitation energies in eV for molecule cyclopentadiene.

State	TBE	CASPT2[a]	CASPT2[b]	CC2	CCSD	CC3	ESMP2	lvl-ESMP2
1^1B_2	5.55	5.27	5.51	5.69	5.87	5.73	5.23	5.36
2^1A_1	6.31	6.31	6.31	7.05	7.05	6.61	4.83	6.60

Table A.63: Absolute ESMF, ESMP2 and level shifted ESMP2 (level shift = 0.50 a.u.) results vs. the Thiel best estimates (TBEs) for cyclopentadiene.

State	TBE	ESMF	error	ESMP2	error	shift=0.50 a.u.	error
1^1B_2	5.55	5.40	0.15	5.23	0.32	5.36	0.19
2^1A_1	6.31	8.27	1.96	4.83	1.48	6.60	0.29

Table A.64: Absolute ESMF, ESMP2 and level shifted ESMP2 (level shift = 0.50 a.u.) errors vs. the Thiel best estimates (TBEs) and the corresponding norm of the doubles amplitudes calculated from the norm of the first order ESMP wave function for cyclopentadiene.

State	lvl=0.0 error	norm	lvl=0.5 error	norm
1^1B_2	0.32	0.23	0.19	0.17
2^1A_1	1.48	0.59	0.29	0.28

Table A.65: SA-CASSCF percentages for the amount of singles, doubles, and triples character for the excitations of cyclopentadiene.

State	%singles	%doubles	%triples
2^1A_1	42.65	56.41	0.13
1^1B_2	99.19	0.59	0.05

Table A.66: Singles amplitudes with magnitudes above 0.2 from the ESMF and EOM-CCSD wave functions for the calculated states for cyclopentadiene.

State	ESMF	EOM
1^1B_2		
	H→L(0.69)	H→L(-0.96)
2^1A_1		
	H−1→L(0.49)	H−1→L(0.67)
	H→L+7(0.47)	H→L+7(-0.59)

A.14 Norbornadiene

Table A.67: All methods singlet excitation energies in eV for molecule norbornadiene.

State	TBE	CASPT2[a]	CASPT2[b]	CC2	CCSD	CC3	ESMP2	lvl-ESMP2
1^1A_2	5.34	5.28	5.34	5.57	5.80	5.64	5.09	5.31
1^1B_2	6.11	6.20	6.11	6.37	6.69	6.49	5.79	6.31

Table A.68: Absolute ESMF, ESMP2 and level shifted ESMP2 (level shift = 0.50 a.u.) results vs. the Thiel best estimates (TBEs) for norbornadiene.

State	TBE	ESMF	error	ESMP2	error	shift=0.50 a.u.	error
1^1A_2	5.34	5.49	0.15	5.09	0.25	5.31	0.03
1^1B_2	6.11	7.12	1.01	5.79	0.32	6.31	0.20

Table A.69: Absolute ESMF, ESMP2 and level shifted ESMP2 (level shift = 0.50 a.u.) errors vs. the Thiel best estimates (TBEs) and the corresponding norm of the doubles amplitudes calculated from the norm of the first order ESMP wave function for norbornadiene.

State	lvl=0.0 error	norm	lvl=0.5 error	norm
1^1A_2	0.25	0.25	0.03	0.18
1^1B_2	0.32	0.28	0.20	0.20

Table A.70: SA-CASSCF percentages for the amount of singles, doubles, and triples character for the excitations of norbornadiene.

State	%singles	%doubles	%triples
1^1A_2	99.93	0.00	0.00
1^1B_2	99.47	0.00	0.53

Table A.71: Singles amplitudes with magnitudes above 0.2 from the ESMF and EOM-CCSD wave functions for the calculated states for norbornadiene.

State	ESMF	EOM
1^1A_2		
	H→L(0.68)	H→L(0.95)
1^1B_2		
	H−1→L(0.67)	H−1→L(0.89)
		H→L(-0.29)

A.15 Benzene

Table A.72: All methods singlet excitation energies in eV for molecule benzene.

State	TBE	CASPT2[a]	CASPT2[b]	CC2	CCSD	CC3	ESMP2	lvl-ESMP2
1^1B_{2u}	5.08	4.84	5.05	5.27	5.19	5.07	4.03	4.98
1^1B_{1u}	6.54	6.30	6.45	6.68	6.74	6.68	6.07	6.24
1^1E_{1u}	7.13	7.03	7.07	7.44	7.65	7.45	6.48	7.11
2^1E_{2g}	8.41	7.90	8.21	9.03	9.21	8.43	7.60	9.37

Table A.73: Absolute ESMF, ESMP2 and level shifted ESMP2 (level shift = 0.50 a.u.) results vs. the Thiel best estimates (TBEs) for benzene.

State	TBE	ESMF	error	ESMP2	error	shift=0.50 a.u.	error
1^1B_{2u}	5.08	6.08	1.00	4.03	1.05	4.98	0.10
1^1B_{1u}	6.54	6.22	0.32	6.07	0.47	6.24	0.30
1^1E_{1u}	7.13	7.89	0.76	6.48	0.65	7.11	0.02
2^1E_{2g}	8.41	10.65	2.24	7.60	0.81	9.37	0.96

Table A.74: Absolute ESMF, ESMP2 and level shifted ESMP2 (level shift = 0.50 a.u.) errors vs. the Thiel best estimates (TBEs) and the corresponding norm of the doubles amplitudes calculated from the norm of the first order ESMP wave function for benzene.

State	lvl=0.0 error	norm	lvl=0.5 error	norm
1^1B_{2u}	1.05	0.42	0.10	0.26
1^1B_{1u}	0.47	0.27	0.30	0.18
1^1E_{1u}	0.65	0.31	0.02	0.21
2^1E_{2g}	0.81	0.60	0.96	0.26

Table A.75: SA-CASSCF percentages for the amount of singles, doubles, and triples character for the excitations of benzene.

State	%singles	%doubles	%triples
1^1B_{2u}	79.74	17.13	1.25
1^1B_{1u}	94.77	3.46	0.09
1^1E_{1u}	45.42	46.89	5.00
2^1E_{2g}	88.11	5.47	3.59

Table A.76: Singles amplitudes with magnitudes above 0.2 from the ESMF and EOM-CCSD wave functions for the calculated states for benzene.

State	ESMF	EOM
1^1B_{2u}		
	H−1→L(0.50)	H→L+1(0.66)
	H→L+1(0.50)	H−1→L(-0.66)
1^1B_{1u}		
	H→L(-0.50)	H−1→L+1(0.68)
	H−1→L+1(0.50)	H→L(0.68)
1^1E_{1u}		
	H→L+1(-0.48)	H−1→L(0.66)
	H−1→L(0.49)	H→L+1(0.66)
2^1E_{2g}		
	H−4→L+1(0.69)	H−4→L+1(0.84)
		H−1→L+9(-0.32)
		H−1→L+1(0.20)

A.16 Naphthalene

Table A.77: All methods singlet excitation energies in eV for molecule naphthalene.

State	TBE	CASPT2[a]	CASPT2[b]	CC2	CCSD	CC3	ESMP2	lvl-ESMP2
1^1B_{3u}	4.24	4.03	4.24	4.45	4.41	4.27	3.22	4.13
1^1B_{2u}	4.77	4.56	4.77	4.96	5.21	5.03	4.33	4.73
2^1A_g	5.90	5.39	5.90	6.22	6.23	5.98	5.06	6.11
1^1B_{1g}	6.00	5.53	6.00	6.21	6.53	6.07	5.96	6.37
2^1B_{3u}	6.07	5.54	6.07	6.25	6.55	6.33	5.33	5.99
2^1B_{1g}	6.48	5.87	6.48	6.82	6.97	6.79	4.96	6.30
2^1B_{2u}	6.33	5.93	6.33	6.57	6.77	6.57	5.42	6.22
3^1A_g	6.71	6.04	6.71	7.34	7.77	6.90	N/A	N/A

Table A.78: Absolute ESMF, ESMP2 and level shifted ESMP2 (level shift = 0.50 a.u.) results vs. the Thiel best estimates (TBEs) for naphthalene.

State	TBE	ESMF	error	ESMP2	error	shift=0.50 a.u.	error
1^1B_{3u}	4.24	5.17	0.93	3.22	1.02	4.13	0.11
1^1B_{2u}	4.77	5.04	0.27	4.33	0.44	4.73	0.04
2^1A_g	5.90	7.28	1.38	5.06	0.84	6.11	0.21
1^1B_{1g}	6.00	6.69	0.69	5.96	0.04	6.37	0.37
2^1B_{3u}	6.07	6.85	0.78	5.33	0.74	5.99	0.08
2^1B_{1g}	6.48	7.76	1.28	4.96	1.52	6.30	0.18
2^1B_{2u}	6.33	7.11	0.78	5.42	0.91	6.22	0.11

Table A.79: Absolute ESMF, ESMP2 and level shifted ESMP2 (level shift = 0.50 a.u.) errors vs. the Thiel best estimates (TBEs) and the corresponding norm of the doubles amplitudes calculated from the norm of the first order ESMP wave function for naphthalene.

State	lvl=0.0 error	norm	lvl=0.5 error	norm
1^1B_{3u}	1.02	0.42	0.11	0.26
1^1B_{2u}	0.44	0.33	0.04	0.21
2^1A_g	0.84	0.42	0.21	0.26
1^1B_{1g}	0.04	0.31	0.37	0.20
2^1B_{3u}	0.74	0.33	0.08	0.22
2^1B_{1g}	1.52	0.49	0.18	0.27
2^1B_{2u}	0.91	0.36	0.11	0.23

Table A.80: SA-CASSCF percentages for the amount of singles, doubles, and triples character for the excitations of naphthalene.

State	%singles	%doubles	%triples
1^1B_{3u}	71.64	12.61	1.91
1^1B_{2u}	84.65	7.18	0.92
2^1A_g	57.47	19.95	1.18
1^1B_{1g}	54.81	25.21	0.02
2^1B_{3u}	37.34	39.74	2.00
2^1B_{1g}	81.32	4.94	1.69
2^1B_{2u}	80.81	7.34	1.77
3^1A_g	49.10	28.97	0.15

Table A.81: Singles amplitudes with magnitudes above 0.2 from the ESMF and EOM-CCSD wave functions for the calculated states for naphthalene.

State	ESMF	EOM
1^1B_{3u}		
	H−1→L(-0.49)	H−1→L(-0.66)
	H→L+1(-0.49)	H→L+1(-0.65)
1^1B_{2u}		
	H→L(0.62)	H→L(-0.92)
	H−1→L+1(-0.30)	H−1→L+1(0.27)
2^1A_g		
	H−1→L+2(-0.57)	H−1→L+2(-0.66)
	H−2→L+1(-0.35)	H−2→L+1(-0.59)
1^1B_{1g}		
	H→L+2(-0.62)	H→L+2(0.87)
	H−2→L(-0.29)	H−2→L(-0.34)
2^1B_{3u}		
	H→L+1(0.49)	H→L+1(-0.67)
	H−1→L(-0.48)	H−1→L(0.66)
2^1B_{1g}		
	H−2→L(-0.58)	H−2→L(-0.88)
	H→L+2(0.38)	H→L+2(-0.34)
2^1B_{2u}		
	H−1→L+1(0.60)	H→L+1(0.90)
	H→L(0.31)	H→L(0.23)

A.17 Furan

Table A.82: All methods singlet excitation energies in eV for molecule furan.

State	TBE	CASPT2[a]	CASPT2[b]	CC2	CCSD	CC3	ESMP2	lvl-ESMP2
1^1B_2	6.32	6.04	6.43	6.43	6.80	6.60	6.18	6.32
2^1A_1	6.57	6.16	6.52	6.87	6.89	6.62	5.04	6.50
3^1A_1	8.13	7.66	8.22	8.83	8.83	8.53	7.87	8.38

Table A.83: Absolute ESMF, ESMP2 and level shifted ESMP2 (level shift = 0.50 a.u.) results vs. the Thiel best estimates (TBEs) for furan.

State	TBE	ESMF	error	ESMP2	error	shift=0.50 a.u.	error
1^1B_2	6.32	6.34	0.02	6.18	0.14	6.32	0.00
2^1A_1	6.57	8.04	1.47	5.04	1.53	6.50	0.07
3^1A_1	8.13	8.96	0.83	7.87	0.26	8.38	0.25

Table A.84: Absolute ESMF, ESMP2 and level shifted ESMP2 (level shift = 0.50 a.u.) errors vs. the Thiel best estimates (TBEs) and the corresponding norm of the doubles amplitudes calculated from the norm of the first order ESMP wave function for furan.

State	lvl=0.0 error	norm	lvl=0.5 error	norm
1^1B_2	0.14	0.24	0.00	0.17
2^1A_1	1.53	0.51	0.07	0.28
3^1A_1	0.26	0.28	0.25	0.19

Table A.85: SA-CASSCF percentages for the amount of singles, doubles, and triples character for the excitations of furan.

State	%singles	%doubles	%triples
1^1B_2	91.75	7.15	0.37
2^1A_1	71.71	25.43	1.15
3^1A_1	64.33	30.51	2.62

Table A.86: Singles amplitudes with magnitudes above 0.2 from the ESMF and EOM-CCSD wave functions for the calculated states for furan.

State	ESMF	EOM
1^1B_2		
	H→L(0.68)	H→L(-0.94)
2^1A_1		
	H−1→L(0.53)	H−1→L(-0.69)
	H→L+5(0.43)	H→L+5(-0.59)
3^1A_1		
	H→L+5(-0.50)	H→L+5(-0.68)
	H−1→L(0.45)	H−1→L(0.59)

A.18 Pyrrole

Table A.87: All methods singlet excitation energies in eV for molecule pyrrole.

State	TBE	CASPT2[a]	CASPT2[b]	CC2	CCSD	CC3	ESMP2	lvl-ESMP2
2^1A_1	6.37	5.92	6.31	6.61	6.61	6.40	5.30	6.41
1^1B_2	6.57	6.00	6.33	6.83	6.87	6.71	6.25	6.45
3^1A_1	7.91	7.46	8.17	8.44	8.44	8.17	7.50	8.04

Table A.88: Absolute ESMF, ESMP2 and level shifted ESMP2 (level shift = 0.50 a.u.) results vs. the Thiel best estimates (TBEs) for pyrrole.

State	TBE	ESMF	error	ESMP2	error	shift=0.50 a.u.	error
2^1A_1	6.37	7.54	1.17	5.30	1.07	6.41	0.04
1^1B_2	6.57	6.57	0.00	6.25	0.32	6.45	0.12
3^1A_1	7.91	8.69	0.78	7.50	0.41	8.04	0.13

Table A.89: Absolute ESMF, ESMP2 and level shifted ESMP2 (level shift = 0.50 a.u.) errors vs. the Thiel best estimates (TBEs) and the corresponding norm of the doubles amplitudes calculated from the norm of the first order ESMP wave function for pyrrole.

State	lvl=0.0 error	norm	lvl=0.5 error	norm
2^1A_1	1.07	0.45	0.04	0.26
1^1B_2	0.32	0.25	0.12	0.18
3^1A_1	0.41	0.29	0.13	0.19

Table A.90: SA-CASSCF percentages for the amount of singles, doubles, and triples character for the excitations of pyrrole.

State	%singles	%doubles	%triples
2^1A_1	76.61	21.95	0.94
1^1B_2	88.43	10.67	0.42
3^1A_1	68.47	27.59	2.63

Table A.91: Singles amplitudes with magnitudes above 0.2 from the ESMF and EOM-CCSD wave functions for the calculated states for pyrrole.

State	ESMF	EOM
2^1A_1		
	H−1→L+1(-0.55)	H−1→L+1(0.71)
	H→L+6(-0.42)	H→L+6(-0.57)
1^1B_2		
	H→L+1(0.67)	H→L+1(-0.92)
		H−1→L+6(-0.22)
3^1A_1		
	H→L+6(-0.51)	H→L+6(0.71)
	H−1→L+1(0.45)	H−1→L+1(0.57)

A.19 Imidazole

Table A.92: All methods singlet excitation energies in eV for molecule imidazole.

State	TBE	CASPT2[a]	CASPT2[b]	CC2	CCSD	CC3	ESMP2	lvl-ESMP2
$1^1A''$	6.81	6.52	6.81	6.86	7.01	6.82	6.80	6.72
$2^1A'$	6.19	6.72	6.19	6.73	6.80	6.58	5.65	6.49
$3^1A'$	6.93	7.15	6.93	7.28	7.27	7.10	7.01	7.36

Table A.93: Absolute ESMF, ESMP2 and level shifted ESMP2 (level shift = 0.50 a.u.) results vs. the Thiel best estimates (TBEs) for imidazole.

State	TBE	ESMF	error	ESMP2	error	shift=0.50 a.u.	error
$1^1A''$	6.81	6.11	0.70	6.80	0.01	6.72	0.09
$2^1A'$	6.19	7.08	0.89	5.65	0.54	6.49	0.30
$3^1A'$	6.93	7.77	0.84	7.01	0.08	7.36	0.43

Table A.94: Absolute ESMF, ESMP2 and level shifted ESMP2 (level shift = 0.50 a.u.) errors vs. the Thiel best estimates (TBEs) and the corresponding norm of the doubles amplitudes calculated from the norm of the first order ESMP wave function for imidazole.

State	lvl=0.0 error	norm	lvl=0.5 error	norm
$1^1A''$	0.01	0.19	0.09	0.15
$2^1A'$	0.54	0.43	0.30	0.22
$3^1A'$	0.36	0.27	0.43	0.19

Table A.95: SA-CASSCF percentages for the amount of singles, doubles, and triples character for the excitations of imidazole.

State	%singles	%doubles	%triples
$1^1A''$	84.99	8.79	1.90
$2^1A'$	75.30	20.32	0.86
$3^1A'$	88.29	6.96	0.30

Table A.96: Singles amplitudes with magnitudes above 0.2 from the ESMF and EOM-CCSD wave functions for the calculated states for imidazole.

State	ESMF	EOM
$1^1A''$		
	H−2→L+1(-0.56)	H−2→L+1(-0.88)
	H−2→L+4(0.30)	H−2→L+4(-0.28)
$2^1A'$		
	H→L+1(0.52)	H→L+1(0.70)
	H→L+4(0.36)	H→L+4(0.46)
		H−1→L+1(0.37)
$3^1A'$		
	H→L+4(-0.50)	H→L+1(0.61)
	H→L+1(+0.43)	H−1→L+1(-0.50)
		H→L(-0.47)

A.20 Pyridine

Table A.97: All methods singlet excitation energies in eV for molecule pyridine.

State	TBE	CASPT2[a]	CASPT2[b]	CC2	CCSD	CC3	ESMP2	lvl-ESMP2
1^1B_2	4.85	4.84	5.02	5.32	5.27	5.15	4.52	5.19
1^1B_1	4.59	4.91	5.14	5.12	5.25	5.05	4.93	4.98
2^1A_2	5.11	5.17	5.47	5.39	5.73	5.50	5.25	5.50
2^1A_1	6.26	6.42	6.39	6.88	6.94	6.85	6.22	6.45
3^1A_1	7.18	7.23	7.46	7.72	7.94	7.70	6.55	7.29
2^1B_2	7.27	7.48	7.29	7.61	7.81	7.59	6.54	7.25

Table A.98: Absolute ESMF, ESMP2 and level shifted ESMP2 (level shift = 0.50 a.u.) results vs. the Thiel best estimates (TBEs) for pyridine.

State	TBE	ESMF	error	ESMP2	error	shift=0.50 a.u.	error
1^1B_2	4.85	5.97	1.12	4.52	0.33	5.19	0.34
1^1B_1	4.59	4.70	0.11	4.93	0.34	4.98	0.39
2^1A_2	5.11	5.65	0.54	5.25	0.14	5.50	0.39
2^1A_1	6.26	6.47	0.21	6.22	0.04	6.45	0.19
3^1A_1	7.18	8.21	1.03	6.55	0.63	7.29	0.11
2^1B_2	7.27	8.14	0.87	6.54	0.73	7.25	0.02

Table A.99: Absolute ESMF, ESMP2 and level shifted ESMP2 (level shift = 0.50 a.u.) errors vs. the Thiel best estimates (TBEs) and the corresponding norm of the doubles amplitudes calculated from the norm of the first order ESMP wave function for pyridine.

State	lvl=0.0 error	norm	lvl=0.5 error	norm
1^1B_2	0.33	0.36	0.34	0.23
1^1B_1	0.34	0.24	0.39	0.17
2^1A_2	0.14	0.26	0.39	0.19
2^1A_1	0.04	0.29	0.19	0.19
3^1A_1	0.63	0.33	0.11	0.22
2^1B_2	0.73	0.34	0.02	0.22

Table A.100: SA-CASSCF percentages for the amount of singles, doubles, and triples character for the excitations of pyridine.

State	%singles	%doubles	%triples
1^1B_2	78.62	17.20	1.25
1^1B_1	88.99	3.14	2.28
2^1A_2	88.52	3.97	1.96
2^1A_1	74.85	19.76	0.82
3^1A_1	62.70	30.38	1.14
2^1B_2	45.87	45.28	4.91

Table A.101: Singles amplitudes with magnitudes above 0.2 from the ESMF and EOM-CCSD wave functions for the calculated states for pyridine.

State	ESMF	EOM
1^1B_2		
	H→L(0.67)	H→L(0.77)
		H−1→L+1(0.52)
1^1B_1		
	H−2→L(-0.62)	H−2→L(-0.92)
2^1A_2		
	H−2→L+1(0.65)	H−2→L+1(0.94)
2^1A_1		
	H→L+1(0.53)	H→L+1(0.76)
	H−1→L(-0.44)	H−1→L(-0.59)
3^1A_1		
	H→L+1(-0.48)	H−1→L(-0.73)
	H−1→L(-0.47)	H→L+1(-0.56)
2^1B_2		
	H−1→L+1(0.56)	H−1→L+1(+0.77)
	H→L(-0.39)	H→L(-0.51)

A.21 Pyrazine

Table A.102: All methods singlet excitation energies in eV for molecule pyrazine.

State	TBE	CASPT2[a]	CASPT2[b]	CC2	CCSD	CC3	ESMP2	lvl-ESMP2
1^1B_{3u}	3.95	3.63	4.12	4.26	4.42	4.24	3.34	4.00
1^1A_u	4.81	4.52	4.70	4.95	5.29	5.05	3.84	4.81
1^1B_{2u}	4.64	4.75	4.85	5.13	5.14	5.02	4.25	4.86
1^1B_{2g}	5.56	5.17	5.68	5.92	6.02	5.74	4.92	5.65
1^1B_{1g}	6.60	6.13	6.41	6.70	7.13	6.75	5.42	6.69
1^1B_{1u}	6.58	6.70	6.89	7.10	7.18	7.07	6.48	6.66
2^1B_{1u}	7.72	7.57	7.79	8.13	8.34	8.06	6.91	7.62
2^1B_{2u}	7.60	7.70	7.65	8.07	8.29	8.05	6.99	7.76

Table A.103: Absolute ESMF, ESMP2 and level shifted ESMP2 (level shift = 0.50 a.u.) results vs. the Thiel best estimates (TBEs) for pyrazine.

State	TBE	ESMF	error	ESMP2	error	shift=0.50 a.u.	error
1^1B_{3u}	3.95	4.94	0.99	3.34	0.61	4.00	0.05
1^1A_u	4.81	6.61	1.80	3.84	0.97	4.81	0.00
1^1B_{2u}	4.64	5.57	0.93	4.25	0.39	4.86	0.22
1^1B_{2g}	5.56	6.38	0.82	4.92	0.64	5.65	0.09
1^1B_{1g}	6.60	8.71	2.11	5.42	1.18	6.69	0.09
1^1B_{1u}	6.58	6.63	0.05	6.48	0.10	6.66	0.08
2^1B_{1u}	7.72	8.54	0.82	6.91	0.81	7.62	0.10
2^1B_{2u}	7.60	8.64	1.04	6.99	0.61	7.76	0.16

Table A.104: Absolute ESMF, ESMP2 and level shifted ESMP2 (level shift = 0.50 a.u.) errors vs. the Thiel best estimates (TBEs) and the corresponding norm of the doubles amplitudes calculated from the norm of the first order ESMP wave function for pyrazine.

State	lvl=0.0 error	norm	lvl=0.5 error	norm
1^1B_{3u}	0.61	0.34	0.05	0.23
1^1A_u	0.97	0.36	0.00	0.25
1^1B_{2u}	0.39	0.34	0.22	0.23
1^1B_{2g}	0.64	0.37	0.09	0.23
1^1B_{1g}	1.18	0.41	0.09	0.26
1^1B_{1u}	0.10	0.28	0.08	0.19
2^1B_{1u}	0.81	0.32	0.10	0.22
2^1B_{2u}	0.61	0.35	0.16	0.23

Table A.105: SA-CASSCF percentages for the amount of singles, doubles, and triples character for the excitations of pyrazine.

State	%singles	%doubles	%triples
1^1B_{3u}	81.32	10.79	1.98
1^1B_{2u}	78.63	17.69	0.00
1^1A_u	78.34	14.48	2.14
1^1B_{2g}	71.18	20.54	1.83
1^1B_{1g}	71.21	20.48	1.69
1^1B_{1u}	92.51	4.53	0.00
2^1B_{2u}	86.97	7.43	3.21
2^1B_{1u}	90.31	3.76	3.15

Table A.106: Singles amplitudes with magnitudes above 0.2 from the ESMF and EOM-CCSD wave functions for the calculated states for pyrazine.

State	ESMF	EOM
1^1B_{3u}		
	H−1→L(0.68)	H−1→L(-0.94)
1^1A_u		
	H→L(0.68)	H→L(-0.84)
		H−2→L+1(0.39)
1^1B_{2u}		
	H−1→L+1(-0.69)	H−1→L+1(0.95)
1^1B_{2g}		
	H−3→L(-0.65)	H−3→L(0.92)
	H−1→L+7(0.20)	
1^1B_{1g}		
	H−3→L+1(-0.69)	H−3→L+1(0.94)
1^1B_{1u}		
	H→L+1(0.56)	H→L+1(-0.85)
	H−2→L(-0.40)	H−2→L(-0.45)
2^1B_{1u}		
	H−2→L+1(0.61)	H−2→L+1(0.84)
	H→L(-0.30)	H→L(0.39)
2^1B_{2u}		
	H−2→L(0.54)	H−2→L(0.81)
	H→L+1(0.40)	H→L+1(-0.41)

A.22 Pyrimidine

Table A.107: All methods singlet excitation energies in eV for molecule pyrimidine.

State	TBE	CASPT2[a]	CASPT2[b]	CC2	CCSD	CC3	ESMP2	lvl-ESMP2
1^1B_1	4.55	3.81	4.44	4.49	4.70	4.50	3.65	4.24
1^1A_2	4.91	4.12	4.81	4.84	5.12	4.93	4.18	4.83
1^1B_2	5.44	4.93	5.24	5.51	5.49	5.36	4.96	5.55
2^1A_1	6.95	6.72	6.64	7.12	7.17	7.06	6.36	7.25

Table A.108: Absolute ESMF, ESMP2 and level shifted ESMP2 (level shift = 0.50 a.u.) results vs. the Thiel best estimates (TBEs) for pyrimidine.

State	TBE	ESMF	error	ESMP2	error	shift=0.50 a.u.	error
1^1B_1	4.55	5.17	0.62	3.65	0.90	4.24	0.31
1^1A_2	4.91	5.89	0.98	4.18	0.73	4.83	0.08
1^1B_2	5.44	6.20	0.76	4.96	0.48	5.55	0.11
2^1A_1	6.95	8.31	1.36	6.36	0.59	7.25	0.30

Table A.109: Absolute ESMF, ESMP2 and level shifted ESMP2 (level shift = 0.50 a.u.) errors vs. the Thiel best estimates (TBEs) and the corresponding norm of the doubles amplitudes calculated from the norm of the first order ESMP wave function for pyrimidine.

State	lvl=0.0 error	norm	lvl=0.5 error	norm
1^1B_1	0.90	0.32	0.31	0.23
1^1A_2	0.73	0.33	0.08	0.23
1^1B_2	0.48	0.34	0.11	0.23
2^1A_1	0.59	0.38	0.30	0.23

Table A.110: SA-CASSCF percentages for the amount of singles, doubles, and triples character for the excitations of pyrimidine.

State	%singles	%doubles	%triples
1^1B_1	84.42	6.35	1.80
1^1A_2	83.35	8.23	1.23
1^1B_2	75.86	19.81	2.27
2^1A_1	67.47	24.97	0.74

Table A.111: Singles amplitudes with magnitudes above 0.2 from the ESMF and EOM-CCSD wave functions for the calculated states for pyrimidine.

State	ESMF	EOM
1^1B_1		
	H−1→L(-0.67)	H−1→L(-0.94)
1^1A_2		
	H−1→L+1(0.66)	H−1→L+1(0.94)
1^1B_2		
	H→L(0.66)	H→L(0.77)
		H−2→L+1(0.53)
2^1A_1		
	H→L+1(-0.51)	H→L+1(0.81)
	H−2→L(-0.38)	H−2→L(-0.49)

A.23 Pyridazine

Table A.112: All methods singlet excitation energies in eV for molecule pyridazine.

State	TBE	CASPT2[a]	CASPT2[b]	CC2	CCSD	CC3	ESMP2	lvl-ESMP2
1^1B_1	3.78	3.48	3.78	3.90	4.11	3.92	3.26	3.67
1^1A_2	4.32	3.66	4.32	4.40	4.76	4.49	3.66	4.25
2^1A_1	5.18	4.86	5.18	5.37	5.35	5.22	4.28	5.16
2^1A_2	5.77	5.09	5.77	5.81	6.00	5.74	4.82	5.53

Table A.113: Absolute ESMF, ESMP2 and level shifted ESMP2 (level shift = 0.50 a.u.) results vs. the Thiel best estimates (TBEs) for pyridazine.

State	TBE	ESMF	error	ESMP2	error	shift=0.50 a.u.	error
1^1B_1	3.78	4.33	0.55	3.26	0.52	3.67	0.11
1^1A_2	4.32	5.18	0.86	3.66	0.66	4.25	0.07
2^1A_1	5.18	6.20	1.02	4.28	0.90	5.16	0.02
2^1A_2	5.77	6.54	0.77	4.82	0.95	5.53	0.24

Table A.114: Absolute ESMF, ESMP2 and level shifted ESMP2 (level shift = 0.50 a.u.) errors vs. the Thiel best estimates (TBEs) and the corresponding norm of the doubles amplitudes calculated from the norm of the first order ESMP wave function for pyridazine.

State	lvl=0.0 error	norm	lvl=0.5 error	norm
1^1B_1	0.52	0.30	0.11	0.22
1^1A_2	0.66	0.31	0.07	0.22
2^1A_1	0.90	0.40	0.02	0.26
2^1A_2	0.95	0.35	0.24	0.24

Table A.115: SA-CASSCF percentages for the amount of singles, doubles, and triples character for the excitations of pyridazine.

State	%singles	%doubles	%triples
1^1B_1	87.74	8.18	1.80
1^1A_2	86.20	8.37	2.77
2^1A_1	79.39	17.82	0.26
2^1A_2	74.52	21.37	1.33

Table A.116: Singles amplitudes with magnitudes above 0.2 from the ESMF and EOM-CCSD wave functions for the calculated states for pyridazine.

State	ESMF	EOM
1^1B_1		
	H−2→L(0.67)	H−2→L(-0.94)
1^1A_2		
	H−2→L+1(0.64)	H−2→L+1(0.94)
2^1A_1		
	H→L(0.65)	H→L(-0.75)
	H−1→L+1(0.26)	H−1→L+1(0.54)
2^1A_2		
	H−3→L(0.59)	H−3→L(0.91)
	H−2→L+1(0.26)	

A.24 Triazine

Table A.117: All methods singlet excitation energies in eV for molecule triazine.

State	TBE	CASPT2[a]	CASPT2[b]	CC2	CCSD	CC3	ESMP2	lvl-ESMP2
$1^1A_1''$	4.60	3.90	4.60	4.70	4.96	4.78	3.23	4.44
$1^1A_2''$	4.66	4.08	4.68	4.80	4.98	4.76	3.65	4.48
$1^1E''$	4.71	4.36	4.71	4.77	5.01	4.81	3.49	4.48
$1^1A_2'$	5.79	5.33	5.79	5.82	5.84	5.71	4.34	5.48

Table A.118: Absolute ESMF, ESMP2 and level shifted ESMP2 (level shift = 0.50 a.u.) results vs. the Thiel best estimates (TBEs) for triazine.

State	TBE	ESMF	error	ESMP2	error	shift=0.50 a.u.	error
$1^1A_1''$	4.60	6.04	1.44	3.23	1.37	4.44	0.16
$1^1A_2''$	4.66	6.14	1.48	3.65	1.01	4.48	0.18
$1^1E''$	4.71	6.16	1.45	3.49	1.22	4.48	0.23
$1^1A_2'$	5.79	6.95	1.16	4.34	1.45	5.48	0.31

Table A.119: Absolute ESMF, ESMP2 and level shifted ESMP2 (level shift = 0.50 a.u.) errors vs. the Thiel best estimates (TBEs) and the corresponding norm of the doubles amplitudes calculated from the norm of the first order ESMP wave function for triazine.

State	lvl=0.0 error	norm	lvl=0.5 error	norm
$1^1A_1''$	1.37	0.37	0.16	0.25
$1^1A_2''$	1.01	0.39	0.18	0.25
$1^1E''$	1.22	0.37	0.23	0.25
$1^1A_2'$	1.45	0.44	0.31	0.28

Table A.120: SA-CASSCF percentages for the amount of singles, doubles, and triples character for the excitations of triazine.

State	%singles	%doubles	%triples
$1^1A_1''$	76.65	13.15	1.41
$1^1A_2''$	79.27	12.32	1.11
$1^1E''$	79.27	13.18	0.69
$1^1A_2'$	76.20	18.86	2.63

Table A.121: Singles amplitudes with magnitudes above 0.2 from the ESMF and EOM-CCSD wave functions for the calculated states for triazine.

State	ESMF	EOM
$1^1A_1''$		
	H−3→L+1(-0.51)	H−2→L(-0.67)
	H−2→L(0.44)	H−3→L+1(0.67)
$1^1A_2''$		
	H−2→L+1(0.48)	H−3→L(-0.66)
	H−3→L(-0.48)	H−2→L+1(-0.66)
$1^1E''$		
	H−2→L+1(-0.49)	H−2→L+1(-0.66)
	H−3→L(-0.46)	H−3→L(0.66)
$1^1A_2'$		
	H→L+1(-0.48)	H−1→L(-0.66)
	H−1→L(0.46)	H→L+1(-0.66)

A.25 Tetrazine

Table A.122: All methods singlet excitation energies in eV for molecule tetrazine.

State	TBE	CASPT2[a]	CASPT2[b]	CC2	CCSD	CC3	ESMP2	lvl-ESMP2
1^1B_{3u}	2.24	1.96	2.24	2.47	2.71	2.53	1.36	2.12
1^1A_u	3.48	3.06	3.48	3.67	4.07	3.79	2.48	3.55
1^1B_{1g}	4.73	4.51	4.73	5.10	5.32	4.97	4.06	4.94
1^1B_{2u}	4.91	4.89	4.91	5.20	5.27	5.12	3.98	4.86
2^1A_u	5.47	5.28	5.47	5.50	5.70	5.46	3.61	4.75
1^1B_{2g}	5.18	5.05	5.18	5.53	5.70	5.34	4.25	5.28

Table A.123: Absolute ESMF, ESMP2 and level shifted ESMP2 (level shift = 0.50 a.u.) results vs. the Thiel best estimates (TBEs) for tetrazine.

State	TBE	ESMF	error	ESMP2	error	shift=0.50 a.u.	error
1^1B_{3u}	2.24	3.34	1.10	1.36	0.88	2.12	0.12
1^1A_u	3.48	5.39	1.91	2.48	1.00	3.55	0.07
1^1B_{1g}	4.73	5.99	1.26	4.06	0.67	4.94	0.21
1^1B_{2u}	4.91	5.96	1.05	3.98	0.93	4.86	0.05
2^1A_u	5.47	6.53	1.06	3.61	1.86	4.75	0.72
1^1B_{2g}	5.18	6.41	1.23	4.25	0.93	5.28	0.10

Table A.124: Absolute ESMF, ESMP2 and level shifted ESMP2 (level shift = 0.50 a.u.) errors vs. the Thiel best estimates (TBEs) and the corresponding norm of the doubles amplitudes calculated from the norm of the first order ESMP wave function for tetrazine.

State	lvl=0.0 error	norm	lvl=0.5 error	norm
1^1B_{3u}	0.88	0.36	0.12	0.25
1^1A_u	1.00	0.37	0.07	0.25
1^1B_{1g}	0.67	0.41	0.21	0.24
1^1B_{2u}	0.93	0.40	0.05	0.26
2^1A_u	1.86	0.41	0.72	0.27
1^1B_{2g}	0.93	0.43	0.10	0.25

Table A.125: SA-CASSCF percentages for the amount of singles, doubles, and triples character for the excitations of tetrazine.

State	%singles	%doubles	%triples
1^1B_{3u}	86.53	10.71	0.59
1^1A_u	83.26	11.30	2.09
1^1B_{2u}	86.75	10.76	1.33
1^1B_{1g}	75.30	20.55	1.02
2^1A_u	79.40	16.40	1.06
1^1B_{2g}	70.51	24.45	1.02

Table A.126: Singles amplitudes with magnitudes above 0.2 from the ESMF and EOM-CCSD wave functions for the calculated states for tetrazine.

State	ESMF	EOM
1^1B_{3u}		
	H→L(-0.68)	H→L(0.95)
1^1A_u		
	H→L+1(0.67)	H→L+1(-0.94)
1^1B_{1g}		
	H−1→L(-0.67)	H−1→L(0.82)
		H−2→L+1(0.43)
1^1B_{2u}		
	H−4→L(-0.61)	H−4→L(-0.93)
	H→L+6(0.26)	
2^1A_u		
	H−3→L(0.61)	H−3→L(0.93)
	H→L+1(-0.30)	
1^1B_{2g}		
	H−5→L(0.65)	H−5→L(-0.92)

A.26 Cytosine

Table A.127: All methods singlet excitation energies in eV for molecule cytosine.

State	TBE	CASPT2[a]	CASPT2[b]	CC2	CCSD	CC3	ESMP2	lvl-ESMP2
$2^1A'$	4.66	4.39	4.68	4.80	4.98	4.72	N/A	N/A
$1^1A''$	4.87	5.00	5.12	5.13	5.45	5.16	4.47	5.06
$2^1A''$	5.26	6.53	5.54	5.01	5.99	5.52	5.83	5.80
$3^1A'$	5.62	5.36	5.54	5.71	5.95	5.61	4.78	5.56

Table A.128: Absolute ESMF, ESMP2 and level shifted ESMP2 (level shift = 0.50 a.u.) results vs. the Thiel best estimates (TBEs) for cytosine.

State	TBE	ESMF	error	ESMP2	error	shift=0.50 a.u.	error
$1^1A''$	4.87	6.03	1.16	4.47	0.40	5.06	0.19
$2^1A''$	5.26	5.12	0.14	5.83	0.57	5.80	0.54
$3^1A'$	5.62	6.64	1.02	4.78	0.84	5.56	0.06

Table A.129: Absolute ESMF, ESMP2 and level shifted ESMP2 (level shift = 0.50 a.u.) errors vs. the Thiel best estimates (TBEs) and the corresponding norm of the doubles amplitudes calculated from the norm of the first order ESMP wave function for cytosine.

State	lvl=0.0 error	norm	lvl=0.5 error	norm
$1^1A''$	0.40	0.32	0.19	0.23
$2^1A''$	0.57	0.21	0.54	0.16
$3^1A'$	0.84	0.37	0.06	0.23

Table A.130: SA-CASSCF percentages for the amount of singles, doubles, and triples character for the excitations of cytosine.

State	%singles	%doubles	%triples
$2^1A'$	79.24	9.35	0.54
$1^1A''$	81.26	9.49	0.60
$3^1A'$	74.66	15.52	0.69
$2^1A''$	80.49	9.57	0.64

Table A.131: Singles amplitudes with magnitudes above 0.2 from the ESMF and EOM-CCSD wave functions for the calculated states for cytosine.

State	ESMF	EOM
$1^1A''$		
	H−2→L(0.66)	H−2→L(0.80)
		H−3→L(-0.39)
		H−2→L+4(0.28)
$2^1A''$		
	H−3→L+4(0.44)	H−3→L+4(-0.56)
	H−2→L+4(0.41)	H−2→L+4(-0.56)
		H−3→L(-0.43)
$3^1A'$		
	H−1→L(0.60)	H−1→L(0.90)

A.27 Thymine

Table A.132: All methods singlet excitation energies in eV for molecule thymine.

State	TBE	CASPT2[a]	CASPT2[b]	CC2	CCSD	CC3	ESMP2	lvl-ESMP2
$1^1A''$	4.82	4.39	4.94	4.94	5.14	4.98	4.91	4.90
$2^1A'$	5.20	4.88	5.06	5.39	5.60	5.34	4.84	5.29
$3^1A'$	6.27	5.88	6.15	6.46	6.78	6.34	4.56	5.94
$2^1A''$	6.16	5.91	6.38	6.33	6.57	6.45	6.55	6.44
$4^1A'$	6.53	6.10	6.52	6.80	7.05	6.71	4.91	6.45

Table A.133: Absolute ESMF, ESMP2 and level shifted ESMP2 (level shift = 0.50 a.u.) results vs. the Thiel best estimates (TBEs) for thymine.

State	TBE	ESMF	error	ESMP2	error	shift=0.50 a.u.	error
$1^1A''$	4.82	4.26	0.56	4.91	0.09	4.90	0.08
$2^1A'$	5.20	5.96	0.76	4.84	0.36	5.29	0.09
$3^1A'$	6.27	7.50	1.23	4.56	1.71	5.94	0.33
$2^1A''$	6.16	5.62	0.54	6.55	0.39	6.44	0.28
$4^1A'$	6.53	8.68	2.15	4.91	1.62	6.45	0.08

Table A.134: Absolute ESMF, ESMP2 and level shifted ESMP2 (level shift = 0.50 a.u.) errors vs. the Thiel best estimates (TBEs) and the corresponding norm of the doubles amplitudes calculated from the norm of the first order ESMP wave function for thymine.

State	lvl=0.0 error	norm	lvl=0.5 error	norm
$1^1A''$	0.09	0.23	0.08	0.17
$2^1A'$	0.36	0.29	0.09	0.21
$3^1A'$	1.71	0.50	0.33	0.27
$2^1A''$	0.39	0.19	0.28	0.15
$4^1A'$	1.62	0.48	0.08	0.29

Table A.135: SA-CASSCF percentages for the amount of singles, doubles, and triples character for the excitations of thymine.

State	%singles	%doubles	%triples
$1^1A''$	81.88	10.38	0.24
$2^1A'$	82.75	7.70	0.00
$2^1A''$	83.17	5.98	0.71
$3^1A'$	71.05	21.01	0.02
$4^1A'$	76.55	13.02	0.02

Table A.136: Singles amplitudes with magnitudes above 0.2 from the ESMF and EOM-CCSD wave functions for the calculated states for thymine.

State	ESMF	EOM
$1^1A''$		
	H−2→L(0.54)	H−2→L(0.81)
	H−2→L+4(-0.22)	H−2→L+4(0.30)
	H−3→L(0.22)	H−3→L(0.26)
$2^1A'$		
	H→L(0.67)	H→L(-0.90)
$3^1A'$		
	H−1→L(0.71)	H−1→L(-0.88)
$2^1A''$		
	H−3→L+4(-0.52)	H−3→L+4(0.64)
	H−2→L+4(0.29)	H−2→L+4(-0.54)
		H−3→L(-0.26)
$4^1A'$		
	H→L+4(0.68)	H→L+4(0.89)

A.28 Uracil

Table A.137: All methods singlet excitation energies in eV for molecule uracil.

State	TBE	CASPT2[a]	CASPT2[b]	CC2	CCSD	CC3	ESMP2	lvl-ESMP2
$1^1A''$	4.80	4.54	4.90	4.91	5.11	4.90	4.82	4.83
$2^1A'$	5.35	5.00	5.23	5.52	5.70	5.44	4.80	5.36
$3^1A'$	6.26	5.82	6.15	6.43	6.76	6.29	N/A	N/A
$3^1A''$	6.56	6.37	6.97	6.73	7.68	6.77	5.63	6.93
$2^1A''$	6.10	6.00	6.27	6.26	6.50	6.32	6.49	6.39
$4^1A'$	6.70	6.46	6.75	6.96	7.19	6.87	5.14	6.40

Table A.138: Absolute ESMF, ESMP2 and level shifted ESMP2 (level shift = 0.50 a.u.) results vs. the Thiel best estimates (TBEs) for uracil.

State	TBE	ESMF	error	ESMP2	error	shift=0.50 a.u.	error
$1^1A''$	4.80	4.24	0.56	4.82	0.02	4.83	0.03
$2^1A'$	5.35	6.18	0.83	4.80	0.55	5.36	0.01
$3^1A''$	6.56	8.98	2.42	5.63	0.93	6.93	0.37
$2^1A''$	6.10	5.56	0.54	6.49	0.39	6.39	0.29
$4^1A'$	6.70	8.12	1.42	5.14	1.56	6.40	0.30

Table A.139: Absolute ESMF, ESMP2 and level shifted ESMP2 (level shift = 0.50 a.u.) errors vs. the Thiel best estimates (TBEs) and the corresponding norm of the doubles amplitudes calculated from the norm of the first order ESMP wave function for uracil.

State	lvl=0.0 error	norm	lvl=0.5 error	norm
$1^1A''$	0.02	0.23	0.03	0.17
$2^1A'$	0.55	0.32	0.01	0.21
$3^1A''$	0.93	0.42	0.37	0.27
$2^1A''$	0.39	0.19	0.29	0.15
$4^1A'$	1.56	0.43	0.30	0.27

Table A.140: SA-CASSCF percentages for the amount of singles, doubles, and triples character for the excitations of uracil.

State	%singles	%doubles	%triples
$1^1A''$	81.94	9.81	0.14
$2^1A'$	83.11	6.81	0.01
$2^1A''$	83.11	6.14	0.58
$3^1A'$	72.34	18.53	0.03
$4^1A'$	77.40	12.86	0.01
$3^1A''$	61.21	27.02	1.23

Table A.141: Singles amplitudes with magnitudes above 0.2 from the ESMF and EOM-CCSD wave functions for the calculated states for uracil.

State	ESMF	EOM
$1^1A''$		
	H−2→L(0.53)	H−2→L(0.80)
	H−2→L+3(0.24)	H−2→L+3(0.33)
	H−3→L(0.21)	H−3→L(0.24)
$2^1A'$		
	H→L(-0.67)	H→L(-0.90)
$3^1A''$		
	H−3→L(0.50)	H−3→L(0.76)
	H−2→L+3(-0.39)	H−2→L+3(-0.52)
$2^1A''$		
	H−3→L+3(-0.51)	H−3→L+3(0.62)
	H−2→L+3(0.27)	H−2→L+3(-0.54)
		H−3→L(-0.31)
		H−2→L(0.23)
		H−3→L+11(-0.21)
$4^1A'$		
	H→L+3(0.49)	H→L+3(0.90)
	H−1→L(0.38)	

A.29 Adenine

Table A.142: All methods singlet excitation energies in eV for molecule adenine.

State	TBE	CASPT2[a]	CASPT2[b]	CC2	CCSD	CC3	ESMP2	lvl-ESMP2
$2^1A'$	5.25	5.13	5.20	5.28	5.37	5.18	4.41	5.36
$3^1A'$	5.25	5.20	5.30	5.42	5.61	5.39	4.90	5.37
$1^1A''$	5.12	6.15	5.21	5.27	5.58	5.34	4.87	5.44
$2^1A''$	5.75	6.86	5.97	5.91	6.19	5.96	5.12	5.84

Table A.143: Absolute ESMF, ESMP2 and level shifted ESMP2 (level shift = 0.50 a.u.) results vs. the Thiel best estimates (TBEs) for adenine.

State	TBE	ESMF	error	ESMP2	error	shift=0.50 a.u.	error
$2^1A'$	5.25	6.52	1.27	4.41	0.84	5.36	0.11
$3^1A'$	5.25	5.94	0.69	4.90	0.35	5.37	0.12
$1^1A''$	5.12	6.33	1.21	4.87	0.25	5.44	0.32
$2^1A''$	5.75	7.00	1.25	5.12	0.63	5.84	0.09

Table A.144: Absolute ESMF, ESMP2 and level shifted ESMP2 (level shift = 0.50 a.u.) errors vs. the Thiel best estimates (TBEs) and the corresponding norm of the doubles amplitudes calculated from the norm of the first order ESMP wave function for adenine.

State	lvl=0.0 error	norm	lvl=0.5 error	norm
$2^1A'$	0.84	0.41	0.11	0.26
$3^1A'$	0.35	0.32	0.12	0.22
$1^1A''$	0.25	0.32	0.32	0.23
$2^1A''$	0.63	0.34	0.09	0.24

Table A.145: SA-CASSCF percentages for the amount of singles, doubles, and triples character for the excitations of adenine.

State	%singles	%doubles	%triples
$2^1A'$	76.38	9.57	0.00
$1^1A''$	78.60	6.53	0.09
$3^1A'$	81.27	6.62	0.00
$2^1A''$	77.69	7.84	0.69

Table A.146: Singles amplitudes with magnitudes above 0.2 from the ESMF and EOM-CCSD wave functions for the calculated states for adenine.

State	ESMF	EOM
$2^1A'$		
	H−1→L(0.50)	H→L+2(-0.70)
	H→L+2(0.29)	H−1→L(-0.57)
$3^1A'$		
	H→L(0.65)	H→L(-0.88)
		H−2→L+5(-0.27)
$1^1A''$		
	H−2→L(-0.49)	H−2→L(0.89)
	H−2→L+2(0.33)	H−2→L+5(-0.27)
	H−2→L+5(0.23)	
$2^1A''$		
	H−2→L+2(0.66)	H−2→L+2(0.92)

Bibliography

[1] Denis Jacquemin, Lluís Blancafort, and Young Min Rhee. "Computational Photochemistry". In: *ChemPhotoChem* 3.9 (2019), pp. 664–665.

[2] Thomas L. C. Jansen. "Computational spectroscopy of complex systems". In: *The Journal of Chemical Physics* 155.17 (Nov. 2021).

[3] Diptarka Hait and Martin Head-Gordon. "Excited State Orbital Optimization via Minimizing the Square of the Gradient: General Approach and Application to Singly and Doubly Excited States via Density Functional Theory". In: *Journal of Chemical Theory and Computation* 16.3 (2020), pp. 1699–1710.

[4] Neepa T. Maitra. "Charge transfer in time-dependent density functional theory". In: *J. Phys.: Condens. Matter* 49 (2017), p. 423001.

[5] Neepa T. Maitra. "Double and Charge-Transfer Excitations in Time-Dependent Density Functional Theory". In: *Annual Review of Physical Chemistry* 73 (2022), pp. 117–140.

[6] J. J. Benson-Smith et al. "Formation of a Ground-State Charge-Transfer Complex in Polyfluorene//[6,6]-Phenyl-C61 Butyric Acid Methyl Ester (PCBM) Blend Films and Its Role in the Function of Polymer/PCBM Solar Cells". In: *Advanced Functional Materials* 17.3 (2007), pp. 451–457.

[7] Saeed-Uz-Zaman Khan et al. "Multiple Charge Transfer States in Donor-Acceptor Heterojunctions with Large Frontier Orbital Energy Offsets". In: *Chemistry of Materials* 31.17 (2019), pp. 6808–6817.

[8] MM Martin and JT Hynes. "Ultrafast photoinduced charge transfer in fluorinated derivatives". In: *Femtochemistry and Femtobiology: Ultrafast Events in Molecular Science* (2004), p. 323.

[9] Balazs Kozma et al. "A New Benchmark Set for Excitation Energy of Charge Transfer States: Systematic Investigation of Coupled Cluster Type Methods". In: *Journal of Chemical Theory and Computation* 16.7 (2020), pp. 4213–4225.

[10] David Mester and Mihaly Kallay. "Charge-Transfer Excitations within Density Functional Theory: How Accurate Are the Most Recommended Approaches?" In: *Journal of Chemical Theory and Computation* 18.3 (2022), pp. 1646–1662.

[11] R. Clune, J. A. R. Shea, and E. Neuscamman. "N-5-Scaling Excited-State-Specific Perturbation Theory". In: *Journal of Chemical Theory and Computation* 16.10 (2020), pp. 6132–6141.

[12] Rachel Clune et al. *Studying excited-state-specific perturbation theory on the Thiel set*. 2023. arXiv: `2302.07240 [physics.chem-ph]`.

[13] Attila Szabo and Neil S. Ostlund. *Modern quantum chemistry : introduction to advanced electronic structure theory*. 1st. New York: McGraw-Hill, 1989, xiv, 466 p.

[14] J. Grant Hill. "Gaussian basis sets for molecular applications". In: *International Journal of Quantum Chemistry* 113.1 (2013), pp. 21–34.

[15] Marko Schreiber et al. "Benchmarks for electronically excited states: CASPT2, CC2, CCSD, and CC3". In: *J. Chem. Phys.* 128.13 (2008), p. 134110.

[16] C. C. J. Roothaan. "New Developments in Molecular Orbital Theory". In: *Rev. Mod. Phys.* 23 (2 1951), pp. 69–89.

[17] G. G. Hall and John Edward Lennard-Jones. "The molecular orbital theory of chemical valency VIII. A method of calculating ionization potentials". In: *Proceedings of the Royal Society of London. Series A. Mathematical and Physical Sciences* 205.1083 (1951), pp. 541–552.

[18] Tracy P. Hamilton and Peter Pulay. "Direct inversion in the iterative subspace (DIIS) optimization of open-shell, excited-state, and small multiconfiguration SCF wave functions". In: *The Journal of Chemical Physics* 84.10 (1986), pp. 5728–5734.

[19] Haskell B. Curry. "The Method of Steepest Descent for Non-Linear Minimization Problems". eng. In: *Quarterly of applied mathematics* 2.3 (1944), pp. 258–261.

[20] Rodney J. Bartlett and John F. Stanton. "Applications of Post-Hartree—Fock Methods: A Tutorial". In: *Reviews in Computational Chemistry*. John Wiley & Sons, Ltd, 1994, pp. 65–169.

[21] R. D. Johnson. *NIST Computational Chemistry Comparison and Benchmark Database*. Online Database. 2019. URL: `http://cccbdb.nist.gov/`.

[22] Dieter Cremer. "Møller–Plesset perturbation theory: from small molecule methods to methods for thousands of atoms". In: *WIREs Computational Molecular Science* 1.4 (2011), pp. 509–530.

[23] T. Helgaker, P. Jøgensen, and J. Olsen. *Molecular Electronic Structure Theory*. West Sussex, England: John Wiley and Sons, Ltd, 2000, p. 162.

[24] R J Bartlett. "Many-Body Perturbation Theory and Coupled Cluster Theory for Electron Correlation in Molecules". In: *Annual Review of Physical Chemistry* 32.1 (1981), pp. 359–401.

[25] Rodney J. Bartlett and Monika Musiał. "Coupled-cluster theory in quantum chemistry". In: *Rev. Mod. Phys.* 79 (1 2007), pp. 291–352.

[26] John F. Stanton. "Why CCSD(T) works: a different perspective". In: *Chemical Physics Letters* 281.1 (1997), pp. 130–134.

[27] Jan Řezáč and Pavel Hobza. "Describing Noncovalent Interactions beyond the Common Approximations: How Accurate Is the "Gold Standard," CCSD(T) at the Complete Basis Set Limit?" In: *Journal of Chemical Theory and Computation* 9.5 (2013), pp. 2151–2155.

[28] Rodney J. Bartlett. "Coupled-cluster theory and its equation-of-motion extensions". In: *WIREs Computational Molecular Science* 2.1 (2012), pp. 126–138.

[29] Dermot Hegarty and Michael A. Robb. "Application of unitary group methods to configuration interaction calculations". In: *Molecular Physics* 38.6 (1979), pp. 1795–1812.

[30] Richard H.A. Eade and Michael A. Robb. "Direct minimization in mc scf theory. the quasi-newton method". In: *Chemical Physics Letters* 83.2 (1981), pp. 362–368.

[31] Peter Pulay. "A perspective on the CASPT2 method". In: *International Journal of Quantum Chemistry* 111.13 (2011), pp. 3273–3279.

[32] James Finley et al. "The multi-state CASPT2 method". In: *Chemical Physics Letters* 288.2 (1998), pp. 299–306.

[33] Henryk A. Witek et al. "Intruder state avoidance multireference Møller–Plesset perturbation theory". In: *Journal of Computational Chemistry* 23.10 (2002), pp. 957–965.

[34] Björn O. Roos and Kerstin Andersson. "Multiconfigurational perturbation theory with level shift — the Cr2 potential revisited". In: *Chemical Physics Letters* 245.2 (1995), pp. 215–223.

[35] Stefano Battaglia et al. "Regularized CASPT2: an Intruder-State-Free Approach". In: *Journal of Chemical Theory and Computation* 18.8 (2022), pp. 4814–4825.

[36] Niclas Forsberg and Per-Åke Malmqvist. "Multiconfiguration perturbation theory with imaginary level shift". In: *Chemical Physics Letters* 274.1 (1997), pp. 196–204.

[37] Luke W. Bertels, Joonho Lee, and Martin Head-Gordon. "Third-Order Møller–Plesset Perturbation Theory Made Useful? Choice of Orbitals and Scaling Greatly Improves Accuracy for Thermochemistry, Kinetics, and Intermolecular Interactions". In: *The Journal of Physical Chemistry Letters* 10.15 (2019), pp. 4170–4176.

[38] Joonho Lee and Martin Head-Gordon. "Regularized Orbital-Optimized Second-Order Møller–Plesset Perturbation Theory: A Reliable Fifth-Order-Scaling Electron Correlation Model with Orbital Energy Dependent Regularizers". In: *Journal of Chemical Theory and Computation* 14.10 (2018), pp. 5203–5219.

[39] Francesco A. Evangelista. "A driven similarity renormalization group approach to quantum many-body problems". In: *The Journal of Chemical Physics* 141.5 (Aug. 2014).

[40] Adele D Laurent and Denis Jacquemin. "TD-DFT benchmarks: a review". In: *International Journal of Quantum Chemistry* 113.17 (2013), pp. 2019–2039.

[41] J. D. Whitfield et al. "Computational complexity of time-dependent density functional theory". In: *New Journal of Phyiscs* 16 (2014).

[42] John P. Perdew and Karla Schmidt. "Jacob's ladder of density functional approximations for the exchange-correlation energy". In: *AIP Conference Proceedings* 577.1 (July 2001), pp. 1–20.

[43] M. Crouzeix, B. Philippe, and M. Sadkane. "The Davidson Method". In: *SIAM Journal on Scientific Computing* 15.1 (1994), pp. 62–76.

[44] Xinle Liu et al. "Communication: Adjusting charge transfer state energies for configuration interaction singles: Without any parameterization and with minimal cost". In: *The Journal of Chemical Physics* 136.16 (2012).

[45] J. M. Foster and S. F. Boys. "Canonical Configurational Interaction Procedure". In: *Rev. Mod. Phys.* 32 (2 1960), pp. 300–302.

[46] Joseph E. Subotnik. "Communication: Configuration interaction singles has a large systematic bias against charge-transfer states". In: *J. Chem. Phys.* 135 (2011).

[47] Leszek Meissner. "On perturbative corrections to excitation energies from configuration interaction singles". In: *Molecular Physics* 104.13-14 (2006), pp. 2073–2083.

[48] P. F. Loos, A. Scemama, and D. Jacquemin. "The Quest for Highly Accurate Excitation Energies: A Computational Perspective". In: *J. Phys. Chem. Lett.* 11.6 (2020).

[49] John F. Stanton and Rodney J. Bartlett. "The equation of motion coupled-cluster method. A systematic biorthogonal approach to molecular excitation energies, transition probabilities, and excited state properties". In: *The Journal of Chemical Physics* 98.9 (May 1993), pp. 7029–7039.

[50] Benjamin Meyer et al. "Charge transfer processes: the role of optimized molecular orbitals". In: *Dalton Trans.* 43 (29 2014), pp. 11209–11215.

[51] Ove Christiansen, Henrik Koch, and Poul Jørgensen. "The second-order approximate coupled cluster singles and doubles model CC2". In: *Chemical Physics Letters* 243.5-6 (1995), pp. 409–418.

[52] Ove Christiansen, Henrik Koch, and Poul Jo/rgensen. "Response functions in the CC3 iterative triple excitation model". In: *The Journal of chemical physics* 103.17 (1995), pp. 7429–7441.

[53] Harrison Tuckman and Eric Neuscamman. *An Excited-State-Specific Projected Coupled-Cluster Theory*. 2023. arXiv: `2302.06731 [physics.chem-ph]`.

[54] Lan Nguyen Tran, Jacqueline A. R. Shea, and Eric Neuscamman. "Tracking Excited States in Wave Function Optimization Using Density Matrices and Variational Principles". In: *Journal of Chemical Theory and Computation* 15.9 (2019), pp. 4790–4803.

[55] Lan Nguyen Tran and Eric Neuscamman. "Improving Excited-State Potential Energy Surfaces via Optimal Orbital Shapes". In: *The Journal of Physical Chemistry A* 124.40 (2020), pp. 8273–8279.

[56] Rebecca Hanscam and Eric Neuscamman. *Applying generalized variational principles to excited-state-specific complete active space self-consistent field theory.* 2022. arXiv: 2111.02590 [physics.chem-ph].

[57] J. A. R. Shea and E. Neuscamman. "Communication: A mean field platform for excited state quantum chemistry". In: *Journal of Chemical Physics* 149.8 (2018).

[58] T. S. Hardikar and E. Neuscamman. "A self-consistent field formulation of excited state mean field theory". In: *Journal of Chemical Physics* 153.16 (2020).

[59] J. A. R. Shea, E. Gwin, and E. Neuscamman. "A Generalized Variational Principle with Applications to Excited State Mean Field Theory". In: *Journal of Chemical Theory and Computation* 16.3 (2020), pp. 1526–1540.

[60] Stefan Grimme et al. "Dispersion-corrected mean-field electronic structure methods". In: *Chem. Rev.* 116.9 (2016), pp. 5105–5154.

[61] Tom Ziegler et al. "On the relation between time-dependent and variational density functional theory approaches for the determination of excitation energies and transition moments". In: *J. Chem. Phys.* 130 (2009), p. 154102.

[62] Young Choon Park, Mykhaylo Krykunov, and Tom Ziegler. "On the relation between adiabatic time dependent density functional theory (TDDFT) and the Δ SCF-DFT method. Introducing a numerically stable Δ SCF-DFT scheme for local functionals based on constricted variational DFT". In: *Mol. Phys.* 113.13-14 (2015), pp. 1636–1647.

[63] L. Zhao and E. Neuscamman. "Density Functional Extension to Excited-State Mean-Field Theory". In: *J. Chem. Theory Comput.* 16 (2020), p. 164.

[64] M. Filatov and S. Shaik. "A spin-restricted ensemble-referenced Kohn-Sham method and its application to diradicaloid situations". In: *Chem. Phys. Lett.* 304 (1999), pp. 429–437.

[65] Tim Kowalczyk et al. "Excitation energies and Stokes shifts from a restricted open-shell Kohn-Sham approach". In: *J. Chem. Phys.* 138 (2013), p. 164101.

[66] Paula Mori-Sánchez, Aron J Cohen, and Weitao Yang. "Localization and delocalization errors in density functional theory and implications for band-gap prediction". In: *Phys. Rev. Lett.* 100.14 (2008), p. 146401.

[67] Christine M Isborn et al. "The charge transfer problem in density functional theory calculations of aqueously solvated molecules". In: *J. Phys. Chem. B* 117.40 (2013), pp. 12189–12201.

[68] Jonathan D Gledhill, Michael J G Peach, and David J Tozer. "Assessment of tuning methods for enforcing approximate energy linearity in range-separated hybrid functionals". In: *J. Chem. Theory Comput.* 9.10 (2013), pp. 4414–4420.

[69] Luning Zhao and Eric Neuscamman. "Excited State Mean-Field Theory without Automatic Differentiation". In: *arXiv* (2020), p. 2002.00322.

[70] Chr Møller and Milton S Plesset. "Note on an approximation treatment for many-electron systems". In: *Phys. Rev.* 46.7 (1934), p. 618.

[71] Martin Head-Gordon. "An improved semidirect MP2 gradient method". In: *Mol. Phys.* 96.4 (1999), pp. 673–679.

[72] R. L. Martin. "Natural transition orbitals". In: *J. Chem. Phys.* 118 (2003), p. 4775.

[73] Martin Head-Gordon et al. "A doubles correction to electronic excited states from configuration interaction in the space of single substitutions". In: *Chem. Phys. Lett.* 219.1-2 (1994), pp. 21–29.

[74] Chenyang Li et al. "A low-cost approach to electronic excitation energies based on the driven similarity renormalization group". In: *J. Chem. Phys.* 147.7 (2017), p. 074107.

[75] Björn O Roos et al. "A simple method for the evaluation of the second-order-perturbation energy from external double-excitations with a CASSCF reference wavefunction". In: *Chem. Phys.* 66.1-2 (1982), pp. 197–207.

[76] Kerstin Andersson, Per-Åke Malmqvist, and Björn O Roos. "Second-order perturbation theory with a complete active space self-consistent field reference function". In: *J. Chem. Phys.* 96.2 (1992), pp. 1218–1226.

[77] Celestino Angeli et al. "Introduction of n-electron valence states for multireference perturbation theory". In: *J. Chem. Phys.* 114.23 (2001), pp. 10252–10264.

[78] Christoph Riplinger and Frank Neese. "An efficient and near linear scaling pair natural orbital based local coupled cluster method". In: *J. Chem. Phys.* 138.3 (2013), p. 034106.

[79] Piotr Piecuch, Jared A. Hansen, and Adeayo O. Ajala. "Benchmarking the completely renormalised equation-of-motion coupled-cluster approaches for vertical excitation energies". In: *Mol. Phys.* 113.19-20 (2015), pp. 3085–3127.

[80] Piotr Piecuch et al. "Efficient computer implementation of the renormalized coupled-cluster methods: The R-CCSD[T], R-CCSD(T), CR-CCSD[T], CR-CCSD(T) approaches". In: *Comput. Phys. Commun.* 149.2 (2002), pp. 71–96.

[81] Piotr Piecuch, Jeffrey R. Gour, and Marta Włoch. "Left-eigenstate completely renormalized equation of motion coupled-cluster methods: Review of key concepts, extension to excited states of open-shell systems and comparison with electron-attached and ionized approaches". In: *Int. J. Quantum Chem.* 109.14 (2009), pp. 3268–3304.

[82] Karol Kowalski and Piecuch Piotr. "New coupled-cluster methods with singles, doubles, and noniterative triples for high accuracy calculations of excited electronic states". In: *J. Chem. Phys* 120.4 (2004), pp. 1715–1738.

[83] M. W. Schmidt et al. "General Atomic and Molecular Electronic Structure System". In: *J. Comput. Chem.* 14 (1993), pp. 1347–1363.

[84] Giuseppe M. J. Barca et al. "Recent developments in general atomic and molecular electronic structure system". In: *J. Chem. Phys* 152.15 (2020), p. 154102.

[85] Yihan Shao et al. "Advances in molecular quantum chemistry contained in the Q-Chem 4 program package". In: *Mol. Phys.* 113.2 (2015), pp. 184–215.

[86] Hans-Joachim Werner et al. "Molpro: a general-purpose quantum chemistry program package". In: *Wiley Interdiscip. Rev. Comput. Mol. Sci.* 2.2 (2012), pp. 242–253.

[87] Hans-Joachim Werner. "Third-order multireference perturbation theory The CASPT3 method". In: *Mol. Phys.* 89.2 (1996), pp. 645–661.

[88] Paolo Celani and Hans-Joachim Werner. "Multireference perturbation theory for large restricted and selected active space reference wave functions". In: *J. Chem. Phys.* 112.13 (2000), pp. 5546–5557.

[89] P.-F. Loos et al. "A Mountaineering Strategy to Excited States: Highly-Accurate Energies and Benchmarks for Medium Size Molecules". In: *J. Chem. Theory Comput.* 16.3 (2020), pp. 1711–1741.

[90] Heidi H. Falden et al. "Benchmarking Second Order Methods for the Calculation of Vertical Electronic Excitation Energies: Valence and Rydberg States in Polycyclic Aromatic Hydrocarbons". In: *J. Phys. Chem. A.* 113.43 (2009), pp. 11995–12012.

[91] J. Lorentzon et al. "A CASPT2 Study of the Valence and Lowest Rydberg Electronic States of Benzene and Phenol". In: *Theor. Chim. Acta* 91 (1995), p. 91.

[92] Janet E Del Bene, John D Watts, and Rodney J Bartlett. "Coupled-cluster calculations of the excitation energies of benzene and the azabenzenes". In: *J. Chem. Phys.* 106.14 (1997), pp. 6051–6060.

[93] Huub JJ van Dam, Joop H van Lenthe, and Paul JA Ruttink. "Exact size consistency of multireference Møller–Plesset perturbation theory". In: *Int. J. Quantum Chem.* 72.6 (1999), pp. 549–558.

[94] I. R. Ariyarathna, C. R. Duan, and H. J. Kulik. "Understanding the chemical bonding of ground and excited states of HfO and HfB with correlated wavefunction theory and density functional approximations". In: *Journal of Chemical Physics* 156.18 (2022).

[95] D. Tuna et al. "Semiempirical Quantum-Chemical Orthogonalization-Corrected Methods: Benchmarks of Electronically Excited States". In: *Journal of Chemical Theory and Computation* 12.9 (2016), pp. 4400–4422.

[96] N. Beizaei and S. P. A. Sauer. "Benchmarking Correlated Methods for Static and Dynamic Polarizabilities: The T145 Data Set Evaluated with RPA, RPA(D), HRPA, HRPA(D), SOPPA, SOPPA(CC2), SOPPA(CCSD), CC2, and CCSD". In: *Journal of Physical Chemistry A* 125.17 (2021), pp. 3785–3792.

[97] P. O. Dral, X. Wu, and W. Thiel. "Semiempirical Quantum-Chemical Methods with Orthogonalization and Dispersion Corrections". In: *J Chem Theory Comput* 15.3 (2019), pp. 1743–1760.

[98] M. W. Jorgensen et al. "Benchmarking Correlated Methods for Frequency-Dependent Polarizabilities: Aromatic Molecules with the CC3, CCSD, CC2, SOPPA, SOPPA(CC2), and SOPPA(CCSD) Methods". In: *Journal of Chemical Theory and Computation* 16.5 (2020), pp. 3006–3018.

[99] J. Pedersen and K. V. Mikkelsen. "A benchmark study of aromaticity indexes for benzene, pyridine and the diazines - I. Ground state aromaticity". In: *Rsc Advances* 12.5 (2022), pp. 2830–2842.

[100] P. Piecuch, J. A. Hansen, and A. O. Ajala. "Benchmarking the completely renormalised equation-of-motion coupled-cluster approaches for vertical excitation energies". In: *Molecular Physics* 113.19-20 (2015), pp. 3085–3127.

[101] S. P. A. Sauer et al. "Performance of SOPPA-based methods in the calculation of vertical excitation energies and oscillator strengths". In: *Molecular Physics* 113.13-14 (2015), pp. 2026–2045.

[102] J. Sharma and P. A. Champagne. "Benchmark of density functional theory methods for the study of organic polysulfides". In: *Journal of Computational Chemistry* 43.32 (2022), pp. 2131–2138.

[103] A. Tajti, B. Kozma, and P. G. Szalay. "Improved Description of Charge-Transfer Potential Energy Surfaces via Spin-Component-Scaled CC2 and ADC(2) Methods". In: *Journal of Chemical Theory and Computation* 17.1 (2021), pp. 439–449.

[104] Anna I. Krylov. "Equation-of-Motion Coupled-Cluster Methods for Open-Shell and Electronically Excited Species: The Hitchhiker's Guide to Fock Space". In: *Annu. Rev. Phys. Chem.* 59.1 (2008), pp. 433–462.

[105] Kristian Sneskov and Ove Christiansen. "Excited state coupled cluster methods". In: *Wiley Interdisciplinary Reviews: Computational Molecular Science* 2.4 (2012), pp. 566–584.

[106] Henrik Koch et al. "The CC3 model: An iterative coupled cluster approach including connected triples". In: *The Journal of chemical physics* 106.5 (1997), pp. 1808–1818.

[107] T. J. Watson et al. "Benchmarking for Perturbative Triple-Excitations in EE-EOM-CC Methods". In: *Journal of Physical Chemistry A* 117.12 (2013), pp. 2569–2579.

[108] J. D. Watts and R. J. Bartlett. "Economical triple excitation equation-of-motion coupled-cluster methods for excitation-energies". In: *Chemical Physics Letters* 233.1-2 (1995), pp. 81–87.

[109] Andreas Dreuw and M. Head-Gordon. "Single-Reference ab Initio Methods for the Calculations of Excited States of Large Molecules". In: *Chem. Rev.* 105 (2005), p. 4009.

[110] C. Kollmar, K. Sivalingam, and F. Neese. "An alternative choice of the zeroth-order Hamiltonian in CASPT2 theory". In: *Journal of Chemical Physics* 152.21 (2020).

[111] G. Levi, A. V. Ivanov, and H. Jonsson. "Variational Density Functional Calculations of Excited States via Direct Optimization". In: *Journal of Chemical Theory and Computation* 16.11 (2020), pp. 6968–6982.

[112] C. A. A. McKeon et al. "An optimally tuned range-separated hybrid starting point for ab initio GW plus Bethe-Salpeter equation calculations of molecules". In: *Journal of Chemical Physics* 157.7 (2022).

[113] S. P. Neville and M. S. Schuurman. "A perturbative approximation to DFT/MRCI: DFT/MRCI(2)". In: *Journal of Chemical Physics* 157.16 (2022).

[114] K. Pernal and O. V. Gritsenko. "Embracing local suppression and enhancement of dynamic correlation effects in a CAS pi DFT method for efficient description of excited states". In: *Faraday Discussions* 224.0 (2020), pp. 333–347.

[115] S. P. Sauer et al. "Benchmarks for Electronically Excited States: A Comparison of Noniterative and Iterative Triples Corrections in Linear Response Coupled Cluster Methods: CCSDR(3) versus CC3". In: *J Chem Theory Comput* 5.3 (2009), pp. 555–64.

[116] Y. Y. Song et al. "The Static-Dynamic-Static Family of Methods for Strongly Correlated Electrons: Methodology and Benchmarking". In: *Topics in Current Chemistry* 379.6 (2021).

[117] C. Bannwarth et al. "Hole-hole Tamm-Dancoff-approximated density functional theory: A highly efficient electronic structure method incorporating dynamic and static correlation". In: *Journal of Chemical Physics* 153.2 (2020).

[118] S. Battaglia et al. "Regularized CASPT2: an intruder-state-free approach". In: *Journal of Chemical Theory and Computation* 18.8 (2022), pp. 4814–4825.

[119] M. Feldt and A. Brown. "Assessment of local coupled cluster methods for excited states of BODIPY/Aza-BODIPY families". In: *Journal of Computational Chemistry* 42.3 (2021), pp. 144–155. ISSN: 0192-8651.

[120] S. Haldar, T. Mukhopadhyay, and A. K. Dutta. "A similarity transformed second-order approximate coupled cluster method for the excited states: Theory, implementation, and benchmark". In: *Journal of Chemical Physics* 156.1 (2022).

[121] M. Hodecker et al. "Third-Order Unitary Coupled Cluster (UCC3) for Excited Electronic States: Efficient Implementation and Benchmarking". In: *Journal of Chemical Theory and Computation* 16.6 (2020), pp. 3654–3663.

[122] C. Holzer. "An improved seminumerical Coulomb and exchange algorithm for properties and excited states in modern density functional theory". In: *Journal of Chemical Physics* 153.18 (2020).

[123] M. Hubert, E. D. Hedegård, and H. J. Jensen. "Investigation of Multiconfigurational Short-Range Density Functional Theory for Electronic Excitations in Organic Molecules". In: *J Chem Theory Comput* 12.5 (2016), pp. 2203–13.

[124] E. M. Kempfer-Robertson, T. D. Pike, and L. M. Thompson. "Difference projection-after-variation double-hybrid density functional theory applied to the calculation of vertical excitation energies". In: *J Chem Phys* 153.7 (2020), p. 074103.

[125] Dániel Kánnár and Péter G Szalay. "Benchmarking coupled cluster methods on valence singlet excited states". In: *J. Chem. Theory Comput.* 10.9 (2014), pp. 3757–3765.

[126] Dániel Kánnár and Péter G Szalay. "Benchmarking coupled cluster methods on singlet excited states of nucleobases". In: *Journal of molecular modeling* 20 (2014), pp. 1–8.

[127] Richard L Martin. "Natural transition orbitals". In: *The Journal of chemical physics* 118.11 (2003), pp. 4775–4777.

[128] Amir Karton et al. "W4 theory for computational thermochemistry: In pursuit of confident sub-kJ/mol predictions". In: *The Journal of chemical physics* 125.14 (2006), p. 144108.

[129] Timothy J Lee and Peter R Taylor. "A diagnostic for determining the quality of single-reference electron correlation methods". In: *International Journal of Quantum Chemistry* 36.S23 (1989), pp. 199–207.

[130] Ansgar Schäfer, Hans Horn, and Reinhart Ahlrichs. "Fully optimized contracted Gaussian basis sets for atoms Li to Kr". In: *J. Chem. Phys.* 97.4 (1992), pp. 2571–2577.

[131] Qiming Sun et al. *PySCF: the Python-based simulations of chemistry framework*. 2017.

[132] H.-J. Werner et al. *MOLPRO, version 2019.2, a package of ab initio programs*. see https://www.molpro.net. Cardiff, UK, 2019.

[133] Gijs Schaftenaar, Elias Vlieg, and Gerrit Vriend. "Molden 2.0: quantum chemistry meets proteins". In: *J. Comput.-Aided Mol. Des.* 31.9 (2017), pp. 789–800.

[134] Mario R. Silva-Junior et al. "Benchmarks for electronically excited states: Time-dependent density functional theory and density functional theory based multireference configuration interaction". In: *J. Chem. Phys.* 129.10 (2008), p. 104103.

[135] J. M. Barrera-Andrade et al. "Incorporation of amide functional groups to graphene oxide during the photocatalytic degradation of free cyanide". In: *Materials Letters* 280 (2020).

[136] D. D. Bume et al. "Ketones as directing groups in photocatalytic sp(3) C-H fluorination". In: *Chemical Science* 8.10 (2017), pp. 6918–6923.

[137] M. X. Deng et al. "Synthesis and Characterization of Biodegradable Poly(ester amide)s with Pendant Amine Functional Groups and In Vitro Cellular Response". In: *Biomacromolecules* 10.11 (2009), pp. 3037–3047.

[138] S. Gnaim et al. "Tagging the Untaggable: A Difluoroalkyl-Sulfinate Ketone-Based Reagent for Direct C-H Functionalization of Bioactive Heteroarenes". In: *Bioconjugate Chemistry* 27.9 (2016), pp. 1965–1971.

[139] Tim Kowalczyk et al. "Excitation energies and Stokes shifts from a restricted open-shell Kohn-Sham approach". In: *J. Chem. Phys.* 138.16 (2013), p. 164101.

[140] Kenneth B. Wiberg, Anselmo E. de Oliveira, and Gary Trucks. "A Comparison of the Electronic Transition Energies for Ethene, Isobutene, Formaldehyde, and Acetone Calculated Using RPA, TDDFT, and EOM-CCSD. Effect of Basis Sets". In: *J. Phys. Chem. A* 106.16 (2002), pp. 4192–4199.

[141] Kenichi Nakayama, Haruyuki Nakano, and Kimihiko Hirao. "Theoretical study of the $\pi \rightarrow \pi^*$ excited states of linear polyenes: The energy gap between 11Bu+ and 21Ag- states and their character". In: *International journal of quantum chemistry* 66.2 (1998), pp. 157–175.

[142] M. Krauss and S. R. Mielczarek. "Minima in generalized oscillator strengths . C2H4". In: *Journal of Chemical Physics* 51.12 (1969), p. 5241.

[143] R. Lindh and B. O. Roos. "A theoretical study of the diffuseness of the V(1B1u) state of planar ethylene". In: *International Journal of Quantum Chemistry* 35.6 (1989), pp. 813–825.

[144] Luis Serrano-Andrés et al. "Theoretical study of the electronic spectra of cyclopentadiene, pyrrole, and furan". In: *J. Am. Chem. Soc.* 115.14 (1993), pp. 6184–6197.

[145] Yannick J. Bomble et al. "On the vertical excitation energy of cyclopentadiene". In: *The Journal of Chemical Physics* 121.11 (2004), pp. 5236–5240.

[146] Bjoern O. Roos et al. "Theoretical and Experimental Determination of the Electronic Spectrum of Norbornadiene". In: *J. Am. Chem. Soc.* 116.13 (1994), pp. 5927–5936.

[147] J. P. Doering and Ruth McDiarmid. "An electron impact investigation of the forbidden and allowed transitions of norbornadiene". In: *J. Chem. Phys.* 75.1 (1981), pp. 87–91.

[148] Ove Christiansen et al. "Large-scale calculations of excitation energies in coupled cluster theory: The singlet excited states of benzene". In: *J. Chem. Phys.* 105.16 (1996), pp. 6921–6939.

[149] Marco Caricato et al. "Electronic Transition Energies: A Study of the Performance of a Large Range of Single Reference Density Functional and Wave Function Methods on Valence and Rydberg States Compared to Experiment". In: *J. Chem. Theory Comput.* 6.2 (2010), pp. 370–383.

[150] Ove Christiansen et al. "The electronic spectrum of pyrrole". In: *J. Chem. Phys.* 111.2 (1999), pp. 525–537.

[151] Ove Christiansen and Poul Jørgensen. "The Electronic Spectrum of Furan". In: *J. Am. Chem. Soc.* 120.14 (1998), pp. 3423–3430.

[152] Luis Serrano-Andrés et al. "Theoretical Study of the Electronic Spectrum of Imidazole". In: *J. Phys. Chem.* 100.16 (1996), pp. 6484–6491.

[153] "Physical methods in heterocyclic chemistry". In: *Index to Reviews, Symposia Volumes and Monographs in Organic Chemistry*. Ed. by Norman Kharasch and Walter Wolf. Pergamon, 1966, p. 195.

[154] S. A. Asher and J. L. Murtaugh. "UV Raman excitation profiles of imidazole, imidazolium, and water". In: *Applied Spectroscopy* 42.1 (1988), pp. 83–90.

[155] E. Bernarducci et al. "Electronic-structure of alkylated imidazoles and electronic-spectra of tetrakis(imidazole)copper(II) complexs - molecular-structure of tetrakis(1,4, 5-trimethylimidazole)copper(II) diperchlroate". In: *Journal of the American Chemical Society* 105.12 (1983), pp. 3860–3866.

[156] D. S. Caswell and T. G. Spiro. "Ultraviolet resonance Raman-spectroscopy of imidazole, histidine, and Cu(imidazole) - implications for protein studies". In: *Journal of the American Chemical Society* 108.21 (1986), pp. 6470–6477.

[157] T. G. Fawcett et al. "charge-transfer absorption of Cu(II)-imidazole and Cu(II)-imidazole chromophores". In: *Journal of the American Chemical Society* 102.8 (1980), pp. 2598–2604.

[158] M. Gelus and J. M. Bonnier. "UV spectrophotometry of some heterocycles". In: *Journal De Chimie Physique Et De Physico-Chimie Biologique* 64.11-1 (1967), p. 1602.

[159] P. E. Grebow and T. M. Hooker. "conformation of histidine model peptides .2. spectroscopic properties of imidazole chromophore". In: *Biopolymers* 14.4 (1975), pp. 871–881.

[160] Jian Wan et al. "Electronic excitation and ionization spectra of azabenzenes: Pyridine revisited by the symmetry-adapted cluster configuration interaction method". In: *J. Chem. Phys.* 114.12 (2001), pp. 5117–5123.

[161] P. F. Loos et al. "A Mountaineering Strategy to Excited States: Highly Accurate Energies and Benchmarks for Medium Sized Molecules". In: *J Chem Theory Comput* 16.3 (2020), pp. 1711–1741.